DISSERTATION

USE OF STABLE ISOTOPES IN THE STUDY OF CO_2 FLUXES IN SHORTGRASS STEPPE

Submitted by

Jee H. Shim

Forest, Rangeland, and Watershed Stewardship

In partial fulfillment of the requirements

For the Degree of Doctorate of Philosophy

Colorado State University

Fort Collins, Colorado

Spring 2005

COLORADO STATE UNIVERSITY

March 3, 2005

WE HERBY RECOMMEND THAT THE DISSERTATION PREPARED UNDER OUR SUPERVISON BY JEE HYUN SHIM ENTITIED:
USE OF STABLE ISOTOPES IN THE STUDY OF CO_2 FLUXES IN SHORTGRASS STEPPE, BE ACCEPTED AS FULFILLING IN PART REQUIREMENTS FOR THE DEGREE OF DOCTORATE OF PHIOLOSOPHY.

Committee on Graduate Work

Advisor

Department Head

ABSTRACT OF DISSERTATION

USE OF STABLE ISOTOPES IN THE STUDY OF CO_2 FLUXES IN SHORTGRASS STEPPE

The shortgrass steppe in northeastern Colorado has brief periods of water availability, and as a consequence, distinct carbon isotopes of C_3 and C_4 plants. We investigated 1) what environmental controls are responsible for the dynamics of $\delta^{13}C$ of ecosystem respiration ($\delta^{13}C_R$) and how plant functional groups contribute to $\delta^{13}C_R$, and 2) what environmental controls are responsible for $\delta^{18}O$ of ecosystem water pools and respiratory fluxes and how plant functional groups interact with different environmental conditions (moist versus dry). Last, we determined whether or not isotopic fluxes of $^{13}CO_2$ and $C^{18}O^{16}O$ could be used for partitioning NEE into gross photosynthesis and respiration.

We hypothesized that time lags between pulse precipitation events, net CO_2 exchange (NEE) and $\delta^{13}C$ of ecosystem respiration ($\delta^{13}C_R$) are related to antecedent moisture conditions. Time lags of two weeks occurred between a rainfall event and a NEE response after extended dry periods. During extreme dry periods, soil respiration measurements indicated older plant carbon compounds were emitted. Plant responses related to precipitation events seem to correlate well with variations of $\delta^{13}C_R$.

Dominant influence of very enriched $\delta^{18}O$ of soil surface water caused decoupling between $\delta^{18}O$ of atmospheric CO_2 and inverse CO_2 concentrations during the

dry seasons. The changes in $\delta^{18}O$ of leaf water pools and respiratory CO_2 fluxes responded rapidly to pulse precipitation. Isotopic $\delta^{18}O$ partitioning suggested that soil respiration accounted for about 89 % of the total ecosystem respiration, and the strong contribution was more pronounced in dry conditions.

Photosynthesis did not alter the $C^{18}O^{16}O$ signal during prolonged dry conditions. It appeared that water vapor and carbon were weakly coupled during rainy sampling periods. Restricted usage of partitioning with carbon isotopic analysis was also revealed in dry condition during July 2001. Despite the limitations, photosynthetic CO_2 fluxes partitioned by both stable isotopes agreed well, and the relationship was stronger when isotopic disequilibrium between photosynthetic assimilation and $\delta^{13}C_R$ was strong.

Jee H. Shim
Forest, Rangeland, and Watershed Stewardship
Colorado State University
Fort Collins, CO 80253
Spring 2005

TABLE OF CONTENTS

1. Introduction 1

2. Contributions of precipitation pulses and plant functional types to ^{13}C of ecosystem respiration in shortgrass steppe 17

2.1 Abstract 17

2.2 Introduction 18

2.3 Materials and methods 22

2.4 Results 29

2.5 Discussions 37

2.6 Conclusions 44

2.7 References 45

3. The contribution of C_3 and C_4 plants, and dynamics of ^{18}O water pools to variations in respiratory ^{18}O signals in shortgrass steppe 62

3.1 Abstract 62

3.2 Introduction 63

3.3 Materials and methods 67

3.4 Results 79

3.5 Discussions 86

3.6 Conclusion 94

3.7 References 97

4. Partitioning gross photosynthesis and respiration in shortgrass steppe ecosystem: Relation to the climatic and plant community dynamics 120

4.1 Abstract 120

4.2 Introduction 121

4.3 Materials and methods 124

4.4 Results 138

4.5 Discussions 144

4.6 Conclusions 147

4.7 References 151

1. Introduction

Understanding net ecosystem exchange (NEE) of carbon dioxide between the biosphere and atmosphere is a critical issue due to its contribution to changes in global atmospheric CO_2 concentrations and net primary production in terrestrial ecosystem. Net ecosystem exchange has been defined as the balance of gross primary production (GPP) and ecosystem respiration (Re) and expressed as the difference between the two. The complexities of controlling factors governing the dynamics of gas exchange and on the interactions at the interface between the atmosphere and canopy contribute to substantial uncertainties in field measurements and model estimates of net gas fluxes.

Coordinated international networks of ecosystem studies have been organized (EUROFLUX, AMERIFLUX; http://www.bgc-jena.mpg.de/public/carboeur/, http://public.ornl.gov/ameriflux/, respectively) to measure NEE over short time scales (e.g., seconds to hours) and longer periods (e.g., days to years), and to assesses the environmental constraints on ecosystem carbon exchange (Baldocchi et al. 2001). Recent research has incorporated the measurements of stable isotope composition of atmospheric CO_2 combined with micrometeorological measurements such as Bowen Ratio Energy Balance (BREB) or eddy covariance techniques to provide unique and additional ways of partitioning NEE into photosynthesis and ecosystem respiration, land/ocean sink partitioning (Yakir and Wang 1996; Bowling et al. 1999; Ciais et al. 1995; Battle et al. 2000) because stable isotopes offer distinct labeling of flux components. Isotopic

compositions of ecosystem water and CO_2 are illustrated in Fig. 1.1. The following two sections provide background information of stable isotopic techniques and micrometeorological methods employed for carbon exchange studies.

Isotopic Discrimination of Photosynthesis and Respiration

Carbon isotopes

Photosynthesis discriminates against the heavier ^{13}C in CO_2 and preferentially assimilates $^{12}CO_2$ into plant biomass, creating leaf tissue depleted in ^{13}C of CO_2 (Farquhar et al. 1989) and enrichment in $^{13}CO_2$ of air near terrestrial ecosystems. Discrimination of ^{13}C at the leaf level is dependent on enzymatic discrimination and diffusion linked to the ratio of CO_2 of the internal leaf concentration to atmospheric concentrations (c_i/c_a) (Farquhar et al. 1989; Ehleringer et al. 1993). C_3 plants discriminate more against ^{13}C than C_4 plants due to higher ratio of c_i/c_a and higher discrimination of Rubisco-controlled photosynthesis of C_3 plants (Farquhar et al. 1989). Intra-specific variations often exist in ^{13}C discrimination since ci/ca is tightly related with stomatal conductance that is subject to change with species response to variations in environmental parameters such as soil water availability (Lauteri et al. 1993), vapor pressure deficit (VPD) and sunlight (Berry et al. 1997).

The Keeling plot approach is frequently used to interpret fluctuations in the $\delta^{13}C$ values of ambient CO_2 and to identify the integrated value of CO_2 sources in ecosystems (Keeling 1958, 1961; Buchmann et al. 1997a, 1997b; Flanagan et al. 1995; Pataki et al. 2002). The $\delta^{13}C$ of ecosystem respiration ($\delta^{13}C_R$) derived from the Keeling plot method is

one of the key parameters in mass balance equation that are used to partition net ecosystem fluxes of CO_2 into their photosynthetic and respiratory fluxes and to assess the magnitude of the terrestrial carbon sink (Bowling et al. 1999; Yakir and Wang 1996; Fung et al. 1997; Randerson et al. 2002). $\delta^{13}C_R$ provides an estimate of the decomposing plant and soil substrates that break down during decomposition and respiration, assuming no fractionation occurs during theses process (Lin and Ehleringer 1997; but refer to Duranceau et al. 1999 and Ghashghaie et al. 2001). Interplay between the $\delta^{13}C$ of assimilation and respiration of carbon can be dependent on multi-level interactions involving plant and ecosystem levels. In addition to spatially related interactions from the leaf to canopy scale, temporally driven isotopic disequilibrium associated with different turn-over rates of fast-versus slow-responding carbon pools can also be an important consideration for investigating $\delta^{13}C_R$ dynamics. Observations made in systems characterized by fast growing forest canopies and large soil organic matter turnover show that vapor pressure deficit (VPD) of the preceding couple of days served as a good indicator of recently fixed carbon (Bowling et al. 2002; Ekblad and Högberg 2001). The effect of time lagged VPD on $\delta^{13}C_R$ has been reported in C_3 ecosystems where the bulk of respired CO_2 was derived from recent assimilates (a few days to two weeks old), showing that $\delta^{13}C_R$ is directly controlled by canopy scale discrimination. If suppression of photosynthesis results from prolonged drought, and VPD influences ^{13}C discrimination by plant functional groups differentially in mixed C_3 and C_4 ecosystems, then these other mechanisms are required to understand the variability of $\delta^{13}C_R$.

Oxygen isotopes

Ecosystem CO_2 exchange can also significantly influence the oxygen ratio of atmospheric CO_2 through net photosynthesis (Farquhar et al. 1993; Gillon and Yakir 2000) and soil and foliar respiration (Tans 1998; Miller et al. 1999; Bowling et al. 2003a, b). The Keeling plot approach has also been applied to estimate the $\delta^{18}O$ of nocturnal ecosystem respiration (Yakir and Wang 1996; Flanagan et al. 1997). A conceptual diagram of controlling factors influencing $\delta^{18}O$ of ecosystem respiration ($\delta^{18}O_R$) is shown in Figure 1.2.

The isotopic composition of precipitation varies mainly with temperature and storm tracks (Rozanski et al. 1982), and initially controls $\delta^{18}O$ of soil water. Evaporation taking place at the soil surface enriches $\delta^{18}O$ of soil water, resulting in an isotopic gradient within the soil. Hydration of respiratory CO_2 produced within soils (by roots or heterotrophs) equilibrates isotopically with soil water (Miller et al. 1999). Plants probably use a mixture of source water that has been mixed with evaporatively enriched soil water. Leaf water is enriched in $\delta^{18}O$ compared to stem and soil water because transpiration results in a lower evaporation rate for $H_2{}^{18}O$ than $H_2{}^{16}O$ (Flanagan et al. 1991; Wang and Yakir 1995). Enrichments of leaf water vary with environmental conditions such as variations in VPD (Roden and Ehleringer 1999), leaf temperature (Flanagan et al. 1991), the $\delta^{18}O$ of atmospheric water vapor which is controlled by local precipitation and air temperature. The $\delta^{18}O$ of leaves also varies with plant species due to specific rooting zones and different leaf anatomy between C_3 and C_4 grasses (Helliker and Ehleringer 2000).

The $^{18}O_R$ is a combined product of $\delta^{18}O$ of leaf and soil respired CO_2 ($\delta^{18}O_{LR}$ and $\delta^{18}O_{SR}$, respectively). Isotopic signatures of leaf and soil respired $C^{18}O^{16}O$ are influenced by $\delta^{18}O$ of leaf water ($\delta^{18}O_{LW}$) and soil water ($\delta^{18}O_{SW}$), respectively. There are two major processes that influence the changes in $\delta^{18}O$ of soil respired CO_2. First, oxygen isotopes in CO_2 are subject to a kinetic isotopic fractionation factor associated with diffusion. The heavier CO_2 molecules diffuse slower than molecules with ^{16}O. Second, once this CO_2 interacts with soil water, oxygen in water can exchange readily with oxygen in CO_2 due to the presence of an enzyme called carbonic anhydrase (CA). The presence of CA in soil, especially near the soil surface, results in the CO_2 to be near isotopic equilibrium with soil water. The kinetic fractionation factor during diffusion depends on the relative rate of CO_2 production, equilibration between CO_2 and H_2O, and invasion of atmospheric CO_2 into soil (Hesterberg and Siegenthaler 1991; Tans 1998).

The two main processes influencing the $\delta^{18}O$ of soil respired CO_2 also have dominant effects on discrimination against $C^{18}O^{16}O$ during photosynthetic gas exchange (Farquhar and Lloyd 1993). Equilibration of respired CO_2 with leaf water and fractionation during diffusion are the major processes. Once inside the leaf in liquid phase, oxygen in water can exchange readily with oxygen in CO_2 due to CA. The leaf water is equilibrated with CO_2 facilitated by CA and is followed by retrodiffusion of two thirds of equilibrating CO_2 with an altered oxygen isotope (Flanagan et al. 1997).

The $C^{18}O^{16}O$ discrimination ($\Delta^{18}O$) during photosynthesis accounts for possible incomplete isotopic equilibrium and can be expressed as

$$\Delta^{18}O = \varepsilon_k' + c_\varepsilon[\theta_{eq}(\delta_e - \delta_{a\_co_2}) - (1-\theta_{eq})\varepsilon_k'/(c_\varepsilon + 1)]$$

where ε_k' is the average diffusional fractionation of CO_2 from air to leaf chloroplast. This is dominated by the diffusion from the atmosphere into leaf pore space, which is theoretically 8.8 ‰ based on the differences in diffusivity between $C^{16}O_2$ and $C^{18}O_2$. δ_e refers to the $\delta^{18}O$ of CO_2 in equilibrium with chloroplast water. δ_a is the oxygen isotope ratio of CO_2 in the atmosphere; $C_\varepsilon = c_{cs}/(c_a-c_{cs})$; c_{cs} and c_a are CO_2 concentrations at the site of CO_2-H_2O exchange in leaves and in ambient air, respectively. θ_{eq} is isotopic equilibrium factor considering the extent of CO_2-H_2O equilibrium in the chloroplast (i.e. CA activity). In plants with low CA activity, there is incomplete equilibration between CO_2 and chloroplast water and, therefore, low $\Delta^{18}O$ values are expected. The $\delta^{18}O$ of atmospheric CO_2 is more enriched during active isotopic exchange with enriched leaf water through a process of evaporative enrichment during transpiration compared to the soil respired $\delta^{18}O$-CO_2 signature because the latter is controlled by relatively ^{18}O-depleted sub-surface soil water (Miller et al. 1999).

A few studies have examined the controls of $\delta^{18}O$ of respiratory CO_2 including leaf and soil components (Bowling et al. 2003 a b; Flanagan et al. 1994, 1995 and 1997). The quantification of ^{18}O discrimination and investigation of major controls governing dynamics of ^{18}O signatures from respiratory sources will add to our critical understanding of ecosystem controls on carbon exchange to the atmosphere.

Micrometeorological Approach to CO_2 and H_2O Exchange

Detection of variations of net carbon exchange is relatively straightforward using eddy correlation or Bowen ratio techniques. However, obtaining the process details of

how gross photosynthesis and respiration contribute differentially to NEE is not feasible from these techniques without the use of isotopic analysis or models based on respiration-temperature relationships. The isotopic mass balance approach for partitioning was first applied in concert with combinations of meteorological knowledge and stable isotope measurements by Yakir and Wang (1996) in wheat, cotton and corn fields, followed by Bowling et al. (1999, 2003c) in forests and Lai et al. (2003) in tallgrass prairie. However, an isotopic partitioning approach has never been applied to the short grass steppe. In order to evaluate how gross fluxes of photosynthesis (P) and respiration (R) change with environmental perturbation such as variations in climate change and atmospheric CO_2 concentrations, this technique should be tested in other ecosystem types and over several growing seasons.

Even though grasslands comprise 32% of the earth's natural vegetation (Adams et al. 1990) studies on CO_2 exchange have not been initiated in these ecosystems until recently (Dugas et al. 1999; Frank and Dugas 2001; Sims and Bradford 2001; Suyker and Verma 2001; Suyker et al. 2003; Flanagan et al. 2002). In particular, few studies have investigated the partitioning of NEE and the associated changes in $\delta^{13}C$ of CO_2. What studies which are available have been carried out in forest ecosystems (Buchmann et al. 1997 a b; Bowling et al. 2002; McDowell et al. 2003). Relations between environmental parameters and $\delta^{13}C_R$ can be complicated in a mixed C_3 and C_4 ecosystem which has variable periods of adequate water availability (Sala et al. 1992) and of distinct $\delta^{13}C$ signatures of C_3 and C_4 plants. Co-existence of C_3 and C_4 plant species lead to a more complicated interpretation of $\delta^{13}C$ of canopy uptake and respiration (Still et al. 2003) and to disagreement of modeled versus measured data (Bakwin et al. 1998).

Precipitation pulse size plays an important role in regulating NEE of arid ecosystems through its differential effects on ecosystem respiration and photosynthesis (Huxman et al. 2004). The sensitivities of the processes may be dependent on precipitation amount, distribution of precipitation pulses both within and across seasons, and the response time differences of microbes and plants to wetting events. Understanding the linkage between precipitation pulses to measured $\delta^{13}C_R$, in semi-arid ecosystems, may be very informative.

Very few studies on atmospheric $C^{18}O^{16}O$ signals have been conducted in grasslands. Like the $\delta^{13}C$ research, the contribution of different plant functional groups classified by photosynthetic pathway to atmospheric $C^{18}O^{16}O$ signal and in particular to $\delta^{18}O$ of leaf respiratory CO_2 is needed for improving understanding of carbon sinks/source strengths. Seasonal activity of C_3 and C_4 plants could contribute to dynamics of $\delta^{18}O$ of respired CO_2 because C_4 grass species show less ^{18}O discrimination than C_3 plants because of much lower internal CO_2 concentrations and lower CA hydration rate (Gillon and Yakir 2000; Williams et al. 1996) Improved information about the magnitude of plant functional type's contribution to productivity is particularly important because the C_4 plants cause changes to the $^{13}C/^{12}C$ ratio of atmosphere that are very similar to oceanic exchange.

Therefore, in the first study (chapter 2), I will address a) what environmental controls are responsible for the dynamics of $\delta^{13}C$ of ecosystem respiration ($\delta^{13}C_R$) and b) how plant functional groups contribute to $\delta^{13}C_R$ in the short grass steppe. In chapter 3, I will a) describe the natural variability in $\delta^{18}O$ of ecosystem water pools and respiratory fluxes with seasonal variations, and b) evaluate environmental controls responsible for

the dynamics of those values and c) determine how plant functional groups interact with different environmental conditions (moist versus dry) to quantify the soil and foliar contributions to the total ecosystem respiration fluxes using both chamber based measurements and modeling approach. In chapter 4, I will evaluate the utility of isotopic techniques of $^{13}CO_2$ and $C^{18}O^{16}O$ fluxes for partitioning NEE into gross photosynthesis and respiration on the shortgrass steppe over two consecutive growing seasons.

References

Adams JM, Faure H, Faure-Denard L, McGlade JM, Woodward FI (1990) Increases in terrestrial carbon storage from the last glacial maximum to the present. Nature 348:711-714.

Bakwin PS, Tans PP, White JWC, Andres RJ (1998) Determination of the isotopic ($^{13}C/^{12}C$) discrimination by terrestrial biology from a global network of observations. Global Biogeochemical Cycles 12:555-562.

Baldocchi D, Falge E, Wilson K (2001) A spectral analysis of biosphere-atmosphere trace gas flux densities and meteorological variables across hour to multi-year time scales. Agricultural and Forest Meteorology 107:1-27.

Battle M, Bender ML, Tans PP, White JWC, Ellis JT, Conway T, Francey RJ (2000) Global carbon sinks and their variability inferred from atmospheric O_2 and $\delta^{13}C$. Science 287:2467-2470.

Berry SC, Varney GT, Flanagan LB (1997) Leaf $\delta^{13}C$ in *Pinus resinosa* trees and understory plants: Variation associated with light and CO_2 gradient. Oecologia 109:499-506.

Bowling DR, Baldocchi DD, Monson RK (1999) Dynamics of isotopic exchange of carbon dioxide in a Tennessee deciduous forest. Global Biogeochemical Cycles 13:903-922.

Bowling DR, McDowell NG, Bond BJ, Law BE, Ehleringer JR (2002) ^{13}C content of ecosystem respiration is linked to precipitation and vapor pressure deficit. Oecologia 131:113-124.

Bowling DR, McDowell NG, Welker JM, Bond BJ, Law BE, Ehleringer JR (2003a) Oxygen isotope content of CO_2 in nocturnal ecosystem respiration: 2 Short-term dynamics of foliar and soil component fluxes in an old-growth ponderosa pine forest. Global Biogeochemical Cycles 17:34.

Bowling DR, McDowell NG, Welker JM, Bond BJ, Law BE, Ehleringer JR (2003b) Oxygen isotope content of CO_2 in nocturnal ecosystem respiration: 1. Observations in forests along a precipitation transect in Oregon, USA. Global Biogeochemical Cycles 17(4), 1120, 3oi:10.1029/2003GB002081.

Bowling DR, Pataki DE, Ehleringer JR (2003c) Critical evaluation of micrometeorological methods for measuring ecosystem-atmosphere isotopic exchange of CO_2. Agricultural and Forest Meteorology 116:159-179.

Brenninkmeijer CAM, Kraft P, Mook WG (1983) Oxygen isotope fractionation between CO_2 and H_2O. Isotope Geoscience 1:181-190.

Buchmann N, Guehl J-M, Barigah TS, Ehleringer JR (1997a) Interseasonal comparison of CO_2 concentrations, isotopic composition, and carbon dynamics in an Amazonian rainforest (French Guiana). Oecologia 110:120-131.

Buchmann N, Kao W-Y, Ehleringer J (1997b) Influence of stand structure on carbon-13 of vegetation, soils, and canopy air within deciduous and evergreen forests in Utah, Unites States. Oecologia 110:109-119.

Ciais P, Tans PP, Trolier M, White JWC, Francey RJ (1995) A large Northern Hemisphere terrestrial CO_2 sink indicated by the $^{13}C/^{12}C$ ratio of atmospheric CO_2. Science 269:1089-1102.

Dugas WA, Heuer ML, Mayeux HS (1999) Carbon dioxide fluxes over bermudagrass, native prairie, and sorghum. Agricultural and Forest Meteorology 93:121-139.

Durancean M, Ghashghaie J, Badeck F, Deleens E, Cornic G (1999) Delta C-13 of CO_2 respired in the dark in relation to delta C-13 of leaf carbohydrates in *Phaseolus vulgaris* L-under progressive drought. Plant Cell and Environment 22:515-523.

Ehleringer JR, Hall AE, Farquhar GD (1993) Stable Isotopes and Plant Carbon-Water Relations. Academic, San Diego, California.

Ekbland A, Högberg P (2001) Natural abundance of ^{13}C in CO_2 respired from forest soils reveals speed of link between tree photosynthesis and root respiration. Oecologia 127:305-308.

Farquhar GD, Ehleringer JR, Hubick KT (1989) Carbon isotope discrimination and photosynthesis. Annual Review of Plant Physiology Plant Molecular Biology 40:503-537.

Farquhar GD, Lloyd J (1993) Carbon and oxygen isotope effects in the exchange of carbon dioxide between terrestrial plants and the atmosphere. In: Stable Isotope and Plant Carbon-Water Relations Academic, San Diego, California, pp 47-70.

Flanagan LW, Comstock JP, Ehleringer JR (1991) Comparison of modeled and observed environmental influences on the stable oxygen and hydrogen isotope composition of leaf water in *Phaseolus vulgaris L.* Plant Physiology 96:588-596.

Flanagan LB (1993) Environmental and biological influences on the stable oxygen and hydrogen isotopic composition of leaf water. In: Stable Isotope and Plant Carbon-Water Relations Academic, San Diego, California, pp 71-90.

Flanagan LB, Phillips SL, Ehleringer JR, Lloyd J, Farquhar GD (1994) Effect of changes in leaf water oxygen isotopic composition on discrimination against $C^{18}O^{16}O$ during photosynthetic gas exchange. Australian Journal of Plant Physiology 21:221-234.

Flanagan LB, Varney GT (1995) Influence of vegetation and soil CO_2 exchange on the concentration and stable oxygen isotope ratio of atmospheric CO_2 within a *Pinus resinosa* canopy. Oecologia 101:37-44.

Flanagan LB, Brooks JR, Varney GT, Ehleringer JR (1997) Discrimination against $C^{18}O^{16}O$ during photosynthesis and the oxygen isotope ratio of respired CO_2 in boreal forest ecosystems. Global Biogeochemical Cycles 11:83-98.

Flanagan LB, Wever LA, Carlson PJ (2002) Seasonal and interannual variation in carbon dioxide exchange and carbon balance in a northern temperate grassland. Global Change Biology 8:599-615.

Frank AB, Dugas WA (2001) Carbon dioxide fluxes over a northern, semiarid, mixed-grass prairie. Agricultural and Forest Meteorology 108:317-326.

Fung I, Field CB, Berry JA, Thompson MV, Randerson JT, Malmstrom CM, Vitousek PM, Collaz GJ, Sellers PJ, Randall DA, Denning AS, Badeck F, John J (1997) Carbon^{13} exchanges between the atmosphere and biosphere. Global Biogeochemical Cycles 11:507-533.

Ghashghaie J, Duranceau M, Badeck FW, Cornic G, Adeline MT, Deleens E (2001) Delta C-13 of CO_2 respired in the dark in relation to delta C-13 of leaf metabolites: comparison between *Nicotiana sylvestris* and H*elianthus annuus* under drought. Plant Cell and Environment 4:505-515.

Gillon JS, Yakir D (2000) Naturally low carbonic anhydrase activity in C_4 and C_3 plants limits discrimination against $C^{18}OO$ during photosynthesis. Plant, Cell and Environment 23:903-915.

Helliker BR, Ehleringer JR (2000) Establishing a grassland signature in veins: ^{18}O in the leaf water of C_3 and C_4 grasses. Proceedings of the National Academy of Sciences 97:7894-7898.

Huxman TE, Cable JM, Ignace DD, Eilts JA, English NB, Weltzin J, Williams DG (2004) Response of net ecosystem gas exchange to a simulated precipitation pulse in a semi-arid grassland: the role of native versus non-native grasses and soil texture. Oecologia 141:295-305.

Keeling CD (1958) The concentration and isotopic abundances of atmospheric carbon dioxide in rural areas. Geochemica et Cosmochimica Acta 13: 322-334.

Keeling CD (1961) The concentration and isotopic abundance of carbon dioxide in rural and marine air. Geochemica et Cosmochimica Acta 24:277-298

Lai C-T, Schauer AJ, Owensby C, Ham JM, Ehleringer JR (2003) Isotopic air sampling in a tallgrass prairie to partition net ecosystem CO_2 exchange. Journal of Geophysical Research 108, NO.D18, 4566, dio:10.1029/2029/2002JD003369

Lauteri M, Brugnoli E, Spaccino L (1993) Carbon isotope discrimination in leaf soluble sugars and in whole plant dry matter *in Helianthus annuus L.* grown under different water conditions. In: Ehleringer JR, Hall AE, Farquhar GD (eds.). Stable Isotopes and Plant Carbon-Water Relations Academic Press, San Diego, pp 93-108.

Lin G, Ehleringer JR (1997) Carbon isotopic fractionation does not occur during dark respiration in C_3 and C_4 plants. Plant physiology 114:391-394.

McDowell NG, Bowling DR, Bond BJ, Irvine J, Law BE, Anthoni P, Ehleringer JR (2004) Response of the carbon isotopic content of ecosystem, leaf, and soil respiration to meteorological and physiological driving factors in a *Pinus ponderosa* ecosystem. Global Biogeochemical Cycles 18, dio:10.1029/2003GB002049

Miller JB, Yakir D, White JWC, Tans PP (1999) Measurement of $^{18}O/^{16}O$ in the soil-atmosphere CO_2 flux. Global Biogeochemical Cycles 13:761-774

Pataki DE, Ehleringer JR, Flanagan LB, Yakir D, Bowling DR, Still CS, Buchmann N, Kaplan JO, Berry JA (2003) The application and interpretation of Keeling plots in terrestrial carbon cycle research. Global Biogeochemical Cycles 17(1), 1022, dio:10.1029/2001GB001850

Randerson JT, Collatz GJ, Fessenden JE, Munoz AD, Still CJ, Berry JA, Fung IY, Suits N, Denning AS (2002) A possible global covariance between terrestrial gross primary production and ^{13}C discrimination: Consequences for the atmospheric ^{13}C budget and its response to ENSO. Global Biogeochemical Cycles 16, doi:10.1029/2001GB001845.

Roden JS, Ehleringer JR (1999) Observations of hydrogen and oxygen isotopes in leaf water confirm the Craig-Gordon model under wide-ranging environmental conditions. Plant Physiology 120:1165-1173.

Rozanski KC, Sonntag C, Munnich KO (1982) Factors controlling stable isotope composition of European precipitation. Tellus 34:142-150.

Sala OE, Lauenroth WK, Parton WJ (1992) Long-term soil water dynamics in the shortgrass steppe. Ecology 73:1175-1181.

Sims PL, Bradford JA (2001) Carbon dioxide fluxes in a southern plains prairie. Agricultural and Forest Meteorology 109:117-134.

Still CJ, Berry JA, Ribas-Carbo M, Helliker BR (2003) The contribution of C_3 and C_4 plants to the carbon cycle of a tallgrass prairie: an isotopic approach. Oecologia 136: 347-359.

Suyker AE, Verma SB (2001) Year-round observations of the net ecosystem exchange of carbon dioxide in a native tallgrass prairie. Global Change Biology 7:279-289.

Suyker AE, Verma SB, Burba GG (2003) Interannual variability in net CO^2 exchange of a native tallgrass prairie. Global Change Biology 9: 255-265.

Tans PP (1998) Oxygen isotopic equilibrium between carbon dioxide and water in soils. Tellus Ser. B. 50:163-178.

Wang XF, Yakir D (1995) Temporal and spatial variations in the oxygen^{18} content of leaf water in different plant species. Plant, Cell and Environment 18:1377-1385.

Williams TG, Flanagan LB, Coleman JR (1996) Photosynthetic gas exchange and discrimination against $^{13}CO_2$ and $C^{18}O^{16}O$ in tobacco plants modified by an antisense construct to have low chloroplastic carbonic anhydrase. Plant Physiology 112:319-326.

Yakir D, Wang X-F (1996) Fluxes of CO_2 and water between terrestrial vegetation and the atmosphere estimated from isotope measurements. Nature 380:515-517.

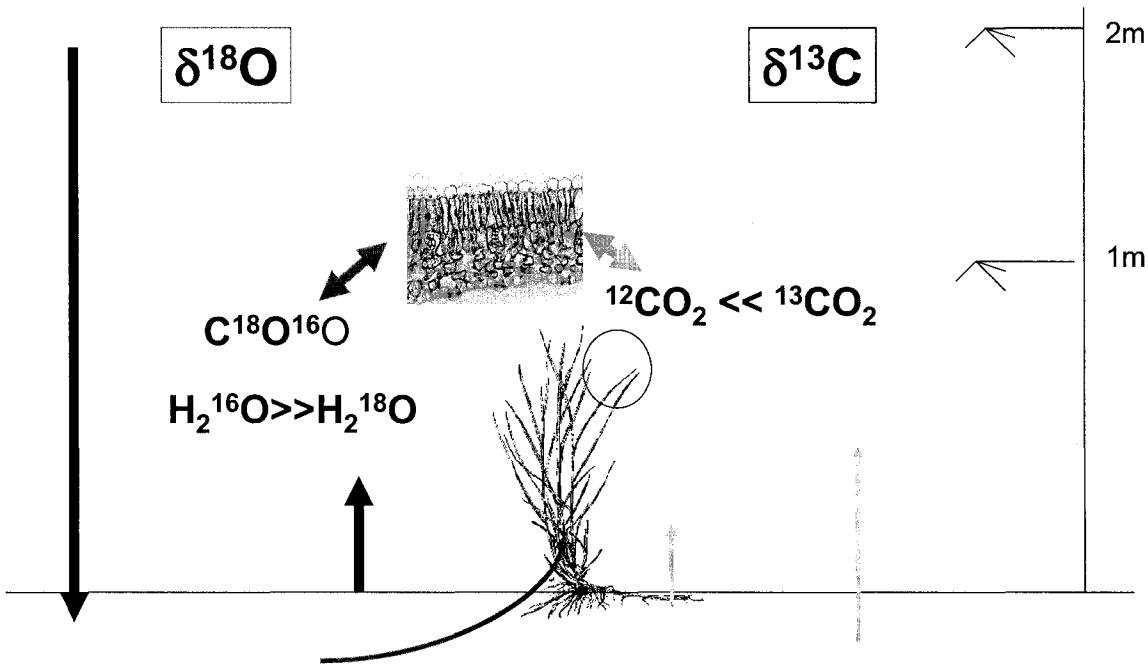

2) $\delta^{18}O_{SR} = \delta_{sw} + \varepsilon_{eq\text{-}CO2} + \varepsilon_{eff\text{-}soil}$

1) $H_2{}^{18}O_{(l)} + CO_{2(g)} \leftrightarrow\!> H^+ + [HCO_2{}^{18}O]^-_{(aq)} \leftrightarrow H_2O_{(l)} + CO^{18}O_{(g)}$

Fig.1.1. Isotopic composition of the major components including soil, plant and atmosphere. Yellow and blue colors represent ^{13}C and ^{18}O labeling, respectively. Root and soil respiration can have distinct ^{13}C signatures; leaf transpiration and soil evaporation have very different isotopic respiratory ^{18}O signals. Equation 1 represents the isotopic equilibration of CO_2 with soil water. $\delta^{18}O$ of CO_2 production by respiration is given by equation 2; where $\delta^{18}O_{SR}$ is the oxygen isotope of soil respiration, δ_{sw} is $\delta^{18}O$ of soil water, $\varepsilon_{eq\text{-}CO2}$ is the equilibrium fraction factor between the oxygen in CO_2 and water, and $\varepsilon_{eff\text{-}soil}$ is the effective kinetic fractionation.

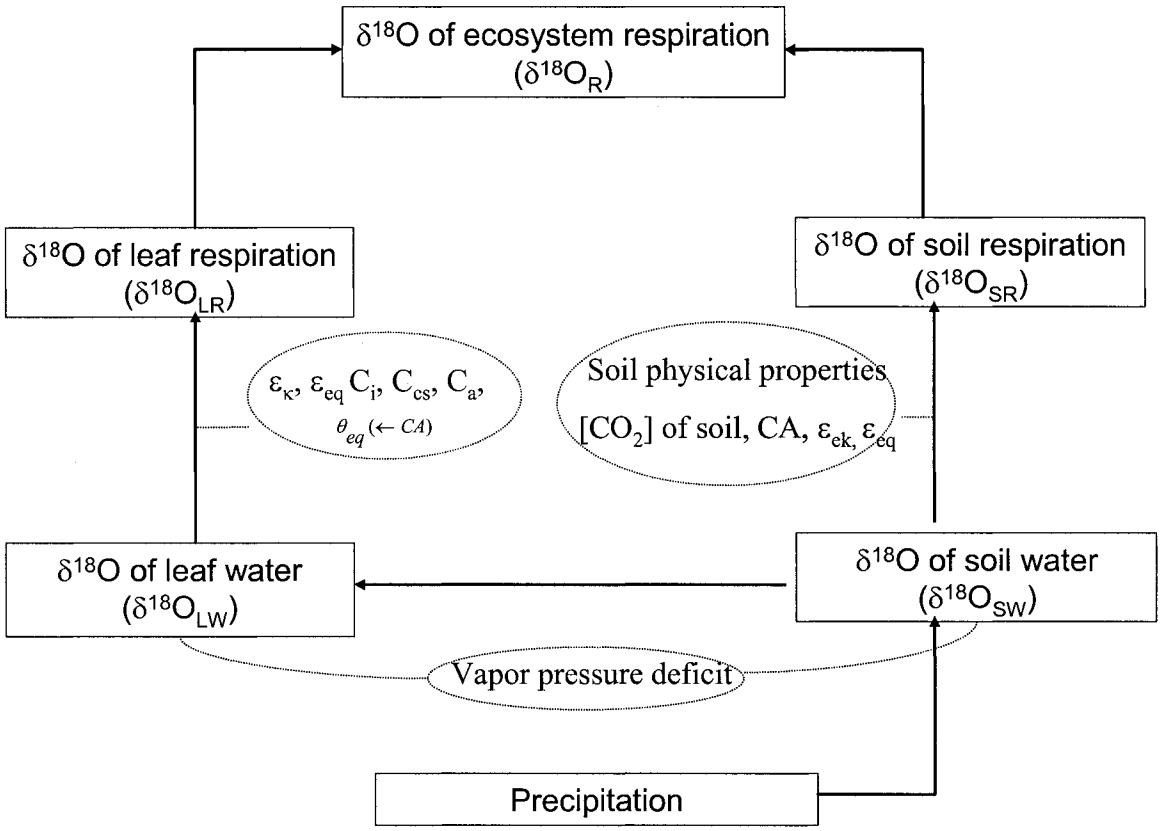

Fig.1.2. A conceptual diagram of eco-physiological drivers influencing $\delta^{18}O$ of respired CO_2 among soil, plants and atmosphere. Boxes represent oxygen isotope compositions of water pools (precipitation, soil and plant) and foliar and soil respiratory fluxes. Ovals represent controlling factors that influence each compartment.

2. Contributions of precipitation pulses and plant functional types to ^{13}C of ecosystem respiration in the Colorado shortgrass steppe

2.1 Abstract

We investigated pulse precipitation events and net CO_2 exchange in the shortgrass steppe to explain seasonal and interannual variability of $\delta^{13}C$ of ecosystem respiration ($\delta^{13}C_R$). We hypothesized that time lags between pulse precipitation events and antecedent moisture conditions interact to determine net CO_2 exchange and $\delta^{13}C_R$. Field measurements including near- surface atmospheric CO_2 flasks, plant and soil sampling, chamber-scale gas samplings, and micrometeorological measurements were conducted over two growing seasons 2000 and 2001. A maximum time lag between a rainfall event and a NEE response occurred after extended dry periods. The time lag was approximately two weeks. Stored photosynthate (C assimilated during the previous two weeks) may be emitted during respiration. There were significant intra-annual and interannual differences in the $\delta^{13}C$ of ecosystem respiration, which varied by as much as 5.2 ‰ and 7.1 ‰ over the 2000 and 2001 growing seasons, respectively. These variations in $\delta^{13}C_R$ were used as a tracer of C cycling, to evaluate how NEE responses to pulses of rainfall might transfer the $\delta^{13}C$ signal from recently assimilated carbon to ecosystem respiration. Both vegetation and NEE responses to the local precipitation regime explained much of the variations of $\delta^{13}C_R$. During moist conditions, labile substrates were respired, indicating an active C cycle, as reflected in significant differences in $\delta^{13}C$ of soil respired CO_2 among different plant community types. The $\delta^{13}C$ of soil respiration from C_3 plots was highly depleted in ^{13}C compared to C_4 and mixed C_3 and C_4 plots. However, labile

substrates are not utilized in microbial respiration under drought conditions. During dry periods, the main part of respiration comes from more stable material, which reduces the effect of recently assimilated root exudations of C_3 and C_4 plants on $\delta^{13}C$ of respired CO_2 from C_3 and mixed C_3 and C_4 plants. Therefore, the influence of plant community type (C_3 versus C_4) on $\delta^{13}C_R$ may not be visible in dry conditions.

2.2 Introduction

Understanding the factors controlling net ecosystem exchange (NEE) of carbon dioxide is necessary for explaining the size and the spatial distribution of the terrestrial carbon sink. To meet this need, large international networks of ecosystem studies have been organized (EUROFLUX, AMERIFLUX) to measure NEE both on short time scales and over long periods and to assess the environmental constraints on carbon exchange (Baldocchi et al. 2001). Incorporation of measurements of stable isotope composition of atmospheric CO_2 combined with micrometeorological measurements such as Bowen Ratio Energy Balance (BREB) or eddy covariance, and simulation and inverse models have tremendous potential to improve our understanding of the global carbon cycle (Fung et al. 1997; Keeling et al. 1995; Lloyd et al. 1996). They allow unique and additional ways of partitioning of NEE into photosynthesis and ecosystem respiration, and also land/ocean sink partitioning (Yakir and Wang 1996; Bowling et al. 1999; Ciais et al. 1995; Battle et al. 2000) since stable isotopes offer distinct labeling of flux components. Determining the ^{13}C variation in ecosystem-level gas exchange processes is critical since partitioning of anthropogenic CO_2 uptake between ocean and terrestrial biosphere is dependent on information from annual variations in atmospheric CO_2 concentration and

the $\delta^{13}C$ of atmospheric CO_2. In particular, $\delta^{13}C$ of ecosystem respiration ($\delta^{13}C_R$) is one of the key parameters in mass balance equation that are used to partition net ecosystem fluxes of CO_2 into their photosynthetic and respiratory fluxes and to assess the magnitude of the terrestrial carbon sink (Bowling et al. 1999; Yakir and Wang 1996; Fung et al. 1997; Randerson et al. 2002). Fixation of C sets the initial signal of $\delta^{13}C_R$, but ecosystem respiration comes from substrates ranging in age from hours to centuries. Measuring variations in $\delta^{13}C_R$ can give insight into the source and relative age of C released from terrestrial ecosystems.

Prediction of ^{13}C discrimination at the leaf level has been improved by mechanistic models that include the processes of enzymatic discrimination and diffusion linked to the ratio of internal to atmospheric CO_2 (C_i/C_a) (Farquhar et al. 1989; Ehleringer et al. 1993). C_3 plants discriminate more against ^{13}C than C_4 plants due to their high ratio of C_i/C_a and strong isotopic discrimination of ribulose bisphosphate carboxylase during photosynthesis (Farquhar et al. 1989). Intra-specific variation of ^{13}C discrimination often exists since C_i/C_a is tightly coupled to stomatal conductance, which varies in response to soil water availability (Lauteri et al. 1993), vapor pressure deficit (VPD) and sunlight (Berry et al. 1997). Dry conditions cause a reduction in stomatal conductance, a decline in C_i/C_a and hence enrichment in $\delta^{13}C$ of assimilated C (Farquhar et al. 1989; Ehleringer et al. 1993). On the other hand, water limitation in C_4 grasses may cause lower $\delta^{13}C$, which can be explained by increasing the leakage of CO_2 out of the bundle sheath cells (Tieszen and Boutton 1989; Buchmann et al. 1996). Higher leakage rates allow for greater discrimination, in other words, for more depletion of ^{13}C. Since leakage rates increase with aridity, ^{13}C discrimination in C_4 plants responds differently to drought than

in C_3 plants. Intra-specific variations in C_4 plants may also exist with soil water availability, salinity stress and sunlight (Bowman et al. 1989; Buchmann et al. 1996).

Scaling from leaf to canopy level, mechanistic understanding of the dominant environmental factors controlling upper level $\delta^{13}C_R$ is very important. Assuming no fractionation occurs during respiratory processes (Lin and Ehleringer 1997; but refer to Duranceau et al. 1999 and Ghashghaie et al. 2001), $\delta^{13}C_R$ provides an estimate of the decomposing plant and soil substrates that break down during decomposition and respiration. Temporally driven isotopic disequilibrium caused by different turn over rates of fast versus slow responding carbon pools is considered to be an important notion for investigating $\delta^{13}C_R$ dynamics. Recent researches have shown that factors that influence leaf level ^{13}C discrimination such as relative humidity and vapor pressure deficit (VPD) linked to canopy level of $\delta^{13}C_R$ in ecosystems where vegetation responses to recent meteorological events are rapid (Ekblad and Högberg 2001; Bowling et al. 2002). However, the response of VPD to $\delta^{13}C_R$ may not be immediate but rather may require lag time for transporting recently fixed C assimilates from leaf to respiring tissue, root exudation, microbial and root turnover, and fungal transport (McDowell et al. 2003). Humidity a few days prior to sampling has been shown to be a good indicator of carrying signals of recently fixed photosynthates to respired $\delta^{13}C$ (Bowling et al. 2002; Ekblad and Högberg 2001). The effect of time lagged VPD on $\delta^{13}C_R$ has been reported in C_3 dominated ecosystems where respiratory signals came from the bulk of respiratory tissues which were assimilated relatively recently and $\delta^{13}C_R$ was directly controlled by canopy scale discrimination. If conditions exist such that suppression of photosynthesis during prolonged drought and the opposite influences of VPD on ^{13}C discrimination by plant

functional groups occurred in mixed C_3 and C_4 ecosystems, then other mechanistic explanations are required to understand the variability of $\delta^{13}C_R$. Relationships between environmental parameters and $\delta^{13}C_R$ can be complicated in a mixed C_3 and C_4 ecosystems, which have variable periods of water availability (Sala et al. 1992) and activity of C_3 and C_4 plants. Co-existence of C_3 and C_4 plant species leads to more complicated interpretation of $\delta^{13}C$ of canopy uptake and respiration (Still et al. 2003) and to disagreement of modeled versus measured data (Bakwin et al. 1998).

Precipitation variables such as event size, timing and frequency have an important impact on ecosystem dynamics including nutrient cycling, net ecosystem productivity (Knapp and Smith 2001) and plant community composition (Epstein et al. 1999; Weltzin 2003). Pulse size plays an important role in regulating NEE of arid ecosystems through its differential effects on ecosystem respiration and photosynthesis (Huxman et al. 2004). The sensitivities of the processes may be dependent on precipitation amount, distribution of precipitation pulses both within and across seasons, and the response time differences of microbes and plants to wetting events. For example, the greatest net CO_2 uptake was observed in the middle of the rainy season, at peak leaf area index in a semiarid grassland and shrubland (Emmerich 2003) because aboveground biomass and LAI responses to precipitation are major determinants of net carbon exchange (Dugas et al. 1999; Frank and Dugas 2001). Near surface soil microbial communities may be highly stimulated by small rainfall events (Austin et al. 2004), while larger events are required to infiltrate to a depth where plants utilize water input and can trigger assimilation processes (Reynolds et al. 2004). Therefore, larger events and/or a series of small events are necessary for eliciting net C gain through autotrophic components (Huxman et al. 2004).

Due to differential response of precipitation pulses between assimilation and respiration processes, overall canopy scale response of net CO_2 exchange may require lag time to change a shift from source to sink, which may be dependent on the previous pulse rainfall history. Hunt et al. (2002) reported a 3 week time delay between major soil water recharge and the ecosystem NEE responses, changing from a carbon source to a small carbon sink in grassland. Understanding the effects of changes in pulse rainfall patterns of precipitation on ecosystem respiration is important and is useful in discerning substrate source of the respiration C exchange.

Even though grasslands comprise 32% of the earth's natural vegetation (Adams et al. 1990) studies on CO_2 exchange have not been initiated in these ecosystems until recently (Dugas et al. 1999; Frank and Dugas 2001; Sims and Bradford 2001; Suyker and Verma 2001; Suyker et al. 2003; Flanagan et al. 2002). In particular, few studies have investigated the partitioning of NEE and the associated changes in $\delta^{13}C$ of CO_2. What studies which are available have been carried out in forest ecosystems (Buchmann et al. 1997 a b; Bowling et al. 2002; McDowell et al. 2003).

Our first objective in this study was to investigate net ecosystem CO_2 exchange associated pulse precipitation events, and plant-soil C dynamics using $\delta^{13}C_R$ in short grass steppe. We hypothesized that time lags between pulse precipitation events and antecedent moisture conditions, and plant community dynamics would interact to determine net CO_2 exchange and $\delta^{13}C_R$. Our second objective was to investigate how $\delta^{13}C_R$ may be an indicator of certain environmental controls. Last, we sought to evaluate how $\delta^{13}C_R$ is a tracer for plant functional group (C_3 or C_4) activity during moist versus dry conditions. The times of strong C_3 or C_4 isotopic signal of respired CO_2 indicate that

more labile C is being respired from roots and microbes, and less older stable substrates are being decomposed. We hypothesized that the extent of which imprint C_3 and C_4 isotopic signal would be relatively well expressed during moist conditions in which both two species actively grow due to the large contribution of labile C to respiration.

2.3 Materials and methods

2.3.1 Site description

This study was conducted during the 2000 and 2001 growing seasons at the USDA-ARS Central Plains Experimental Range (CPER), in the shortgrass steppe region of north-eastern Colorado, 56 km north-east of Fort Collins, CO (lat. 40° 40′ N, long. 104° 45′ W). This site is also part of the Shortgrass Steppe Long Term Ecological Research site (Franklin et al. 1990). Vegetation of this region is dominated by warm-season, C_4 grasses (*Bouteloua gracilis* and *Buchloe dactyloides*), but also includes an abundance of cool-season, C_3 grasses (e.g. *Pascopyrum smithii* and *Stipa comata*), as well as a variety of C_3 forbs and woody vegetation. C_4 forbs and woody vegetation occur primarily in landscape positions with very deep sandy soils. Belowground production represents ~70% of net primary production (Milchunas and Lauenroth, 2001).

Long term (55 year) mean annual precipitation is 320mm, with the majority occurring during May, June and July. Mean air temperatures are 15.6 ^{0}C in summer and 0.6 ^{0}C in winter with maximum July temperatures averaging 30.6 ^{0}C (Lauenroth and Milchunas, 1991).

2.3.2 Plant Biomass

We estimated plant biomass by functional groups was measured by clipping 9 representative 0.25 m^2 quadrats about every month beginning in April through October from 2000 and 2001. Quadrats were located within 30 m of a Bowen ratio energy balance tower (Morgan et al. 1998). Green leaves, green stems, and dead material were oven dried and weighed to obtain total above ground live biomass.

2.3.3 Micro meteorological measurements and CO_2 flux observations

Ecosystem fluxes of CO_2 and relevant meteorological parameters were measured from a Bowen ratio energy balance tower (BREB) using an infra-red gas analyzer (Model LI-6262, LiCor, Inc., Lincoln, NE, USA). The calculations assume the same turbulent transfer coefficient for heat, water vapor, and CO_2. Fluxes were calculated at 20-minute intervals, using methods described by Dugas (1993) and Dugas et al. (1999). Temperature gradients were obtained at the two heights (1 and 2m) above the canopy from fine wire chromel-constantan thermocouples. Ancillary measurements of net radiation and soil heat flux were also taken. Micrometeorological data were stored on a 21X data logger (Campbell Scientific, Inc., Logan, UT, USA). Soil temperatures were measured at 2cm and 6cm depths and were averaged across 4 sensors. Volumetric soil water was measured with soil moisture probe connected with BREB data logger (Campbell Scientific, CS615) at an averaged depth of 0-15 cm corrected to specific soil type. The CO_2 flux was calculated from the following:

$$CO_2 flux = K_c \frac{\Delta \rho_c}{\Delta z} \qquad (2.1)$$

where $\Delta\rho_c$ is the gradient of CO_2 density (g m^{-3}) and Δz is height difference of sensors (m). K_c is the turbulent diffusivity for carbon dioxide (assuming $K_c = K_h$, where K_h is the turbulent diffusivity for sensible heat, m^2 s^{-1}). The CO_2 flux was corrected for temperature and vapor density differences at the two heights (Webb et al. 1980).

2.3.4 Ecosystem scale flask measurements

We observed diurnal and seasonal changes of CO_2, and associated $\delta^{13}C$ values from air flasks above the canopy at 1 and 2m heights, to estimate changes in the activities of C_3 and C_4 plants during the 2000 and 2001 growing seasons. Atmospheric flasks were collected over 15 to 30-minute periods from two heights simultaneously. All flask samples were dried prior to collection using magnesium perchlorate traps to avoid contamination of the $\delta^{18}O$ values. Flasks were analyzed for CO_2 using the high-precision non-dispersive infrared gas analysis system used for the NOAA global flasks (Conway et al. 1994) and analyzed for ^{13}C using a Micromass Optima mass spectrometer at the stable isotope laboratory at the University of Colorado at Boulder (Trolier et al. 1996). We used a simple mixing model developed by Keeling (1958, 1961) to calculate the $\delta^{13}C_R$. Estimates of $\delta^{13}C_R$ were obtained from the y-intercept of the geometric mean linear regression (Sokal and Rohlf 1981) between $\delta^{13}C_R$ and inverse CO_2 concentrations. Uncertainties were reported as the standard error of the intercept.

2.3.5 Small scale chamber measurements

We collected chamber scale measurements in 2001 to investigate the contribution of different ecosystem components to the total $\delta^{13}C$ of ecosystem respiration. We

established 2 blocks to account for possible water gradients in the field. Each block had three randomized sets of sampling locations. Within a set, closed chambers (10cm in height, 10cm in diameter) were placed on four different native grass community treatments, including plots for the C_3 species *Pascopyrum. smithii*, C_4 species *Bouteloua. gracilis*, mixed C_3 and C_4 species and bareground. These plots were established approximately one month prior to experiments to minimize site disturbance. At each site, we placed four spatially distributed chamber rings for each of the 4 community treatments, giving a total of 24 sampling locations. They were located about 30 m from the site of flask collections for $\delta^{13}C_R$. For CO_2 fluxes, we sampled from headspace of each community with a syringe (20ml) and then injected into pre-evacuated tubes at 0, 15, and 30 min after chamber closure. To avoid any pressure decline in the soil chamber during air collections, a sterile sample hang-up bag was placed on an inlet open to atmospheric pressure. As the sample was being collected into the pre-evacuated flasks, atmospheric air was filling the bag, thus maintaining constant pressure inside the soil chamber. CO_2 concentrations were measured with gas chromatograph. Air sampling was performed in 8 hour intervals (around noon (D), midnight (N) and early morning on second day (E) each diurnal set in May, June and July 2001. Due to a violent storm in September, only daytime sampling was possible.

Chamber air sampling was conducted on only one block for stable isotope analysis upon completion of the above procedure. Magnesium perchlorate trap was installed in front of the syringe to dry the air. The samples were also analyzed for CO_2 concentrations and isotope ratios to calculate Keeling plot intercepts with a geometric mean regression. Keeling plots were used to estimate $\delta^{13}C$ of respired CO_2 of each

treatment such as C_3 ($\delta^{13}C_{R\text{-}C3}$), C_4 ($\delta^{13}C_{R\text{-}C4}$), mixed C_3-C_4 grass communities ($\delta^{13}C_{R\text{-}M}$) and bare ground ($\delta^{13}C_{R\text{-}B}$). Data were pooled from all three chambers to generate a single Keeling plot for each set.

2.3.6 $\delta^{13}C$ of leaf materials and soil organic matter in several depths

Leaf samples were collected from the dominant vegetation at the study site at the end of each air sampling collection in 2000. Samples were collected separately for C_3 and C_4 plants in each of the two blocks at the end of each diurnal set in 2001.The leaf samples were dried for 48 h at 70°C then ground with mortar and pestle to a fine powder. Standards were run every ten samples. The standard deviation of the analysis was always below 0.1‰. A 2 mg sub-sample was combusted and analyzed for $^{13}C/^{12}C$ using an isotope ratio mass spectrometer.

We collected soil samples and visible root material removed at several depths from one pit and then repeatedly over the growing season of 2000. Soil samples were collected from each block (one pit per block) for repeated measurements of ^{13}C of soil organic matter in 2001. Soil organic matter samples were analyzed by elemental analysis-mass spectrometry for $\delta^{13}C$ values.

$\delta^{13}C$ values are expressed in parts per thousand differences from the standard using the equation:

$$\delta^{13}C = [(^{13}C/^{12}C_{sample} - {}^{13}C/^{12}C_{standard})/(^{13}C/^{12}Cstandard)]\cdot 1000 \qquad (2.2)$$

2.3.7 Estimates of contributions of 'Old' versus 'New' C substrates used for soil respiration from C_3 and C_4 patches

We estimated relative contributions of old versus new carbon substrates to C_3 and C_4 respiration chambers as follows:

$$\delta^{13}C_{CR} = f * \delta^{13}C_{new\text{-}i} + (1\text{-}f)* \delta^{13}C_{old} \quad (2.3)$$

where $\delta^{13}C_{CR}$ represents Keeling plot intercepts from each chamber; i represents each chamber component such as C_3,and C_4 patches; $\delta^{13}C_{new\text{-}i}$ was assumed to be -26 ‰ and -15 ‰ for C_3 and C_4 , respectively; y intercepts derived from Keeling plots in bareground patches were used for $\delta^{13}C_{old.}$ We averaged three times of day to generate a single value for each vegetation type on a monthly basis.

2.3.8 Comparison of net flux of $^{13}CO_2$ added to the atmosphere by ecosystem respiration with that of $^{13}CO_2$ added to the headspace from chambers via soil and plant respirations

We compared local-scale (up to 200 m; based on a 100:1 fetch/height-above-surface ratio established by Rosenberg et al. (1983)) flask results with observations from chambers (up to 10 m) to assess if plant community dynamics could reflect the net flux of $^{13}CO_2$ at the local scale. The net flux of $^{13}CO_2$ added to the atmosphere by ecosystem respiration was calculated by multiplying nocturnal $^{13}C_R$ and averaged CO_2 flux (measured from BREB) during flasks sampling. For the net flux of $^{13}CO_2$ added to the headspace from each chamber, we multiplied each $\delta^{13}C$ of respired CO_2 including $\delta^{13}C_{R\text{-}C3}$, $\delta^{13}C_{R\text{-}C4}$ and $\delta^{13}C_{R\text{-}B}$ by each CO_2 flux measured by gas chromatography. We defined D_i as the difference between two net fluxes of $^{13}CO_2$ from ecosystem respiration and from respired CO_2 of each vegetation type (eq. 2.3).

$$D_i = |\delta^{13}C_{R\text{-}i} * F_i - \delta^{13}C_R F_R| \quad (2.4)$$

Where i represents each chamber including C_3, C_4 and bareground patches; Fi is CO_2 flux from headspace of each chamber measured by gas chromatography; F_R is averaged nocturnal CO_2 flux calculated from BREB.

Ci is the contribution of the net flux of $^{13}CO_2$ from each respiration chamber to that from total ecosystem respiration.

$$Ci = \frac{(\sum_{i=1}^{3}(D_i)^2) - (D_i)^2}{(n-1)\sum_{i=1}^{3}(D_i)^2} \quad (2.5)$$

2.3.9 Statistical analysis

We tested for differences in CO_2 fluxes from chambers using the PROC MIXED procedure (SAS version 8.0) for a design with fixed effects of block, treatment, month and time of day. Random effects were location (block), treatment * location (block), treatment*month* location (block) and residual. Block was considered as a fixed effect since the blocks encompassed a soil gradient. We performed the PROC MIXED procedure where both month and time of day were repeated measurements. Since isotopic analyses for $\delta^{13}C$ of respired CO_2 from chambers were conducted on only one site, we tested for differences in $\delta^{13}C$ of respired CO_2 from chambers using the PROC MIXED procedure for a design with fixed effects of treatment, month and time of day. Random effects were location, treatment * location, treatment * month * location and residual. For

each vegetation type, data were pooled from three replicates to generate a single y-intercept derived from Keeling plots; there was a significant time of day effect, but no time of day by treatment interaction as expressed under each D column in Table 2.2.

We conducted linear regression analyses to test if any environmental variables were coupled with $\delta^{13}C_R$ and $\delta^{13}C_{R\text{-}C3,\ C4,\ M,\ B}$ over a range of time lags, which were similar to what is described by Bowling et al. (2002) and McDowell (2003). We calculated averages of a given independent factor from one to five days and shifted these averages back in time by zero to 16 days for $\delta^{13}C_R$ and to 8days for $\delta^{13}C_{R\text{-}C3,\ C4,\ M,\ B}$. The variables expected to influence the $\delta^{13}C_R$ included vapor pressure deficit (VPD), air temperature (Tair), soil temperature (Tsoil), photosynthetically active radiation (PAR), soil water content and net ecosystem exchange of CO_2 (NEE).

2.4 Results

2.4.1 Environmental conditions

Daily mean air and soil temperatures during sampling periods in 2000 were relatively higher than during those days in 2001 (Fig.2.1). Generally, the effect of precipitation events on air and soil temperatures declined toward mid-late growing season. Frequent precipitation events during the early growing season in 2001 led to cooler air/soil temperatures compared to 2000. Reduction in air/soil temperatures during the mid-late growing season of 2001 was greater than in 2000 due to more frequent precipitation events in 2001.

2.4.2 Dynamics of net CO_2 exchange and water availability

Mean annual precipitation was similar in 2000 and 2001 (311mm and 348mm, respectively), but the structure of the precipitation regime was different between the two years (Fig.2.2). In 2000, conditions were very dry until a large precipitation event (>25mm) occurred in August 2000. More frequent precipitation events including small (<10mm) and middle (10mm<25mm) sized events occurred in 2001, especially in the early part of the growing season. A single middle size precipitation event one day before sampling in June 2001 resulted in a low VPD (0.49kPa) on DOY 171. In 2000, early season soil moisture generally decreased through July despite small fluctuations triggered by several rainfall events (>7mm). A large precipitation event in August increased soil moisture, which then gradually declined toward late growing season of 2000. In 2001, ample early season precipitation led to relatively moist soil environments until August, then changed to drier conditions in the late growing season. The response of soil moisture to precipitation events was dependent on the intensity of precipitation and history of water conditions (Fig. 2.1 (c) and Fig.2.2). With large water inputs, we observed abrupt increases in soil moisture. However, little fluctuation in soil moisture was triggered by several intermittent small events (less than 4-5 mm). In general, 2000 had higher VPD values than were observed in 2001 from mid-May through July.

CO_2 uptake was generally lower during most days in 2000 than in 2001. Exceptions to this included greater CO_2 uptake occurring in mid July though early August and late August through mid September in 2000. The largest amount of precipitation occurred in mid August, which may account for the large CO_2 uptake in late growing

season of 2000 compared to 2001. We observed pulses of CO_2 efflux from the shortgrass steppe ecosystem following precipitation pulses.

To evaluate precipitation effects on C cycling, we assigned ≥ 5 mm precipitation events and/or cumulative ≥ 5 mm following a series of small water inputs for the minimum influential pulse event to net C gain. The maximum time lag for NEE to switch from a source to a sink following a significant rainfall pulse was 13 days in 2000 compared to 5 for 2001 (Fig.2.2).

Prolonged dry conditions in 2000 may have caused a delay in photosynthetic response to the rainfall events. Even if occasional rainfall contributed to switch the sign of NEE from positive to negative (CO_2 uptake), overall the CO_2 uptake following rainfall events was limited and only attained about ~-1.0g C m^{-2} d^{-1}, at most, during prolonged dry conditions in 2000.

In 2001, CO_2 uptake began approximately three days after a series of consecutive rainy days during the early growing season. We measured maximum daily CO_2 uptake of –5.5 g C m^{-2} d^{-1} in mid June 2001 following large and frequent precipitation events. Values of CO_2 uptake were reduced to near zero and the ecosystem became a CO_2 source during 6-13th July and mid August in 2001. Then a release of CO_2 to the atmosphere followed the precipitation events; 1-2 days were required for the net ecosystem exchange to respond to water additions in 2001.

2.4.3 Plant biomass survey classified by functional group

In 2000, C_3 aboveground biomass averaged 10.2 ± 3.4 (g m^{-2}) and C_4 biomass averaged 23.7 ± 6.4 (g m^{-2}). In 2001, C_3 and C_4 biomass averaged 32.0 ± 19.2 (g m^{-2})

and 29.2 ± 16.2 (g m^{-2}), respectively (Fig.2.3). Aboveground plant biomass in 2000 was generally lower than in 2001, but following one large precipitation event in August, biomass increased by 61% compared to the previous month. Ample spring rains in 2001 led to increased productivity of plant biomass, which reached a maximum of 123.9 g m^{-2} in late May, persisted through June and then gradually decreased towards mid-late growing season. Greater C_4 plant live biomass was consistently observed in the drier 2000 compared to C_3 plant live biomass by 1.6 to 3.1 times. The cooler wetter conditions of 2001 favored C_3 production and C_3 live biomass was greater throughout the growing season until C_4 plants became active in the late growing season (Fig.2.3); these trends were opposite to those normally shown in this shortgrass ecosystem. As cumulative precipitation 6 weeks prior to sampling increased, the ratio of C_3 to C_4 biomass increased (Fig.2.4).

2.4.4 Diurnal and seasonal changes in CO_2 flux from chambers installed on patch scale

We conducted chamber measurements of CO_2 respiration on C_3, C_4, and mixed C_3 and C_4, and bare ground patches during the growing season of 2001. No significant block effect on CO_2 flux was observed for whole data set (PROC MIXED, $F = 0.6$, $p = 0.48$). Differences among monthly averaged CO_2 fluxes were significant (PROC MIXED, $F=31.08$, $p < 0.01$) (Table 2.1). CO_2 fluxes averaged across four chambers were 67.1, 128.4, 43.9 and 35.9 (mg CO_2-C m^{-2} hr^{-1}) in May, June, July and September, respectively. Variations in CO_2 flux can also be explained by aboveground plant live biomass variability as we observed (Fig.2.3). More CO_2 was produced during daylight periods than during midnight and dawn (PROC MIXED, $F = 18.67$, $p < 0.01$). The diurnal

differences in CO_2 respiration disappeared in July. Respired CO_2 from bareground was generally significantly lower than from vegetated patches during daylight measurements. Differences between non-vegetated versus vegetated chambers were greater during early growing season than during late growing season. The spatial difference in CO_2 respiration disappeared in September.

2.4.5 Seasonal variations in $\delta^{13}C_R$, and of leaf and soil organic materials

There were significant intra-annual and interannual differences in the $\delta^{13}C$ of ecosystem respiration (Fig.2.5a). The $\delta^{13}C_R$ values were about -15‰ in early summer and decreased by as much as 5.21‰ and 7.13 ‰ through the growing seasons of 2000 and 2001, respectively. In general, more negative $\delta^{13}C_R$ values were observed during the wetter growing season of 2001.

A similar interannual variation was noticed in C_3 leaf tissue and in SOC in the top soil layer (1cm) (Fig.2.5b and c, respectively). The C_3 foliage carbon isotope ratios changed significantly over two consecutive years (ANOVA, $F = 7.79$, $P = 0.04$) with higher $\delta^{13}C$ values in the dry 2000 growing season than in 2001. The C_3 plants showed variations within the season with more ^{13}C depleted in early growing seasons than in late growing season (ANOVA, $F = 17.75$, $p < 0.01$). However, C_4 plant leaf materials did not change significantly between and within years (ANOVA, $F= 0.31$, $P = 0.6$). Isotopic composition of the SOC (top 1cm) was more depleted in ^{13}C in 2001 than 2000 (ANOVA, $F = 6.30$, $P = 0.04$).

We also observed a consistent increase in the ^{13}C of soil organic carbon with an increase in soil depth (Natelhoffer and Fry 1988; Balesdent et al. 1993). It probably

reflects more depleted atmospheric $\delta^{13}C$ from fossil fuel (Friedli et al. 1987), and enrichment of microbial and fungal products at depth (Ehleringer et al. 2000)

2.4.6 Seasonal variations in $\delta^{13}C$ of respired CO_2 from C_3, C_4, mixed C_3 and C_4 plant communities and bareground plot ($\delta^{13}C_{R\text{-}c3}$, $\delta^{13}C_{R\text{-}c4}$, $\delta^{13}C_{R\text{-}M}$, and $\delta^{13}C_{R\text{-}B}$)

No significant differences between $\delta^{13}C_{R\text{-}C3,\ C4,\ M,\ B}$ or times were shown in May 2001 (Table 2.2) even though high CO_2 respiration was shown in C_3 plots (Table 2.1). Significant differences among different plant community types became visible in June 2001, when $\delta^{13}C$ of soil respiration from C_3 plots was highly depleted in ^{13}C compared to C_4 and mixed C_3 and C_4 plots indicating a large proportion of root respiration. Mixed C_3 and C_4 plots almost always had $\delta^{13}C$ values intermediate between C_3 and C_4 plots. Bareground plots had $\delta^{13}C$ values that tended to be more similar to C_3 plots. However, there were no significant differences between C_3 and mixed C_3 and C_4 plots in July. Interestingly, the most depleted ^{13}C of soil respiration was found in bare ground plots in July for day and early morning measurements. ^{13}C of soil respiration was generally more depleted during daylight than during nighttime measurements in June and July.

2.4.7. Contributions of 'Old' versus 'New' C substrates to ^{13}C of soil respiration in C_3 and C_4 patches

In C_3 patches, approximately half of soil respiration came from new C substrates in May, diminished to 19% in June and almost zero in July (Table 2.3). In C_4 patches, highest new C contribution to soil respiration was shown in June and nearly zero percent contribution was calculated in May.

2.4.8 Contributions of each ecosystem component to total ecosystem respiration

The relative contribution of C_3 and C_4 plant communities in 2001 to the isotopic composition of ecosystem respiration generally followed seasonal trends of C_3/C_4 biomass (Table 2.4 and Fig.2.3). Consistently higher contributions of C_3 patches to the ecosystem level of net flux of $^{13}CO_2$ continued through July then the contribution of C_4 patches increased to parity with the C_3 patches in September. Interestingly, August and September were the only months in 2001 when C_4 biomass contribution was similar to C_3. The respired ^{13}C of CO_2 in bareground patches was close to C_3 patches (Table 2.2), but, since they had low CO_2 fluxes, their contributions were low compared to vegetated patches.

2.4.9 Correlations of $\delta^{13}C_R$ with environmental variables and seasonal variations in plant aboveground production separated by C_3 versus C_4 plants

The strongest correlations between $\delta^{13}C_R$ and environmental variables were with air and soil temperature (Table 2.5). Weaker correlations were found with VPD, soil moisture and precipitation; however, the negative correlations with VPD and soil moisture were opposite to expectations. The $\delta^{13}C_R$ showed marginal correlation with NEE. There was a correlation between $\delta^{13}C_R$ and precipitation for the previous 6 weeks over two consecutive growing seasons.

When negative NEE (CO_2 uptake) was already occurring due to prior precipitation, $\delta^{13}C_R$ was correlated with C_3 biomass in the same month. If NEE was positive, $\delta^{13}C_R$ was correlated with previous month's C_3 biomass (R^2=0.73; Fig.2.6).

2.4.10 Correlations of $\delta^{13}C_{R\text{-}C3,\,C4,\,M}$, and $_B$ with environmental variables

For C_3 plots, significant positive relationships occurred between $\delta^{13}C$ of respired CO_2 ($\delta^{13}C_{R\text{-}C3}$) and environmental variables such as VPD, air/soil temperatures, NEE and PAR with lagged days ranging from two to eight days (Table 2.5). For C_4 plots, $\delta^{13}C$ of respired CO_2 ($\delta^{13}C_{R\text{-}C4}$) had negative relations with VPD, soil temperature and PAR

The response of respired $\delta^{13}C$ in C_3 chambers to VPD was opposite to that of C_4 chambers. We found that high $\delta^{13}C$ occurred in C_3 patches in connection with low air RH and high VPD, a condition causing plant water stress and stomatal closure.

2.5 Discussions

Stable isotopes has been useful to understand global C distributions (Fung et al. 1997; Keeling et al. 1995; Lloyd et al. 1996), partition net ecosystem exchange into gross photosynthesis and respiration (Yakir and Wang 1996; Bowling et al. 1999), quantify the impact of land use changes on ecosystem exchange (Lloyd and Farquhar 1994; Miranda et al. 1997) and study contributions of different ages of soil carbon to soil respiration (Trumbore et al. 1996). Few studies have investigated isotope biogeochemistry in temperate semi-arid ecosystems. We need to first better understand the source of variations of the isotopes then to determine the ^{13}C variation in ecosystem-level gas exchange processes in this ecosystem for the better understanding of global carbon cycle and plant-soil C dynamics.

2.5.1 The influence of pulse precipitation associated with plant species composition on seasonal variations in $\delta^{13}C$ of ecosystem respiration

We found that $\delta^{13}C$ of carbon stocks such as leaves and soil organic matter were poor predictors of $\delta^{13}C$ of carbon fluxes in the short grass steppe for our period of study. The intercepts of nighttime Keeling plots, indicating $\delta^{13}C_R$, showed strong seasonal variations, in contrast to $\delta^{13}C$ of plant leaf materials (C_3 or C_4) and soil organic matter (Fig.2.4).The mean $\delta^{13}C_{R-B}$ was approximately 3-4‰ more depleted than the $\delta^{13}C$ of soil organic matter at a 1cm soil depth. Discrepancies between the two isotopic compositions ($\delta^{13}C$ of soil organic matter and of soil respiratory flux) have been commonly reported in C_3 and C_4 ecosystems (Buchmann and Ehleringer 1998; Ehleringer et al. 2000). This likely occurs because soil organic matter reflects the longer term discrimination of decomposition against the heavier isotope.

If we assume no fractionation occurs during dark respiration and microbial respiration (Lin and Ehleringer 1997), $\delta^{13}C_R$ should be flux weighted by autotrophic and heterotropic respiration. Provided root respiration contributes over 40-70% to ecosystem respiration as suggested by Milchunas and Lauenroth (2001) and Pendall et al. (2003), variations in $\delta^{13}C_R$ can be explained to some degree by recently fixed carbon substrates. However, duration over which newly fixed photosynthate is transferred to $\delta^{13}C_R$ is dependent on local precipitation regime and the intensity of soil water stress. If water is not limiting, plant C allocation, root exudates and root turnover may be detected in a few days after C assimilation occurs (Bowling et al. 2002). However, in our ecosystem, the detecting of $\delta^{13}C$ signatures of recently fixed C assimilates to $\delta^{13}C_R$ was not immediate, but lagged by approximately two weeks, especially during prolonged water stress.

Consequently, no positive correlations were found between $\delta^{13}C_R$ and VPD over a range of time lags.

Plant community composition may also contribute to the $\delta^{13}C$ of respired CO_2, and this can shift in response to growing season rainfall patterns in grasslands (Kuchler 1974; Epstein et al. 1999). The C_3 grasses are more competitive during moist, mild springs and dry summers; on the other hand, in years with dry springs and wet summers, C_4 species are favored (Monson et al. 1983). In 2000, reduced summer precipitation and summer heating might have inhibited C_4 grass activity because of their shallower rooting depth; however, the ratios of C_3/C_4 were lower compared to 2001, possibly due to an extremely dry spring which occurred in 2000. A relatively wet spring allowed for superior growth of C_3 species during 2001 resulting in high value of C_3/C_4 until September. At the ecosystem scale, in order to evaluate the duration or lag of recent photosynthate transfer to an ecosystem respiration $\delta^{13}C$ signal via autotrophic respiration, the vegetation response to pulses of rainfall in terms of NEE dynamics might be useful.

NEE is the ecosystem scale balance of photosynthetic assimilation and respiration. Canopy averaged stomatal conductance regulates both ecosystem photosynthetic assimilation and canopy scale carbon discrimination. Since $\delta^{13}C_R$ is the function of carbon isotope signature of atmospheric CO_2 and carbon isotope discrimination (Buchmann et al. 1998; Brugnoli et al. 1988), NEE should be linked to $\delta^{13}C_R$ to some extent. There was a time delay of about 3 weeks between major soil water recharge and changes in net carbon uptake relative to carbon release in grassland (Hunt et al. 2002). Understanding these effects of changes in pulse precipitation patterns on ecosystems C dynamics, especially related to $\delta^{13}C_R$ may be very informative. Since maximum time

lagged NEE response to precipitation input for a transition from C source to C sink took almost two weeks for dry periods, relatively old photosynthetic assimilates (at least two weeks old) seem to be respired due to low and little new C assimilation.

Where negative NEE (i.e., CO_2 uptake) is already established and soil moisture availability is high, we correlated $\delta^{13}C_R$ with C_3 biomass measured in the corresponding flasks sampling. If the ecosystem did not respond rapidly to a shift from drought to moist conditions following previous very small events or long duration between pulse events, we correlated $\delta^{13}C_R$ with C_3 biomass measured approximately one month prior to sampling periods resulting in high regression coefficient ($R^2 = 0.73$). The transfer of the recently fixed C compounds can be detected as $\delta^{13}C_R$ relatively rapid following large pulse size and frequent pulse events. However, occasional small pulses during severely dry conditions may not be readily associated with net C assimilation as indicated by changes in $\delta^{13}C_R$. The new C assimilates do not appear to be reflected in the $\delta^{13}C_R$ even though improved water status may have occurred, increasing their capacity to respond to larger events (Yan et al. 2000). In linear regression analyses, a correlation between $\delta^{13}C_R$ and 6 weeks lagged cumulative precipitation was observed, indicating a lagged vegetation response to rainfall pulses and the ^{13}C signature of newly assimilated C in the of $\delta^{13}C_R$ signal.

2.5.2 The contribution of plant functional groups to $\delta^{13}C$ values of CO_2 from respiration chambers

In May, no difference was observed between C_3 and C_4 patches, probably because C_4 uptake had not yet started in the cool, early growing season (Ode et al. 1980).

During moist conditions in June, the isotopic composition of CO_2 respired from C_3, C_4, mixed and bareground patches closely reflected the plant community composition; the $\delta^{13}C$ of soil respiration from C_3 plots was highly depleted in ^{13}C compared to C_4 and mixed C_3 and C_4 plots. Mixed C_3 and C_4 plots almost always had $\delta^{13}C$ values intermediate between C_3 and C_4 plots. The explicit different enzymatic discrimination against ^{13}C by functional type overshadowed insignificant differences in CO_2 fluxes in June when water availability was relatively high and VPD was low from previous frequent rainfall. The clear plant community effect could be explained by an important participation in respiration of recent assimilates.

However, the distinct effect of C_3 and mixed C_3 and C_4 plots on respired ^{13}C signature shown in June disappeared in July. Under dry conditions, $\delta^{13}C$ of respired CO_2 from mixed C_3 and C_4 plots were closer to C_3 chambers than C_4 chambers. Dry condition reduced stomatal conductance, ci/ca and thus enrichment in $\delta^{13}C$ of assimilates in C_3 plants (Farquhar et al. 1989; Ehleringer et al. 1993). On the other hand, $\delta^{13}C$ of plant materials is more depleted in C_4 plants because of increasing the leakage out of the bundle sheath cells allowing for greater discrimination by Rubisco, by passing PEP-carboxylase (Buchmann et al. 1996). Interestingly, the effect of VPD on $\delta^{13}C$ of respired CO_2 from C_3 plots was different from C_4 plots (Table 2.5). With high VPD, C_3 plots had more enriched $\delta^{13}C_{CR\text{-}C3}$ and C_4 plots showed more depleted $\delta^{13}C_{CR\text{-}C4}$ as expected. The magnitude of changes in $\delta^{13}C$ values by plant functional type is not certain. The differential plant community response to high VPD may be influencing the $\delta^{13}C_{CR}$ resulting in the $\delta^{13}C_{CR}$ to become more similar during dry conditions.

Another potential explanation is that when short grass steppe goes from good soil moisture to dry conditions, leaf gas exchange of *B. gracilis* may be affected first due to its shallow rooting depth and its sensitivity to water (Morgan et al. 1998; LeCain et al. 2003: Nelson et al. 2003). This may contribute to the mixed C_3/C_4 patches looking more like C_3 patches under prolonged dry conditions.

2.5.3 Contributions of 'Old' versus 'New' C substrates to ^{13}C of soil respiration in C_3 and C_4 patches

We observed no differences in CO_2 respiration rates between vegetated and non-vegetated chambers during prolonged dry conditions. Autotrophic respiration cannot be strictly separated from decomposition through comparison of non-vegetated chambers with vegetated chambers because roots are also included in bareground chambers. However, estimates of relative contributions of 'old' versus 'new' carbon substrates are feasible, depending on how we define the two components and a possibility of acquiring two representative isotopic end members to construct a two mixing model. We assumed bare ground patch be representative for old carbon component at least 3-4 years long and $\delta^{13}C$ of plant leaf materials for new carbon substrates used for respiration. In C_3 chambers, recently assimilated C seems to be readily distinguished in the soil respiration measurements, during relatively moist and cool conditions and became no apparent during extended dry conditions, even after a brief rainfall (Table 2.3). Labile substrates in C_3 patches may not be available for respiration under severe dry conditions, especially in the daylight period of July; therefore, the main part of respiration probably comes from more stable soil organic material with little ^{13}C signal associated with recently C

assimilates in July. Potential shifts in the relative magnitude of root respiration and soil organic matter decomposition were also observed by Hesterberg and Siegenthaler (1991). However, in C_4 patches, recently assimilated C from C_4 plots imprinted $\delta^{13}C$ of respired CO_2 clearly after a rainfall pulse (occurred between daytime and nighttime sampling) even in dry periods of July 2001 and its contribution was less apparent in another 6 hours (Table 2.2). Pulse rainfall appears to stimulate microbial growth and lead to a pulse of root respiration in a few hours. In May, C_4 photosynthesis had likely not been initiated. Nearby C_3 roots or SOM must have contributed to low $\delta^{13}C_{CR}$

2.5.4 The contribution of flux weighted ecosystem components to $\delta^{13}C_R$

If water availability is favorable enough to influence the contribution of plant functional type to $\delta^{13}C_R$, $\delta^{13}C_R$ should reflect flux-weighted ^{13}C signatures from different plant communities and soil components. The relative contribution of C dynamics associated with plant functional type (C_3 versus C_4 plants) is estimated as a distance (D), and corresponded to seasonal trends in C_3/C_4 biomass. This indicates that new C inputs from C_3 and C_4 plants can be readily observed in soil respiration. The influence of plant type on ecosystem scale net flux $^{13}CO_2$ is dependent on the moisture regime. In year 2001, a relatively moist year in early growing season expressed a strong C_3 grass contribution to $\delta^{13}C_R$. As we expected, when water availability is favorable enough to reveal the contribution of plant functional type to $\delta^{13}C_R$, then $\delta^{13}C_R$ reflected flux-weighted ^{13}C signatures from different plant community and soil components. This implies flux weighted plant productivity could be applicable to the study regarding dynamics of $\delta^{13}C$ of ecosystem respiration during moist conditions.

2.6 Conclusions

These variations in $\delta^{13}C_R$ were used as a tracer of C cycling, to evaluate how NEE responses to pulses of rainfall might transfer the $\delta^{13}C$ signal from recently assimilated carbon to ecosystem respiration. The response of NEE from pulse precipitation events was not immediate and it took almost two weeks to shift from C source to C sink in dry season. Considerations of NEE dynamics responding to local precipitation events and plant community composition made fairly good agreement in variations of $\delta^{13}C_R$.

During moist conditions, labile substrates were respired, indicating an active C cycle, as reflected in significant differences in $\delta^{13}C$ of soil respired CO_2 among different plant community types. However, labile substrates are not utilized in microbial respiration under drought conditions, as expressed in no apparent effect of recently assimilated root exudations of C_3 and C_4 plants on $\delta^{13}C$ of respired CO_2 from C_3 and mixed C_3 and C_4 plants.

Flux-weighted ^{13}C of respiration from plant functional groups and bareground patches can explain relative contributions of each component to total net flux of $^{13}CO_2$ at ecosystem level during relatively moist conditions.

References

Adams JM, Faure H, Faure-Denard L, McGlade JM, Woodward FI (1990) Increases in terrestrial carbon storage from the last glacial maximum to the present. Nature 348:711-714.

Austin AT, Yahdjian ML, Stark JM, Belnap J, Porporato A, Norton U, Ravetta DA, Schaeffer SM (2004) Water pulses and biogeochemical cycles in arid and semiarid ecosystems. Oecologia 141:221-235.

Bakwin PS, Tans PP, White JWC, Andres RJ (1998) Determination of the isotopic ($^{13}C/^{12}C$) discrimination by terrestrial biology from a global network of observations. Global Biogeochemical Cycles 12:555-562.

Baldocchi D, Falge E, Wilson K (2001) A spectral analysis of biosphere-atmosphere trace gas flux densities and meteorological variables across hour to multi-year time scales. Agricultural Forest Meteorology 107:1-27.

Balesdent J, Girardin C, Mariotti A (1993) Site-related $\delta^{13}C$ of tree leaves and soil organic matter in a temperate forest. Ecology 74:1713–1721.

Battle M, Bender ML, Tans PP, White JWC, Ellis JT, Conway T, Francey RJ (2000) Global carbon sinks and their variability inferred from atmospheric O_2 and $\delta^{13}C$. Science 287:2467-2470.

Berry SC, Varney GT, Flanagan LB (1997) Leaf $\delta^{13}C$ in *Pinus resinosa* trees and understory plants: Variation associated with light and CO_2 gradient. Oecologia 109:499-506.

Bowling DR, Baldocchi DD, Monson RK (1999) Dynamics of isotopic exchange of carbon dioxide in a Tennessee deciduous forest. Global Biogeochemical Cycles 13:903-922.

Bowling DR, McDowell NG, Bond B.J., Law BE, Ehleringer JR (2002) ^{13}C content of ecosystem respiration is linked to precipitation and vapor pressure deficit. Oecologia 131:113-124.

Bowman WD, Hubick KT, von Caemmerers S, Farquhar GD (1989) Short-Term Changes in Leaf Carbon Isotope Discrimination in Salt- and Water-Stressed C_4 Grasses. Plant Physiology 90: 162–166.

Buchmann N, Brooks JR, Rapp KD, Ehleringer JR (1996) Carbon isotope composition of C_4 grasses is influenced by light and water supply. Plant, Cell and Environment 19:392-402.

Buchmann N, Guehl J-M, Barigah TS, Ehleringer JR (1997a) Interseasonal comparison of CO_2 concentrations, isotopic composition, and carbon dynamics in an Amazonian rainforest (French Guiana). Oecologia 110:120-131.

Buchmann N, Kao W-Y, Ehleringer J (1997b) Influence of stand structure on carbon^{13} of vegetation, soils, and canopy air within deciduous and evergreen forests in Utah, United States. Oecologia 110:109-119.

Buchmann N, Ehleringer JR (1998) CO_2 concentration profiles, and carbon and oxygen isotopes in C_3 and C_4 crop canopies. Agricultural and forest meteorology 89:45-58.

Ciais P, Tans PP, Trolier M, White JWC, Francey RJ (1995) A large Northern Hemisphere terrestrial CO_2 sink indicated by the $^{13}C/^{12}C$ ratio of atmospheric CO_2. Science 269:1089-1102.

Conway TJ, Tans PP, Waterman LS, Thoning KW, Kitzis DR, Masarie KA, Zhang N (1994) Evidence of interannual variability of carbon cycle from the National Oceanic and Atmospheric Administration/Climate Monitoring and Diagnosis Laboratory Global Air Sampling Network. Journal of Geophysical Research 99:22831-22855.

Dugas WA (1993) Micrometeorological and chamber measurements of CO_2 flux from bare soil. Agricultural and Forest Meteorology 67:115-128.

Dugas WA, Heuer ML, Mayeux HS (1999) Carbon dioxide fluxes over bermudagrass, native prairie, and sorghum. Agricultural and Forest Meteorology 93:121-139.

Durancean M, Ghashghaie J, Badeck F, Deleens E, Cornic G (1999) Delta C-13 of CO_2 respired in the dark in relation to delta C-13 of leaf carbohydrates in *Phaseolus vulgaris* L-under progressive drought. Plant and Cell Environment 22:515-523.

Ehleringer JR, Hall AE, Farquhar GD (1993) Stable Isotopes and Plant Carbon-Water Relations. Academic, San Diego, California.

Ehleringer JR, Buchmann N, Flanagan LB (2000) Carbon isotope ratios in belowground carbon cycle processes. Ecological Applications 10:412-422.

Ekbland A, Högberg P (2001) Natural abundance of ^{13}C in CO_2 respired from forest soils reveals speed of link between tree photosynthesis and root respiration. Oecologia 127:305-308.

Emmerich WE (2003) Carbon dioxide fluxes in a semiarid environment with high carbonate soils. Agricultural and Forest Meteorology 116:91-102.

Epstein HE, Burke IC, Lauenroth WK (1999) Response of the shortgrass steppe to changes in rainfall seasonality. Ecosystems 2:139-150.

Farquhar GD, Ehleringer JR, Hubick KT (1989) Carbon isotope discrimination and photosynthesis. Annual Review of Plant Physiology Plant Molecular Biology 40:503-537.

Ferretti DF, Pendall E, Morgan JA, Nelson JA, LeCain D, Mosier AR (2003) Partitioning evapotranspiration fluxes from a Colorado grassland using stable isotopes: Seasonal variations and ecosystem implications of elevated atmospheric CO_2. Plant and Soil 00:1-13

Flanagan LB, Wever LA, Carlson PJ (2002) Seasonal and interannual variation in carbon dioxide exchange and carbon balance in a northern temperature grassland. Global Change Biology 8:599-615.

Flanklin JF, Bledsoe CS, Callahan JT (1990) Contributions of the long-term ecological research program. BioScience 40:509-523.

Frank AB, Dugas WA (2001) Carbon dioxide fluxes over a northern, semiarid, mixed-grass prairie. Agricultural and Forest Meteorology 108:317-326.

Fung I, Field CB, Berry JA, Thompson MV, Randerson JT, Malmstrom CM, Vitousek PM, Collaz GJ, Sellers PJ, Randall DA, Denning AS, Badeck F, John J (1997) Carbon^{13} exchanges between the atmosphere and biosphere. Global Biogeochemical Cycles 11:507-533.

Ghashghaie J, Duranceau M, Badeck FW, Cornic G, Adeline MT, Deleens E (2001) Delta C^{13} of CO_2 respired in the dark in relation to delta C^{13} of leaf metabolites: comparison between *Nicotiana sylvestris* and H*elianthus annuus* under drought. Plant Cell Environment 4:505-515.

Hesterberg R, Siegenthaler U (1991) Production and stable isotopic composition of CO_2 in a soil near Bern, Switzerland. Tellus Ser. B 43:197-205.

Hunt JE, Kelliher FM, McSeveny TM, Byers JN (2002) Evaporation and carbon dioxide exchange between the atmosphere and a tussock grassland during a summer drought. Agricultural and Forest Meteorology 111: 65-82.

Huxman TE, Snyder KA, Tissue D, Leffler AJ, Ogle K, Pockman WT, Sandquist DR, Potts DL, Schwinning S (2004) Precipitation pulses and carbon fluxes in semiarid and arid ecosystems. Oecologia 141:254-268.

Morgan JA, LeCain DR, Read JJ, Hunt HW, Knight WG (1998) Photosynthetic pathway and ontogeny affect on water relations and the impact of CO_2 on *Bouteloua gracilis* (C_4) and *Pascopyrum smithii* (C_3). Oecologia 114:483-493.

Keeling CD (1958) The concentration and isotopic abundances of atmospheric carbon dioxide in rural areas. Geochemica et Cosmochimica Acta 13: 322-334.

Keeling CD (1961) The concentration and isotopic abundance of carbon dioxide in rural and marine air. Geochemica et Cosmochimica Acta 24:277-298.

Keeling CD, Whorf TP, Wahlen M, van der Pflicht J (1995) Interannual extremes in the rate of rise of atmospheric carbon idoxide since 1980. Nature 375:666-670.

Knapp AK, Smith MD (2001) Variation among biomes in temporal dynamics of aboveground primary production. Science 291:481-484.

Kuchler AW (1974) A new vegetation map for Kansas. Ecology 55: 586-604.

Lauteri M, Brugnoli E, Spaccino L (1993) Carbon isotope discrimination in leaf soluble sugars and in whole plant dry matter in Helianthus annuus L. grown under different water conditions. In: Ehleringer JR, Hall AE, Farquhar GD (eds.) Stable Isotopes and Plant Carbon-Water Relations Academic Press, San Diego, pp 93-108.

LeCain DR, Morgan JA, Mosier AR, Nelson JA (2003) Soil and plant water relations determine photosynthetic responses of C_3 and C_4 grasses in a semi-arid ecosystem under elevated CO_2. Annals of Botany 92:41-52.

Lin G, Ehleringer JR (1997) Carbon isotopic fractionation does not occur during dark respiration in C_3 and C_4 plants. Plant Physiology 114:391-394.

Lloyd J, Farquhar GD (1994) ^{13}C discrimination during CO_2 assimilation by the terrestrial biosphere. Oecologia 99:201-215.

Lloyd J, Kruijt B, Hollinger DY, Grace J, Francey RJ, Wong S-C, Kelliher FM, Miranda AC, Farquhar GD, Gash JHC, Vygodskaya NN, Wright IR, Miranda HS, Schulze E-D (1996) Vegetation effects on the isotopic composition of atmospheric CO_2 at local and regional scales: Theoretical aspects and comparison between a rain forest in Amazonia and a boreal forest in Siberia. Australian Journal of Plant Physiology 23:371-399.

McDowell NG, Bowling DR, Bond BJ, Irvine J, Law BE, Anthoni P, Ehleringer JR (2004) Response of the carbon isotopic content of ecosystem, leaf, and soil respiration to meteorological and physiological driving factors in a Pinus ponderosa ecosystem. Global Biogeochemical Cycles 18, doi:1029/2003GB002049

Milchunas DG, Lauenroth WK (2001) Belowground primary production by carbon isotope decay and long-term root biomass dynamics. Ecosystems 4:139-150.

Miranda AC, Miranda HS, Lloyd J, Grace J, Francey RJ, McIntyre, JA, Meir P, Riggan P, Lockwood, R and Brass J (1997) Fluxes of water and energy over Brazilian cerrado: an analysis using eddy covariance and stable isotopes. Plant, Cell and Environment 20: 315-328.

Monson RK, Littlejohn RO, Jr. and Williams GJI (1983) Photosynthetic adaptation to temperature in four species from the Colorado shortgrass steppe: A physiological model for coexistence. Oecologia 58:43-51.

Morgan JA, LeCain DR, Read JJ, Hunt HW, Knight WG (1998) Photosynthetic pathway and ontogeny affect water relations and the impact of CO_2 on *Bouteloua gracilis* (C_4) and *Pascopyrum smithii* (C_3). Oecologia 114:483-493.

Natelhoffer KJ, Fry B (1988) Controls on natural nitrogen-15 and carbon-13 abundances in forest soil organic matter. Soil Science Society of America Journal 52:1633-1640.

Nelson JA, Morgan JA, LeCain DR, Mosier AR, Milchunas DG, Parton WJ (2003) Elevated CO_2 increases soil moisture and enhances plant water relations in a long-term field study in semi-arid shortgrass steppe of Colorado. Plant and Soil 259:169-179.

Ode D, Tieszen LL, Lerman JC (1980) The seasonal contribution of C_3 and C_4 plant species to primary production in a mixed prairie. Ecology 61:1304-1311.

Pendall E, Del Grosso S, King JY, LeCain DR, Milchunas DG, Morgan JA, Mosier AR, Ojima DS, Parton WJ, Tans PP, White JWC (2003) Elevated atmospheric CO_2 effects and soil water feedbacks on soil respiration components in a Colorado grassland. Global Biogeochemical Cycles 17, dio;10.1029.2001GB001821

Randerson JT, Collatz GJ, Fessenden JE, Munoz AD, Still CJ, Berry JA, Fung IY, Suits N, Denning AS (2002) A possible global covariance between terrestrial gross primary production and ^{13}C discrimination: Consequences for the atmospheric ^{13}C budget and its response to ENSO. Global Biogeochemical Cycles 16:1136, doi:10.1029/2001GB001845

Reynolds JF, Kemp PR, Ogle K, Fernandez RJ (2004) Modifying the "pulse-reserve" paradigm for deserts of North America: precipitation pulses, soil water and plant responses. Oecologia 141:194-210.

Rosenberg NJ, Blad BL, Verma SB (1983) Microclimate: the Biological Environment. Wiley, New York.

Sala OE, Lauenroth WK, Parton WJ (1992) Long-term soil water dynamics in the shortgrass steppe. Ecology 73:1175-1181.

Sims PL, Bradford JA (2001) Carbon dioxide fluxes in a southern plains prairie. Agricultural and Forest Meteorology 109: 117-134.

Sokal RR, Rohlf FJ (1981) Biometry. Freeman

Still CJ, Berry JA, Ribas-Carbo M, Helliker BR (2003) The contribution of C_3 and C_4 plants to the carbon cycle of a tallgrass prairie: an isotopic approach. Oecologia 136:347-359.

Suyker AE, Verma SB (2001) Year-round observations of the net ecosystem exchange of carbon dioxide in a native tallgrass prairie. Global Change Biology 7:279-289.

Suyker AE, Verma SB, Burba GG. (2003) Interannual variability in net CO_2 exchange of a native tallgrass prairie. Global Change Biology 9: 255-265.

Tans PP (1993) Observational strategy for assessing the role of terrestrial ecosystems in the global carbon cycle: scaling down to regional levels. In: Scaling physiological processes: leaf to globe. Pp. 179-190.

Tieszen LL, Reed BC, Bliss NB, Wylie BK, Dejong DD (1997) NDVI, C_3 and C_4 production, and distributions in Great Plains grassland land cover classes. Ecological Applications 7:59-78.

Trolier M, White JWC, Tans PP, Masarie KA, Germery PA (1996) Monitoring the isotopic composition of atmospheric CO_2: measurements from the NOAA global air sampling network. Journal of Geophysical Research 101:25897-25916.

Trumbore SE, Chadwick OA, Admundson R (1996) Rapid exchange between soil carbon and atmospheric carbon dioxide driven by temperature change. Science 272:393-396.

Webb EK, Pearman GI, Leuning R (1980) Correction of flux measurements for density effects due to heat and water vapor transfer. Quarterly Journal of the Royal Meteorological Society 106:85-100

Weltzin JF, Loil ME, Schwinning S, Williams DG, Fay PA, Haddad BM, Harte J, Huxman TE, Knapp AK, Lin G, Pockman WT, Shaw MR, Small ER, Smith MD, Smith SD, Tissue DT, Zak JC (2003) Assessing the response of terrestrial ecosystems to potential changes in precipitation. BioScience 53:941-952.

Yan S, Wan C, Sosebee RE, Wester DB, Fish EB, Zartman RE (2000) Responses of photosynthesis and water relations to rainfall in the desert shrub creosote bush (*Larrea tridentata*) as influenced by municipal biosolids. Journal of Arid Environments 46:397-412.

Yakir D, Wang X-F (1996) Fluxes of CO_2 and water between terrestrial vegetation and the atmosphere estimated from isotope measurements. Nature 380:515-517.

Table 2.1 CO_2 fluxes (mg C m^{-2} h^{-1}) from four different patches including C_3, C_4, mixed C_3 and C_4 and bareground components over growing season of 2001. Different letters represent significant difference among chambers (LSMEANS, $p<0.05$). Comparisons were made for each chamber and times when experiments were conducted during 24 hour periods (D: Daytime; N:nighttime; E:Dawn) Parenthesis represent standard error.

	May			June			July			September
	$D^{a'}$	$N^{b'}$	$E^{ab'}$	$D^{a'}$	$N^{b'}$	$E^{b'}$	$D^{a'}$	$N^{a'}$	$E^{a'}$	D
C_3	106.12^{a} (8.59)	73.26^{a} (15.55)	106.77^{a} (20.68)	250.06^{a} (63.29)	97.67^{a} (21.85)	107.38^{a} (19.38)	52.14^{a} (9.01)	44.2^{a} (5.58)	45.0^{a} (7.94)	33.64^{a} (5.21)
C_4	83.50^{ab} (11.59)	50.62^{ab} (13.9)	56.62^{b} (15.14)	256.88^{a} (69.89)	110.34^{a} (29.94)	91.31^{a} (22.15)	64.94^{a} (12.52)	44.44^{a} (11.49)	48.05^{a} (9.55)	45.74^{a} (11.81)
M	54.82^{bc} (18.80)	57.96^{ab} (7.40)	67.41^{b} (9.53)	212.06^{a} (61.0)	110.92^{a} (27.10)	98.08^{a} (13.06)	65.22^{a} (27.93)	51.24^{a} (9.39)	28.35^{a} (4.37)	42.91^{a} (13.30)
B	35.97^{c} (3.35)	25.15^{bc} (4.82)	41.12^{b} (2.81)	91.09^{b} (17.92)	69.16^{b} (16.14)	54.45^{b} (9.90)	17.45^{b} (3.49)	27.57^{b} (2.95)	32.59^{a} (9.13)	21.15^{a} (4.74)

Table 2.2 Carbon isotope ratios (‰) of respired CO_2 from four different types of plots such as C_3, C_4, mixed C_3 and C_4 (M) and bareground (B) components in 2001. Different letters represent significant difference among chambers (LSMEANS, $p<0.05$). Comparisons were made for each chamber and times when experiments were conducted during 24 hour periods (D: daytime; N:nighttime; E:Dawn) Parenthesis represent standard error for intercept. Geometric mean regressions were performed to calculate intercepts (*; $p<0.1$; **;$p<0.05$)

	May			June			July			September
	$D^{a'}$	$N^{a'}$	$E^{a'}$	$D^{a'}$	$N^{b'}$	$E^{ab'}$	$D^{a'}$	$N^{b'}$	$E^{b'}$	D
C_3	-26.00[a] (4.77)	-20.50 (0.59)*	-22.94 (0.97)**	-22.18[a] (1.81)**	-21.71 (0.43)**	-21.18 (1.72)*	-21.24[a] (1.29)**	-20.62 (0.81)**	-20.09 (1.7)*	-19.88 (1.82)*
C_4	-23.99[a] (1.69) **	-23.84 (1.02)**	-20.84 (1.4)**	-16.04[c] (0.9)	-15.36 (0.57)*	-16.46 (0.75)**	-19.10[b] (1.39)**	-15.98 (0.55)**	-17.83 (1.81)	-15.59 (0.92)*
M	-18.49[a] (2.15)	-19.76 (1.30)**	-21.95 (2.02)**	-20.57[b] (1.38)**	-17.71 (2.4)	-18.83 (1.2)**	-20.79[a] (5.78)	-19.32 (0.93)*	-19.28 (0.62)**	-26.14 (3.39)
B	-23.49[a] (2.8)*	-21.83 (1.49)**	-20.93 (2.21)*	-22.70[ab] (4.13)	-19.34 (1.67)*	-19.85 (1.44)**	-23.37[c] (2.07)*	-20.91 (1.88)*	-22.27 (1.58)**	-19.10 (2.05)*

Table 2.3 Fraction (%) of 'Old' versus 'New' C substrates using two mixing model. We used $\delta^{13}C$ of soil respiration in bare ground patches, -26‰ and -15 ‰ for old end member, new C_3, and new C_4 end members, respectively. Parenthesis represents stand error of three times of day within each diurnal.

	%	May	June	July
C_3	Old	0.53 (0.29)	0.81(0.1)	1 (0.01)
	New	0.47 (0.29)	0.19 (0.1)	0 (0.01)
C_4	Old	0.99 (0.01)	0.17 (0.07)	0.35 (0.09)
	New	0.01(0.01)	0.83 (0.07)	0.65 (0.09)

Table 2.4 Contributions of each chamber in 2001 to net flux of $^{13}CO_2$ from nocturnal ecosystem respiration.

% Contribution	May	June	July	September
$\delta^{13}C_{R\text{-}c3} * Fc_3$	42.16	49.81	46.48	49.36
$\delta^{13}C_{R\text{-}c4} * Fc_4$	37.00	37.60	33.63	49.94
$\delta^{13}C_{R\text{-}B} * F_B$	20.84	12.59	19.90	0.70

Fi : CO_2 fluxes measured by GC during night time. Most air samplings were collected from 0100 to 0200 local time (i represents three different chambers including C_3, C_4 and bareground chambers)
$^{13}C_{R\text{-}i}$: Keeling plot intercepts of each chamber

Table 2.5 Regression coefficients from linear regression analysis of $\delta^{13}C_R$, and $\delta^{13}C_{R\text{-}C3,\ C4,\ M,\ B}$ $\delta^{13}C$ versus environmental variables.

	VPD	Tsoil	Tair	θ	NEE	PAR	Precipitation
$\delta^{13}C_R$	0.47* (-, 5, 1)	0.58**(-, 9, 3)	0.73**(-, 11, 2)	0.51 * (+, 3, 2)	0.5 (+, 8, 4)	0.38 (+, 9, 1)	0.39*(-, 6)
$\delta^{13}C_{soil\text{-}c3}$	0.82**(+, 5, 5)	0.81**(+, 6, 5)	0.89**(+, 4, 5)	0.82**(-, 8, 1)	0.7**(+, 2, 1)	0.69**(+, 8, 5)	
$\delta^{13}C_{soil\text{-}c4}$	0.85* (-, 7, 1)	0.96**(-, 0, 2)	----------	----------	----------	0.87**(-, 5, 4)	
$\delta^{13}C_{soil\text{-}M}$	----------	----------	----------	----------	0.78**(-, 0, 3)	0.64*(+, 0, 5)	
$\delta^{13}C_{soil\text{-}B}$	----------	----------	----------	----------	----------	0.6**(-, 8, 5)	

+; positive relations, -; negative relations.
In parenthesis, 1st and 2nd numbers represent number of days lagged and number of days averages, respectively. For precipitation, 1st number represent number of weeks lagged.
* Regression significance P = 0.1
** Regression significance P = 0.05

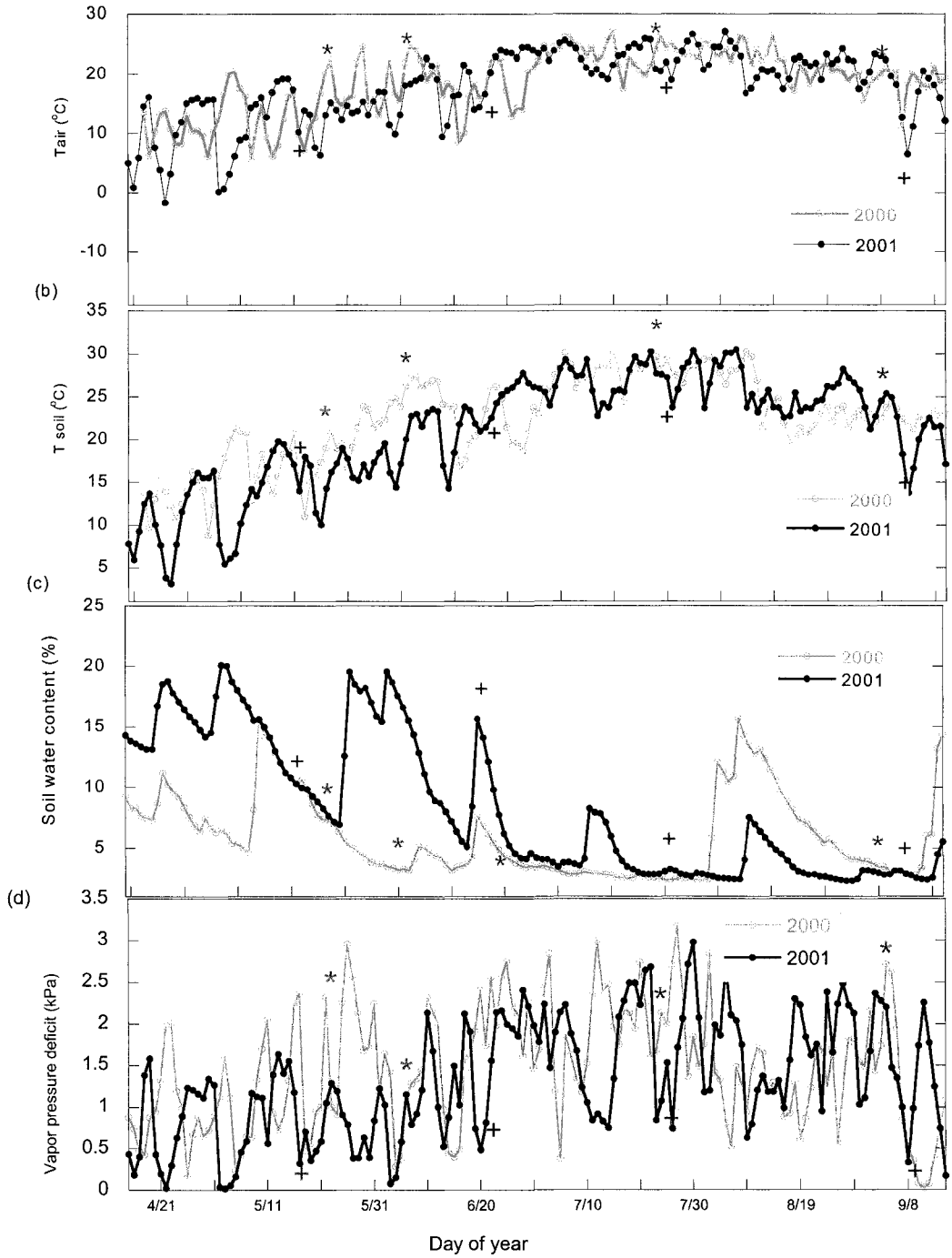

Fig. 2.1 Meteorological variation of (a) air temperature (Ta) (b) soil temperature (Ts), (c) soil moisture and (d) vapor pressure deficit (VPD) over two consecutive years (April 2000 through December 2001), measured at the tower located the air sampling site. Data were collected daily at 20-min intervals (Morgan J.A, unpublished data). Data collection periods were represented for 2000 and 2001 as * and +, respectively.

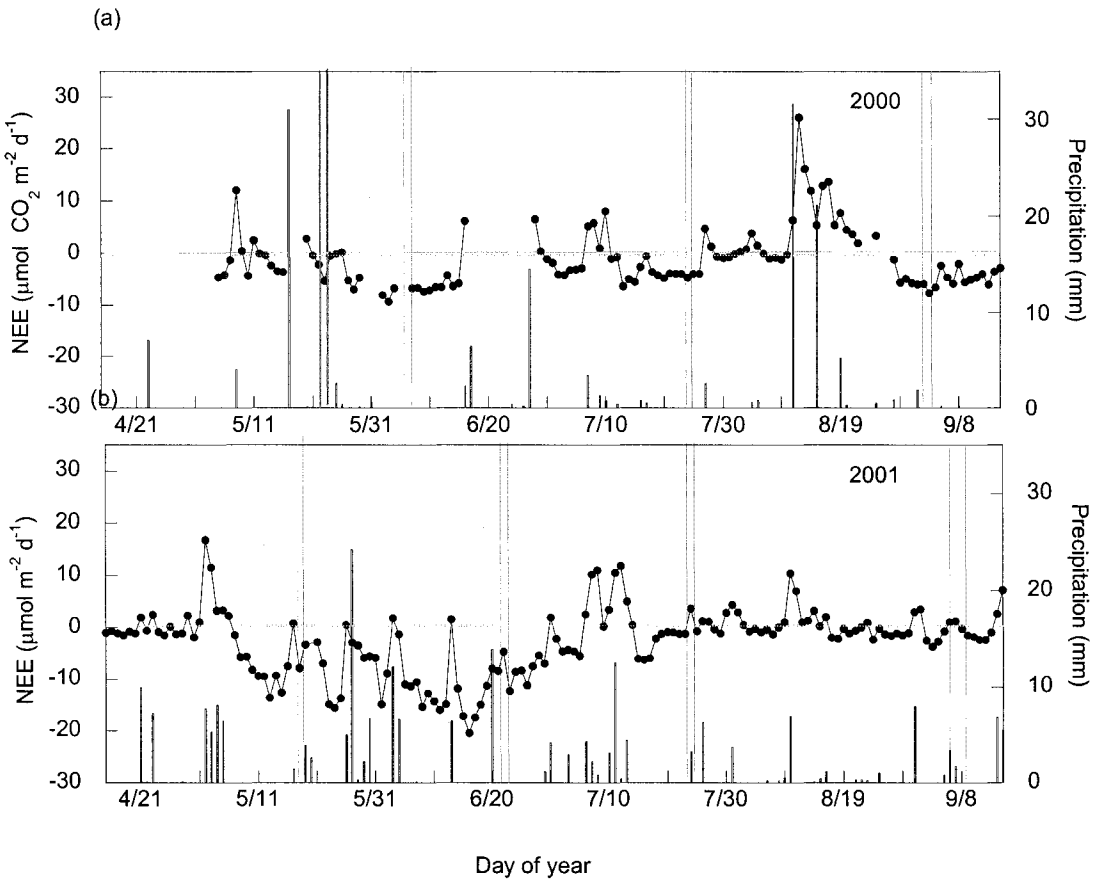

Fig.2.2 Variations of precipitation and NEE (negative values are associated with C-uptake and positive values with net emission) over two consecutive years (a) beginning April 2000 through (b) mid-September 2001, measured at the tower located the air sampling site (Morgan J.A, unpublished data). Data were collected daily at 20-min intervals. Vertical lines represent durations which field experiments were conducted.

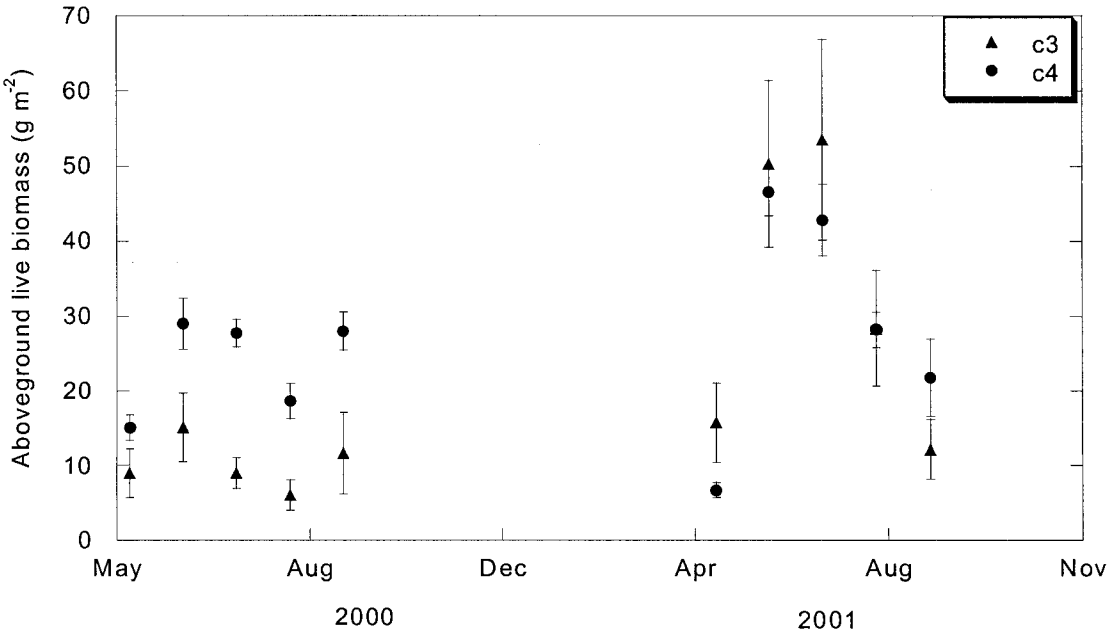

Fig.2.3. Plant above ground live biomass classified by functional groups over two growing seasons of 2000 and 2001 (Morgan J.A, unpublished data).Since C_4 forbs and shrubs are uncommon in the study site, they were grouped as C_3 plants

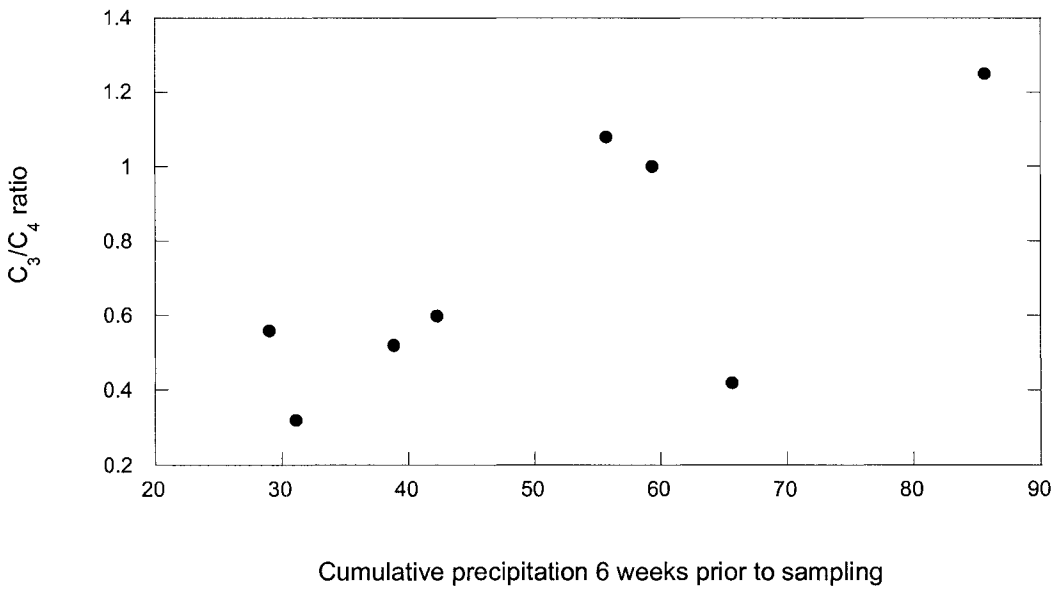

Fig.2.4 Variations in C_3/C_4 with cumulative precipitation 6 weeks prior to sampling over two growing seasons of 2000 and 2001.

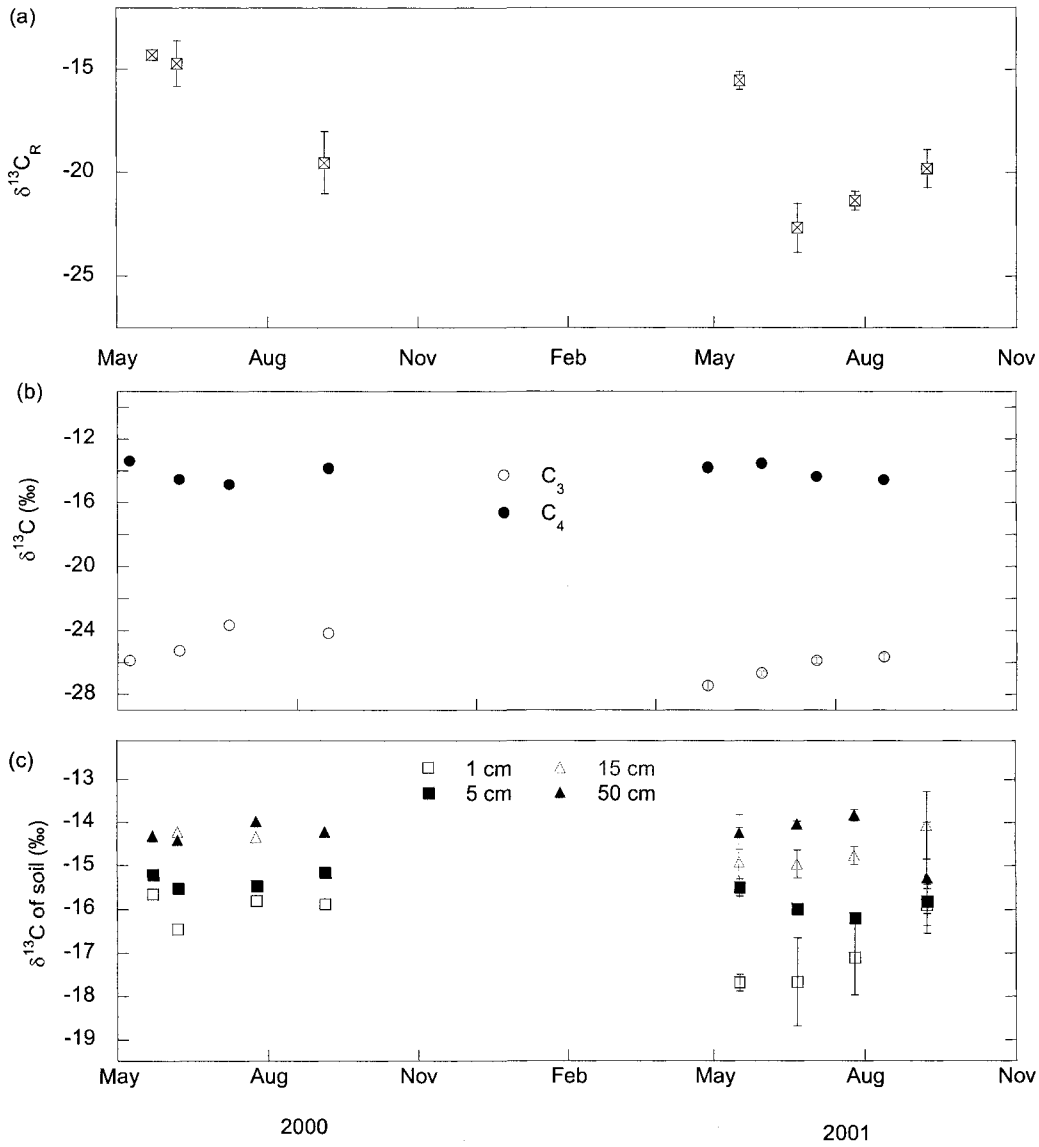

Fig.2.5. Monthly measurements of $\delta^{13}C$ of ecosystem respiration ($\delta^{13}C_R$), (b) bulk organic tissue from C_3 (o) and C_4 plants (•), and (c) soil organic matter from 4 different depths (1, 5, 15 and 50 cm) over two consecutive years (2000 and 2001). Error bars indicate standard error.

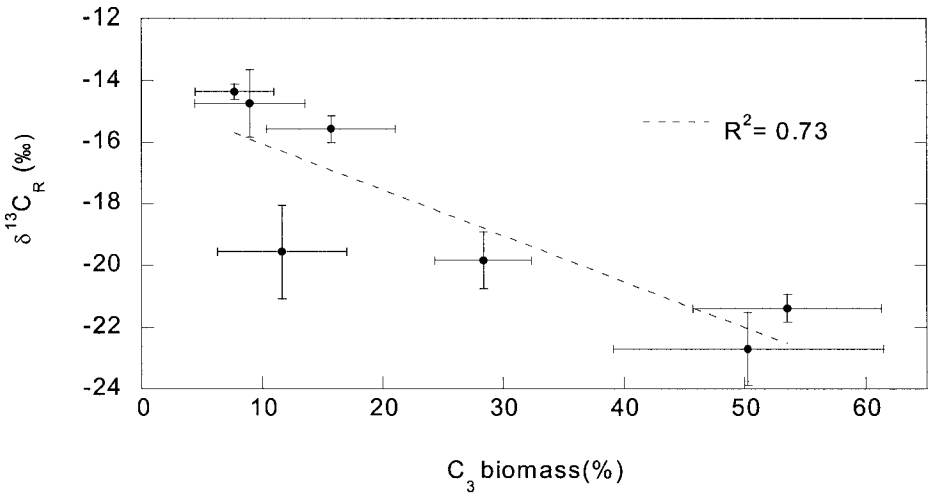

Fig. 2.6. Carbon isotope ratio of ecosystem respiration is compared to aboveground live C_3 biomass over two consecutive years. If negative NEE (CO_2 uptake) is already established from previous water input (Fig. 2.2), we correlated $\delta^{13}C_R$ with C_3 biomass in same month. If ecosystem did not respond rapidly to a shift from drought to moist conditions remaining CO_2 source, we correlated $\delta^{13}C_R$ with C_3 biomass measured approximately one month prior to sampling periods.

3. Contributions of C_3 and C_4 plants, and dynamics of ^{18}O water pools to variations in respiratory ^{18}O signals in the Colorado shortgrass steppe

3.1 Abstract

The contribution of C_3 and C_4 plant functional groups to atmospheric $C^{18}O^{16}O$ signal and in particular to $\delta^{18}O$ of leaf respired CO_2 is needed for improving understanding of carbon sinks/source strengths especially in mixed C_3 and C_4 ecosystems. We sought to 1) describe the natural variability in $\delta^{18}O$ of ecosystem water pools and respiratory fluxes, 2) understand what environmental controls are responsible for the dynamics of those values, and 3) evaluate how plant functional groups interact with different environmental conditions (moist versus dry). We conducted field measurements of oxygen isotopic composition of atmospheric CO_2 from air, soil water, leaf water, soil respiration, and applied modeling approaches to estimate oxygen isotope composition of leaf water pools, and soil and foliar respiratory fluxes. A Keeling plot approach to determine respiratory $C^{18}O^{16}O$ fluxes was valid in the ecosystem during relatively moist conditions without pulse precipitation events. Isotopically enriched soil surface water and low CO_2 production caused decoupling between $\delta^{18}O$ of atmospheric CO_2 and inverse CO_2 concentrations, especially for dry conditions. The amount and timing of precipitation, initial soil moisture content, and abrupt increase in heterotrophic activity from pulse precipitation events are likely to cause immediate changes in $\delta^{18}O$ of soil water pools and

soil respiration. Accordingly, changes in soil respired CO_2 were quite dynamic in chamber measurements. Fractional contribution of soil respiration to total chamber respiration was greater in C_4 patches relative to C_3 patches. Apparently, during moist conditions, foliar retrodiffusional fluxes governed by internal CO_2 concentrations and the extent of isotopic equilibrium between CO_2 and H_2O had dominant influence on $C^{18}O^{16}O$ fluxes. In dry conditions, the explicit differences between C_3 and C_4 patches disappeared, which suggests that the greater $\delta^{18}O$ of the soil water gradient and higher soil respiration contribution to $C^{18}O^{16}O$ fluxes offset the plant community differences.

3.2 Introduction

Many efforts have been made to investigate the role of terrestrial ecosystems in carbon cycling as anthropogenic atmospheric CO_2 concentrations increases. Using oxygen isotopes to detect terrestrial CO_2 uptake at the global scale has been emerging as a promising tool. The latitudinal pattern in the atmospheric oxygen isotope signature of CO_2 is a useful isotopic tracer of C uptake and exchange (Francey and Tans, 1987; Farquhar et al. 1993 b). The ^{18}O isotopic gas exchange has been explored to identify grassland source/sink inputs into the global carbon cycle (Gillon and Yakir 2001; Ehleringer et al. 2002). An advantage of analyzing ^{18}O signal of terrestrial photosynthesis over ^{13}C is that the ^{13}C discrimination by C_4 ecosystems is small and has similar magnitude to oceanic ^{13}C isotopic gas exchange (Fung et al. 1997). Verifying the ^{18}O variation in ecosystem-level gas exchange processes is critical to improve our understanding of the terrestrial carbon cycle.

Measurements of oxygen isotopes of CO_2 are able to distinguish the

contributions of photosynthesis and respiration (Tans and White 1998;Yakir and Wang 1996), of nocturnal leaf and soil respiration (Bowling et al. 2003 a and b), and have led to a better understanding of plant physiological effects on $C^{18}O^{16}O$ signals (Gillon and Yakir 2000; Flanagan et al. 1994) and of the contributions of equilibration and diffusion fractionation to soil respired $C^{18}O^{16}O$ signals (Miller et al. 1999; Tans 1998).

A conceptual diagram of controlling factors influencing $\delta^{18}O$ of ecosystem respiration ($\delta^{18}O_R$) is shown in Figure 1.2. The oxygen isotopic composition of atmospheric CO_2 represents an aspect of eco-physiological exchange processes from the plant-soil system to the atmosphere. In other words, $\delta^{18}O_R$ is a combined product of $\delta^{18}O$ of leaf and soil respired CO_2 ($\delta^{18}O_{LR}$ and $\delta^{18}O_{SR}$, respectively). Isotopic signatures of leaf and soil respired $C^{18}O^{16}O$ are influenced by $\delta^{18}O$ of leaf water ($\delta^{18}O_{LW}$) and soil water ($\delta^{18}O_{SW}$), respectively. $\delta^{18}O_{LR}$ and $\delta^{18}O_{SR}$ are also controlled by a temperature-dependent equilibrium fractionation factor associated with hydration reaction between H_2O and CO_2 (Brenninkmeijer et al. 1983) and a kinetic isotopic fractionation factor associated with diffusion away from the site of respiration (Miller et al. 1999).

Leaf-level exchange of CO_2 to the atmosphere results in an enrichment of ^{18}O due to a process of evaporation at the site of CO_2-H_2O equilibration. Leaf respired CO_2 is influenced by carbonic anhydrase (CA) which catalyzes the isotopic equilibration of CO_2 inside the leaf and undergoes retrodiffusion of two- thirds of the equilibrating CO_2 (Flanagan et al. 1997). Leaf water is enriched in $\delta^{18}O$ compared to stem and soil water because of kinetic and equilibrium fractionation effects (Flanagan et al. 1991; Wang and Yakir 1995). Enrichment of leaf water varies with environmental conditions such as variations in VPD (Roden and Ehleringer 1999), leaf temperature (Flanagan et al.

1991), the $\delta^{18}O$ of atmospheric water vapor which is controlled by local precipitation and air temperature.

The soil respired CO_2 is controlled by relatively ^{18}O-depleted soil water, whose major controls are precipitation input and evaporation from the soil surface (Miller et al. 1999). If CA is present in the soil, then CO_2 should be in isotopic equilibrium with soil water, especially near the soil surface. In addition to equilibrium fractionation in liquid phase, gaseous CO_2 exchanges oxygen atoms with water, and different isotopomers of CO_2 are subject to diffusional fractionation. The $\delta^{18}O$ of soil water is initially controlled by the isotopic content of precipitation, which varies mainly with temperature and storm tracks (Rozanski et al. 1982). Evaporation taking place at the soil surface enriches $\delta^{18}O$ of soil water, resulting in an isotopic gradient within the soil. Hydration of respiratory CO_2 produced within soils (by roots or heterotrophs) leads to isotopic equilibration with soil water (Miller et al. 1999). Soil water is taken up by roots and transported to leaves through the xylem without fractionation effects (Dawson & Ehleringer 1991).

A few studies, mainly focused on C_3 ecosystems, have examined the controls of $\delta^{18}O$ of respiratory CO_2 including leaf and soil components (Bowling et al. 2003 a b; Flanagan et al. 1994,1995 and 1997). Very few studies on atmospheric $C^{18}O^{16}O$ signal have been conducted in semi-arid grasslands which characteristically have brief periods of adequate water availability (Sala et al. 1992). Temperate semi-arid regions frequently contain both C_3 and C_4 plant species, which have distinct $\delta^{18}O$ signatures of leaf respired CO_2 (Gillon and Yakir 2000). Seasonal activity of C_3 and C_4 plants could contribute to dynamics of $\delta^{18}O$ of respired CO_2 because C_4 grass species show less ^{18}O discrimination than C_3 plants because of low internal CO_2 concentrations and lower CA hydration rate

(Gillon and Yakir 2000; Williams et al. 1996). The C_4 plants with low CA activity perform incomplete equilibration between CO_2 and chloroplast water, which limits the extent of ^{18}O exchange. More enrichment of leaf water in C_4 grasses was observed relative to C_3 grasses, which was attributed to the progressive evaporative enrichment along parallel veins with narrow interveinal distances in C_4 grasses (Helliker and Ehleringer 2000). Despite this, CO_2 retrodiffusing from C_4 leaves may be relatively depleted because of much lower internal CO_2 concentrations and low CA activity. In addition, C_3 and C_4 plants may have different $\delta^{18}O$ of source water because of their different root distributions. Root patterns differed between two grass species with more than 95% of *B. gracilis* roots and approximately 72 % *P. smithii* roots distributed in the top 0-20 depth layer (Nelson et al. 2003). The amount of rainfall, distribution of precipitation pulses, the response of soil microbes to rainfall events in terms of CO_2 production, and soil physical properties might create a complicated soil water $\delta^{18}O$ profile and correspondingly the isotope content of respired CO_2 in semi-arid grasslands.

We aim to 1) describe the natural seasonal variability in $\delta^{18}O$ of ecosystem water pools and respiratory fluxes with seasonal variations, 2) understand what environmental controls are responsible for the dynamics of changing $\delta^{18}O$ values and how pulse precipitation events may affect them, 3) evaluate how plant functional groups interact with different environmental conditions (moist versus dry) to quantify the soil and foliar component fluxes of the total ecosystem respiration fluxes using both chamber based measurements and modeling approaches. We expect that $\delta^{18}O$ of soil water gradient would not be large enough to differentiate $\delta^{18}O$ of leaf water between C_3 and C_4 grasses during moist conditions. Therefore, we hypothesize that $\delta^{18}O$ of respired CO_2 from C_3

plots should be more enriched than in C_4 plots as foliar retrodiffusional CO_2 flux governed by internal CO_2 concentrations and CA activity are expected to be higher in C_3 grasses than C_4 grasses. However, in dry conditions, we anticipate that the magnitude of $\delta^{18}O$ of soil water gradient between upper and lower depths would be large enough to make a distinction between $\delta^{18}O$ of C_3 and C_4 leaf water. Therefore, we hypothesize that there should be compensation between $\delta^{18}O$ of C_3 and C_4 leaf water, and foliar retrodiffusion flux leading to no significant difference between the two plot types.

3.3 Materials and methods

3.3.1 Site description

This study was conducted during the 2000 and 2001 growing seasons at the USDA-ARS Central Plains Experimental Range (CPER), in the shortgrass steppe region of north-eastern Colorado, 56 km north-east of Fort Collins, CO (Fig.3.1;lat. 40° 40′ N, long. 104° 45′ W). This site is the Shortgrass Steppe Long Term Ecological Research site (Franklin et al. 1990), such that many long-term data are available. Vegetation of this region is dominated by warm-season, C_4 grasses (*Bouteloua gracilis* and *Buchloe dactyloides*), but also contains an abundance of cool-season, C_3 grasses (e.g., *Pascopyrum smithii* and *Stipa comata.*), as well as a variety of C_3 forbs and woody vegetation. C_4 forbs and woody vegetation occur primarily in landscape positions with very deep sandy soils. Belowground production accounts for ~70% of net primary production (Milchunas and Lauenroth, 2001). Canopy height is less than 1m. Long term (55 year) mean annual precipitation averages 320mm, with the majority occurring

during May, June and July. Mean air temperatures are 15.6°C in summer and 0.6°C in winter with maximum July temperatures averaging 30.6°C (Lauenroth and Milchunas, 1991). The pasture around our sampling site has been moderately grazed but cows were excluded from the sampling area for the duration of the study.

3.3.2 Micrometeorological parameters

Relevant meteorological parameters were measured above the canopy every 20 min from a Bowen ratio energy balance technique (BREB). Measurements included air temperature, relative humidity and soil temperature. Temperature gradients were obtained at 1 m and 2 m heights from fine wire chromel-constantan thermocouples. Soil temperatures were measured at 2 cm and 6 cm depths and were averaged over 4 sensors. Volumetric soil water was measured from 0-15 cm soil depth with a soil moisture probe connected to a data logger (Campbell Scientific, CS615). Soils were classified as Olney-Owlcreek fine sandy loams. Sand, silk and clay contents for A horizon were 67%, 18%, and 15%, respectively.

3.3.3 Midday water potential

Leaf water potential was measured over two growing seasons of 2000 and 2001 on 1-2 leaves each of *B. gracilis* and *P. smithii* with a Scholander-type pressure chamber (PMS instrument Company, Corvallis, OR, USA). Measurements were taken mid-morning (1000-1145 hrs MST) when plants were typically active and sampled leaves were processed immediately after being cut.

3.3.4 Flask measurements

Air samples were collected approximately every four hours during 24- hour periods at two heights (1m and 2m) from tubing located on a BREB tower during the two growing seasons, 2000 and 2001. Samples were collected in glass flasks with a volume of 2.5 L, after flushing at least 10 volumes through the flasks. All samples were dried during collection using magnesium perchlorate to avoid isotopic exchange with minute quantities of liquid water in flasks. Flasks were analyzed for CO_2 using a high-precision non-dispersive infrared gas analysis system used for the NOAA global flask network (Conway et al. 1994). Samples were analyzed for $\delta^{18}O$ of CO_2 via dual-inlet isotope ratio mass spectrometry with a precision of better than ± 0.05 ‰ (Trolier et al. 1996). The ^{18}O of ecosystem respiration was determined with application of Keeling plots and estimated using the y-intercept of a geometric mean regression of $\delta\ ^{18}O$ versus $1/[CO_2]$. The Keeling plot approach assumes that only two sources are present and those sources do not vary over time associated with the measurement period of the observations used to construct the Keeling plots. Uncertainties were reported as the standard error of the intercept.

3.3.5 ^{18}O of CO_2 from headspace on C_3, C_4, mixed C_3 and C_4, and bare ground patches

We used closed chambers (10 cm tall, 10 cm in diameter) to evaluate isotopic composition of CO2 respired from the four cover types, including C_3, C_4, mixed C_3-C_4 patches, and bare ground. We selected *Pascopyrum smithii* and *Bouteloua gracilis* for dominant C_3 and C_4 plant species, respectively. The chamber bases were placed 2 cm into the soil approximately one month before experiments were initiated, to allow for

adjustments of potential disturbance to plant and soil environments. Each cover type had three replicates. They were located about 30m from the site of flask collections (Fig.3.1).

Air sampling was performed at 8 hour intervals (around noon (D), midnight (N) and early morning on second day (E)) each diurnal set in May, June and July 2001. The chamber samples were collected immediately after completion of ecosystem exchange using flask air sampling techniques at BREB tower. Due to a strong storm in September, only daytime sampling was allowed. Static, closed chambers were sampled at time 0 and again 10 minutes later. A sterile air bladder was used in each chamber to maintain constant air pressure in the chamber while syringe samples (20cc) were withdrawn. A magnesium perchlorate trap was installed in front of the greased glass syringe to avoid isotopic exchange with minute quantities of liquid water in syringes. The syringe samples were analyzed within 36 hours for CO_2 concentrations using infrared gas absorption (precision +/- 1 μmol mol^{-1}) and for isotope ratios using continuous flow mass spectrometry (precision +/- 0.1‰; Pendall et al. 2003). We calculated Keeling plots by geometric mean regression to estimate $\delta^{18}O$ of respired CO_2 from C_3, C_4, mixed C_3-C_4, and bare ground patches ($\delta^{18}O_{R\text{-}C3}$, $\delta^{18}O_{R\text{-}C4}$, $\delta^{18}O_{R\text{-}M}$, and $\delta^{18}O_{R\text{-}B}$, respectively). Data were pooled from all three chambers to generate a single Keeling plot for community type. Flask data were used for background values.

3.3.6 ^{18}O of precipitation, soil and leaf water

Precipitation samples were collected for isotope analysis on a daily basis at the Central Plains Experimental Range Headquarters, about 2 km from the BREB tower. Rainfall amounts less than 2mm were excluded from weighted isotopic average values.

Soil samples were collected from 8 depths (1, 3, 5, 7, 10, 15, 25 and 50cm) during each diurnal sampling date during 2000 and 2001 to conduct analysis of soil water content and isotopic composition. In 2001, samples were collected from two separate soil pits located within two blocks to examine variability in the depth profile of $\delta^{18}O$ of soil water. Collected soil samples were sealed and stored frozen in glass vials until analysis for gravimetric soil water content and soil water $\delta^{18}O$. The $\delta^{18}O$ of the water was analyzed after direct equilibration with CO_2 using dual-inlet isotope ratio mass spectrometry.

Leaf samples were collected for analysis of $\delta^{18}O$ of water during air sample collections during the growing season in 2000. The leaf samples were stored in glass vials wrapped with wax film, and kept frozen until analysis. Leaf water was extracted by cryogenic vacuum distillation. Extracts were equilibrated with CO_2 and analyzed for $\delta^{18}O$ by dual-inlet mass spectrometry.

3.3.7 Modeled soil temperature and moisture profiles

We modeled diurnal changes in soil temperature and moisture in order to simulate the diurnal changes in $\delta^{18}O$ of soil respired CO_2 ($\delta^{18}O_{SR}$). We used a model developed by Parton and Logan (1981) for estimating diurnal variations in soil temperature by depth ranging from 0-50 cm given the maximum and minimum soil temperature. A truncated sine wave was used to predict variation of daytime temperature and an exponential function to predict nighttime temperatures (Parton and Logan, 1981).

We estimated diurnal variations in the soil moisture profile by depth, using automatic 20 minute –volumetric soil moisture measurements averaging the top 0-

15cm soil depth and a soil moisture profile from 0 to 50 cm soil depth (3-5 cm intervals) measured on each sampling period. Polynomial equations (provided by KaleidaGraph software) were derived to predict diurnal variations in soil moisture profiles. Soil moisture gradients by depth were corrected based on measured soil moisture data at 0 to 50 cm. Polynomial equations depicting diurnal pattern of soil moisture were applied to each soil layer. When little diurnal variations in surface soil moisture were observed, we assumed measured soil moisture profile by depth was constant throughout a day.

3.3.8 Modeled $\delta\ ^{18}O$ of soil respired CO_2

We used Tans' model to estimate $\delta^{18}O$ of soil respired CO_2 (Tans 1998; Miller et al. 1999). This model has been developed to calculate $\delta^{18}O$ of root and soil respiration as a function of soil water, temperature-dependent equilibrium (ε_{eq}) and kinetic fractionation (ε_k) (Tans 1998; Miller et al. 1999). The boundary conditions of atmospheric ^{13}C and ^{18}O signatures measured in flasks, estimated soil moisture and temperature profiles by each layer on hourly basis and CO_2 production from chamber measurements were used to run the model. The $\delta^{18}O$ of soil water measured once per sampling date was used to produce a continuous time series by assuming that the measured value was representative of a period 12 hours before and after the measurement.

The model incorporates the influence of abiotic or invasion fluxes and uses analytical solutions for the $\delta^{18}O$ value of soil gas CO_2 and surface CO_2 fluxes for a range of environmental conditions. Miller et al. (1999) noted that the magnitude of invasion defined as 'diffusion-equilibration-retrodiffusion process' in natural systems is likely to

be much smaller than in chamber systems. In order to assess natural variability in $\delta^{18}O$ of soil respired CO_2 at the ecosystem scale, we assumed the residence time of air was not greater than tens of seconds and contributions of invasion to δ_a would be small. For comparison between chamber measurements and model results, we assumed the residence time of air in chambers is large so soil water $\delta^{18}O$ values near the surface may magnify the effect of $\delta^{18}O$ of retrodiffused CO_2. Adjustment of model flushing rate was made by comparison of surface $\delta^{13}C$ of CO_2 from the model and those from chamber measurements. Diffusion discrimination factor (4.4‰) was deducted from the surface $\delta^{13}C$ of soil respired CO_2 for the comparison. CO_2 production specific to each chamber measurement was used as input data entry.

We used an empirical equation describing the tight relations between effective kinetic fractionation and volumetric soil water content in the shortgrass steppe (Pendall, unpublished data).

$$Y\ (‰) = 14.48 * X + 3.4\ (R^2 = 0.55) \qquad (3.1)$$

Where Y is effective kinetic fractionation factor (‰) and X is volumetric soil water content. Effective kinetic fractionation was subtracted from the isotopic value of the CO_2 equilibrated with surface soil water because diffusion causes the $\delta^{18}O$ values for soil CO_2 and soil-respired CO_2 to differ.

3.3.9 Modeled $\delta^{18}O$ of leaf water and leaf respired CO_2

Because no ^{18}O signature for leaf water was measured during 2001, evaporative enrichment of leaf water was modeled using the Craig-Gordon model (Craig and Gordon

1965) as described by Flanagan et al. (1991, 1997).

$$\delta^{18}O_{LW} = \delta_{sw} + \varepsilon_{eq} + \varepsilon_{\kappa} + h\,(\delta_a - \varepsilon_{\kappa} - \delta_{sw}) \qquad (3.2)$$

Where δ_{sw} is $\delta^{18}O$ of source water that plants use and δ_a is $\delta^{18}O$ of atmospheric vapor, h is relative humidity at the leaf surface temperature and the fractionation factors are defined below. For the comparison of modeled $\delta^{18}O$ of leaf water with measured values in 2000, we assumed the source water for plant use (δ_{sw}) is average of top 25 cm of soil water for both C_3 and C_4 plants (Ferretti et al. 2003). In order to evaluate contributions of C_3 and C_4 grasses to $\delta^{18}O$ of chamber respirations in detail in 2001, we assumed C_3 and C_4 plants should have different δ_{sw} because of their different root distribution patterns. We used $\delta^{18}O$ of soil water at 25 cm for the representative source water for C_3 plants and at 10 cm for C_4 plants. The amount of soil volumetric water content weighted $\delta^{18}O$ of soil water corresponding to a depth was used for δ_{sw}. We calculated leaf temperature using an energy budget approach for the leaf (Campbell and Norman 1989). Since the boundary layer of grass is rather smooth, the leaf temperature was higher by 1-2 °C than air temperature during daytime. The ε_{κ} is the kinetic fractionation factor. ε_{κ} can be calculated as (Farquhar et al. 1989):

$$\varepsilon_{\kappa} = \frac{32r_s + 21r_b}{r_s + r_b} \qquad (3.3)$$

where r_s and r_b are the stomatal and boundary layer resistances to water vapor diffusion (m^2 s mol^{-1}), and 32 and 21 are their respective fractionation factors (‰). These fractionation values have been revised based on recent experiments showing $^{16}O/^{18}O$=1.032 (Cappa et al. 2003) rather than 1.028 (Merlivat, 1978).

The $\delta^{18}O$ of atmospheric water vapor (δ_a) is estimated by assuming air moisture is near equilibrium with the local precipitation water at corresponding air temperature. The equations of Majoube (1971) were used to calculate the temperature dependent fractionation factor (ε_{eq}) for liquid vapor equilibrium.

Modeled values for $\delta^{18}O_{LW}$ were used to compute $\delta^{18}O_{LR}$. Due to different extent of isotopic equilibrium and different CA hydration rates between C_3 and C_4 plants, the equations of Gillon and Yakir (2000) were applied to each functional group and then $\delta^{18}O$ was scaled to the canopy based on relative productivity. $C^{18}O^{16}O$ discrimination ($\Delta^{18}O$) accounts for possible incomplete isotopic equilibrium and was expressed as:

$$\Delta^{18}O = \varepsilon_k' + c_\varepsilon[\theta_{eq}(\delta_e - \delta_{a\_co_2}) - (1-\theta_{eq})\varepsilon_k'/(c_\varepsilon + 1)] \qquad (3.4)$$

where ε_k' is the weighted mean of discrimination during the diffusion from ambient air to the sites of carboxylation within the chloroplast including smaller fractionations in the laminar boundary layer and during diffusion through solution (7.4‰; Farquhar et al. 1993); δ_e refers to the $\delta^{18}O$ of CO_2 in equilibrium with chloroplast water. We estimated chloroplast water mentioned above at the site of CO_2-H_2O equilibrium. The δ_{a_co2} is the oxygen isotope ratio of CO_2 in the atmosphere; $C_\varepsilon = c_{cs}/(c_a - c_{cs})$; c_{cs} and c_a are CO_2

concentrations at the site of CO_2-H_2O exchange in leaves and in ambient air, respectively. c_{cs} was estimated from $(c_i-c_{cs})/c_a = 0.1$ (Farquhar et al. 1993; Wang et al. 1998). The c_i is CO_2 concentration in the stomatal cavity and estimated from the photosynthesis model mentioned below. The estimation of c_{cs} is necessary because CO_2 mixing ratios at the site of Rubisco (c_c) and of chloroplast surface can be significantly different due to large internal resistances (Gillon and Yakir, 2000). The θ_{eq} is a factor describing the effect of CA on isotopic equilibrium, for which we assumed the constant mean estimates (0.7 and 0.52 for C_3 and C_4 plants, respectively) derived from Gillon and Yakir (2000).

Leaf biomass was used to scale the relative contribution from both functional groups to canopy ^{18}O discrimination following

$$\Delta^{18}O_{canopy} = \sum_{i=3,4} P_i \Delta^{18}O_i \qquad (3.5)$$

P represents % weighted aboveground plant biomass. The i represents plant functional types.

3.3.10 The photosynthesis model for estimating C_i

Independent modeling of canopy assimilation and conductance by plant functional group (C_3 versus C_4) was performed to estimate intercellular CO_2 concentration, C_i. For mixed C_3-C_4 ecosystems to be simulated, photosynthesis subroutines cycle twice, once for each physiological type; separate photosynthetic assimilation rate and overall surface conductance from the two components are calculated.

The parameterizations of photosynthesis and stomatal and canopy conductance are based on equations in Farquhar et al. (1980), Collatz et al. (1991) and Ball et al. (1987). Parameters used for the photosynthesis model are listed and detailed equations are presented in Appendix.

3.3.11 Calculation of contributions of leaf and soil components to $\delta^{18}O$ of respired CO_2 from chamber to ecosystem scales

We anticipated that $\delta^{18}O_R$ would lie between the isotopic compositions of soil-respired ($\delta^{18}O_{SR}$) and leaf-respired fluxes ($\delta^{18}O_{LR}$). Conservation of mass dictates that:

$$\delta^{18}O_R = f\,\delta^{18}O_{SR} + (1-f)\,\delta^{18}O_{LR} \qquad (3.6)$$

where f is the fraction of soil respiration; $\delta^{18}O_R$ represents $\delta^{18}O$ of ecosystem respiration derived from Keeling plots; $\delta^{18}O_{SR}$ and $\delta^{18}O_{LR}$ were estimated from the models mentioned above.

We also estimated contributions of oxygen isotopic compositions of soil respiration and leaf respiration to $\delta^{18}O$ of each chamber respiration from

$$\delta^{18}O_{CR} = f * \delta^{18}O_{LR\text{-}i} + (1-f)* \delta^{18}O_{SR\text{-}i} \qquad (3.7)$$

where $\delta^{18}O_{CR}$ represents Keeling plot intercepts from each chamber; i represents each chamber component such as C_3, C_4 and mixed C_3 and C_4; $\delta^{18}O_{LR\text{-}i}$ is derived from modeled isotopic composition of leaf respiration by each component; $\delta^{18}O_{SR\text{-}i}$ is

estimated from Tans' (1998) model. All oxygen isotope ratios in this paper for water and CO_2 are referenced to the Vienna Standard Mean Ocean Water (V-SMOW) scale (Coplen, 1994) and are presented in dimensionless units of ‰.

3.3.12 Statistical analysis

Since isotopic analyses for $\delta^{18}O$ of respired CO_2 from chambers were conducted on only one site, we tested for differences in $\delta^{18}O$ of respired CO_2 from chambers using the PROC MIXED procedure for a design with fixed effects of treatment, month and time of day. Random effects were location, treatment * location, treatment * month * location and residual. We performed the PROC MIXED procedure where both month and time of day were repeated measurements.

For each vegetation type, data were pooled from three replicates to generate a single y intercept derived from Keeling plots; there was a significant time of day effect, but no time of day by treatment interaction

3.4 Results

3.4.1 Water cycles and vapor pressure deficit (VPD) over two years

The years 2000 and 2001 had similar annual precipitation amounts, but 2000 was dry and 2001 was moist in the early growing season, a critical period for biomass production in the shortgrass steppe (Lauenroth and Milchunas 1991; Table 3.1). In both years, $\delta^{18}O$ of precipitation was low in the early growing season and increased as the season progressed (Table 3.1). In general, vapor pressure deficit (VPD) was higher in 2000 than in 2001 from mid-May through July. The frequency of rainfall events was relatively very low in 2000 compared to 2001 (Fig.3.2).

The response of soil moisture to precipitation events was dependent on the intensity of precipitation and history of water conditions. With large rainfall events (>

7 mm) in mid-May and early August, 2000, soil moisture increased drastically and then gradually decreased. Little fluctuation was triggered by several small events ($\leq$ 7 mm). In 2001, relatively frequent and large rains in the early growing season led to moist soil conditions, then soil moisture conditions became drier toward late growing season. There were no rainfall events during sampling periods in 2000, while light rainfall events were recorded during sampling dates in May and July 2001 (1.4 mm and 6 mm, respectively). The smaller rainfall events had no little effect on soil moisture availability in both months of 2001.

Diurnal patterns in relative humidity illustrated that dry conditions prevailed in 2000 (Fig.3.3). Over all eight sampling periods, July 2000 was notably dry while moist conditions prevailed in May 2001.

3.4.2 Midday leaf water potential

Average leaf water potential for both C_3 and C_4 species was lower in 2000 than in 2001 (Table 3.2). In 2000, lowest leaf water potential was recorded in July indicating severe water stress on plants. The C_3 species, *P. smithii* had consistently lower leaf water potential compared to *B. gracilis*, the C_4 species, throughout the growing seasons.

3.4.3 ^{18}O of soil water

$\delta^{18}O$ values of soil water ($\delta^{18}O_{SW}$) increased over each growing season, especially between 3 and 5 cm-depth in the soil profile (Fig.3.4). Soil water $\delta^{18}O$ values decreased with depth in 2000, which is consistent with large extent of evaporation in the upper 15 cm or so. The highest $\delta^{18}O$ values were observed at 3-5cm depths in most of months in

2000 and May and July 2001. Surficial values may have been lower possibly because of vapor equilibration with moisture in the top cm of the soil. We observed a gradual decrease in $\delta^{18}O_{SW}$ from 3-5 cm to 50 cm, and a gradual increase in $\delta^{18}O$ at each depth over the course of the growing season as soil evaporation and $\delta^{18}O$ of precipitation increased, and soil moisture decreased (Table 3.1; Fig.3.2)

The magnitude of seasonal differences in $\delta^{18}O_{SW}$ was greater in 2001 than in 2000. In general, soil water content and isotopic composition during both growing seasons approximated an evaporating profile (Allison et al. 1985). The soil progressively dried out from May to September. The soil water profile estimate of depth weighted average $\delta^{18}O$ (Figure 3.4) correlates well with the pattern of increasing soil evaporative enrichment during the latter periods of the growing season. The surface $\delta^{18}O$ of soil water is related to evaporative strength that is influenced by VPD to some degree.

3.4.4 ^{18}O of measured and modeled leaf water

In general, there was a tendency for measured $\delta^{18}O$ of leaf water ($\delta^{18}O_{LW}$) to be enriched during the daylight and to be depleted at night in 2000 (Fig.3.5). Variation in vapor pressure deficit is one factor controlling $\delta^{18}O_{LW}$ via transpiration. $\delta^{18}O_{LW}$ was highly enriched during daylight in July and June 2000 when high leaf temperature and more enriched $\delta^{18}O$ of atmospheric water vapor were estimated during those sampling dates.

The modeled values for $\delta^{18}O_{LW}$ were calculated for a 20 min interval corresponding to the time foliage was collected. Modeled values for $\delta^{18}O_{LW}$ were linearly

related to measured values in 2000 (R^2 = 0.88) (Fig.3.5). Best fit between modeled and measured $\delta^{18}O_{LW}$ was observed in September (R^2 = 0.98). Measured $\delta^{18}O_{LW}$ was slightly more depleted relative to modeled values.

The diurnal cycles of modeled $\delta^{18}O_{LW}$ ranged from -10 to 30‰ (Fig.3.6).The modeled $\delta^{18}O_{LW}$ showed the largest variation in June 2000 with the lowest values during early morning of first day and the highest ones during same period of the second day of sampling. Overall modeled $\delta^{18}O_{LW}$ was high in July 2000. In 2001, the lowest modeled $\delta^{18}O_{LW}$ from 1300 to 0800 in May 2001 when shallow rainfall events occurred for 6 hours (Fig.3.2). This coincided with relatively ^{18}O-depleted atmospheric water vapor and source water in top 25 cm below soil surface, low leaf temperature and consistently high relative humidity (Fig.3.3). However, brief rainfall events occurred in July 2001 for 20 minutes (1320-1340 on the first day) and were not persistent enough to induce depleted $\delta^{18}O_{LW}$

There were no apparent differences in modeled values in $\delta^{18}O_{LW}$ between C_3 and C_4 grasses in June 2001 (relatively moist conditions), when soil $\delta^{18}O_{SW}$ did not vary much (Fig. 3.7). Explicit soil $\delta^{18}O_{SW}$ gradient between surface and deep soils enlarged the differences in modeled $\delta^{18}O_{LW}$ between two species in July 2001 (dry conditions) showing consistently higher $\delta^{18}O_{LW}$ values in C_4 plants.

3.4.5 Modeled soil respired and leaf respired ^{18}O in 2001

In general, the modeled $\delta^{18}O$ values of soil respiration ($\delta^{18}O_{SR}$) were higher in 2000 than in 2001 (Fig.3.9). Especially low $\delta^{18}O_{SR}$ was observed in May, 2001. More

dynamic variations in $\delta^{18}O_{SR}$ were observed in 2001 than 2000. There was a tendency for increasing $\delta^{18}O_{SR}$ toward late growing season.

The modeled diurnal patterns of $\delta^{18}O$ of leaf respiration ($\delta^{18}O_{LR}$) were less apparent in 2000 than in 2001 (Fig.3.10) even though more variable diurnal patterns in $\delta^{18}O$ of leaf water were modeled in 2000 (Fig.3.6). The modeled internal CO_2 concentrations at chloroplast surfaces were extremely low in June and July 2000 during the daylight periods possibly because of high VPD (data are not shown). A peak in $\delta^{18}O_{LR}$ was observed in late afternoon of September 2000 (Fig. 3.10a). Modeled $\delta^{18}O_{LR}$ tended to follow the general pattern of modeled $\delta^{18}O$ of leaf water relatively well in 2001.

Diurnal variation in $\delta^{18}O_{LR}$ was greatest in May 2001. The largest diurnal variations of $\delta^{18}O_{LR}$ might be attributed to precipitation events that occurred in the middle of sampling periods. Precipitation produced depleted $\delta^{18}O_{LW}$, $\delta^{18}O_{LR}$, and $\delta^{18}O_{SR}$ compared to before the rain event. Between rainfalls, increases in vapor pressure deficit of air for daytime led to isotopic enrichments of soil and leaf water pools, which influenced ^{18}O of leaf respiration.

Despite no apparent differences in $\delta^{18}O_{LW}$ (modeled) between C_3 and C_4 grasses in June 2001(moist conditions), consistently higher $\delta^{18}O_{LR}$ was modeled in C_3 grasses during daytime periods (Fig.3.8). The diurnal cycle of $\delta^{18}O_{LR}$ in C_4 plants was similar to $\delta^{18}O_{LR}$ in C_3 plants in July 2001 (dry conditions) even though higher $\delta^{18}O_{LW}$ was modeled in C_4 grasses in July 2001.

3.4.6 $\delta^{18}O$ of respired CO_2 measured from headspace of C_3, C_4, mixed C_3 and C_4, and bare ground

Average $\delta^{18}O$ of chamber respiration ($\delta^{18}O_{CR}$) generally increased over the growing season (Fig.3.11). In May, no significant differences among cover types were observed. In June, $\delta^{18}O_R$ was higher in C_3 patches than in C_4 patches throughout the day. There were no significant differences between C_3 and mixed C_3 and C_4 patches. The $\delta^{18}O_{CR}$ was lowest from bare ground patches in June and July. Lower $\delta^{18}O$ values from bare ground patches might be attributable to the exclusion of enriched $\delta^{18}O$ of foliar respiratory fluxes and the isotopic exchange of soil respired CO_2 with the depleted soil water. Interestingly, plant functional group differences were not apparent in July.

3.4.7 Comparisons of modeled $\delta^{18}O$ of soil respired CO_2 with measured $\delta^{18}O$ of respiration from four different vegetation types

Seasonal variations in modeled $\delta^{18}O$ of soil respired CO_2 ($\delta^{18}O_{SR}$) are functions of $\delta^{18}O$ of source water, CO_2 production, soil temperature and moisture conditions. The relationships between modeled and measured $\delta^{18}O_{SR}$ were highly correlated, with $R^2 = 0.85$ and slope = 1.34 during June and July 2001. However, modeled $\delta^{18}O_{SR}$ CO_2 under environments specific to each vegetation type (with varying CO_2 production) were all overestimated relative to Keeling plot intercepts from same vegetation types in May (Table 3.3 and Fig.3.11).

Estimates of $\delta^{18}O_{SR}$ were lowest in June and highest in July. The modeled $\delta^{18}O$ signatures from bare ground patches tend to be higher than patches with plants from May

through July. Such spatial variations might be attributable to differences in CO_2 production rates among each vegetation types (Table 3.3).

3.4.8 Variations of vertical CO_2 concentrations, $\delta^{13}C$ and $\delta^{18}O$ values of air

We observed general diurnal patterns of atmospheric CO_2 concentrations indicating photosynthetic activity consumes ambient CO_2 concentrations during daytime over two years, however, the degree of diurnal variation in CO_2 concentration was dependent on seasonal activity of plants, soil moisture conditions, and aerodynamic conditions. The diurnal differences in CO_2 concentrations were smallest in July 2000 (9.33 μmol mol^{-1}) and largest in June 2001(41.64 μmol mol^{-1}; Table 3.4).

The influence of biotic activity on CO_2 concentrations is expected to be greater at 1m than 2 m height. No significant height gradients were recorded in May, July 2000, or July 2001. The largest sinks and source gradients occurred in June 2000 and 2001.

3.4.9 Variations in ^{18}O of ecosystem respiration ($\delta^{18}O_R$)

Strong positive relations between $\delta^{18}O$ of air and inverse CO_2 concentrations were observed under moist conditions, May and June of 2001 (r^2=0.95 and 0.91). The $\delta^{18}O_R$ determined from Keeling plots, was highly variable within a day. The range of observed $\delta^{18}O_R$ was –5.18 to 27.93 ‰ from May to July, 2001 (Table 3.4). In 2000, we observed increasing $\delta^{18}O$ of atmospheric CO_2 at night in connection with increasing CO_2 concentration (expressed as dashed line in Table 3.4), counter to the expected relationship. Keeling intercepts derived from night and early morning respiration at approximately 4 hour intervals showed remarkably depleted ^{18}O signature in May 2001. The modeled

$\delta^{18}O_{LW}$ beginning 1740 to 0740 (local time) was lower than that of measured $\delta^{18}O_{SW}$ (Fig3.4 and 3.6).

3.4.10 Contributions of leaf and soil components to total $\delta^{18}O$ of respired CO_2 from patch to ecosystem scale

The contribution of soil respiration to ecosystem respiratory $C^{18}O^{16}O$ flux was > 50% and was more pronounced in July than in June 2001 (Table 3.5).

At the patch scale, fractional contribution of soil respiration $C^{18}O^{16}O$ fluxes to the corresponding $\delta^{18}O$ of chamber respiration in C_4 plots were generally higher than in C_3 and mixed C_3 and C_4 plots in June. In July 2001, soil respiratory $C^{18}O^{16}O$ fluxes from all three plots had dominant influence on chamber respiratory $C^{18}O^{16}O$ fluxes.

3.5 Discussions

To understand how the isotopic composition of soil and foliar respiratory fluxes ($\delta^{18}O_{SR}$ and $\delta^{18}O_{LR}$, respectively) influence $\delta^{18}O$ of ecosystem respiration ($\delta^{18}O_R$), we present the sources of variations such as $\delta^{18}O$ of soil and leaf water ($\delta^{18}O_{SW}$ and $\delta^{18}O_{LW}$) then how these water pools influence $\delta^{18}O_{SR}$ and $\delta^{18}O_{LR}$.

3.5.1 Variations in seasonal and diurnal patterns of $\delta^{18}O$ of water pools (precipitation, soil and leaf water) and $\delta^{18}O$ of leaf and soil respired CO_2 over two growing seasons

The isotopic content of precipitation initially controls $\delta^{18}O$ of soil water. The $\delta^{18}O$ of precipitation was more negative during the early growing seasons and more enriched

during later growing seasons. The measured seasonal variations in $\delta^{18}O_{SW}$ generally reflected the seasonal pattern in $\delta^{18}O$ of precipitation to some degree but evaporative enrichment in $\delta^{18}O$ near the soil surface prevailed in 2000 and July and September 2001. The larger seasonal changes in $\delta^{18}O_{SW}$ in 2001 led to more seasonal differences in $\delta^{18}O_{SR}$ compared to 2000.

Very large diurnal changes in $\delta^{18}O_{LW}$ (maximum 38‰) were modeled and attributed to changes in relative humidity (Fig3.3) and leaf temperature. The large diurnal changes in $\delta^{18}O_{LW}$ amplified $\delta^{18}O_{LR}$, especially during moist conditions. Considerable variation in $\delta^{18}O_{LR}$ within a single night were reported in forests (Bowling et al. 2003 a and b). Interestingly, the nocturnal $\delta^{18}O_{LR}$ values in the first day of May and September 2001 were peaked over 65 ‰. Strikingly high $^{18}O_{LR}$ was observed in a leaf dark respiration experiment when there was a relatively large difference between $\delta^{18}O$ of CO_2 in chloroplast and in atmosphere, and when stomata were relatively open (Cernusak et al. 2004).

The controls of $\delta^{18}O_{LW}$ were revealed in variations in $\delta^{18}O_{LR}$ during moist conditions. However, variations in $\delta^{18}O_{LW}$ alone were not sufficient for explaining variations in $\delta^{18}O_{LR}$ in dry conditions. When the initial source water was highly enriched due to high VPD, the variations in $\delta^{18}O_{LR}$ were reduced and became sensitive to other factors such as Ci/Ca and CA controlled equilibrium between CO_2 and H_2O. Plant physiological water stress induced by high VPD was observed in dry conditions during 2000 (Table 3.2). The higher VPD also would lead to a decrease in stomatal conductance. This in turn would decrease C_{cs} and $C^{18}O^{16}O$ discrimination by the plants (Farquhar et al.

1993; Williams et al. 1996). The C_ϵ values ($C_\epsilon = c_{cs}/(c_a-c_{cs})$) were extremely low in dry periods of 2000 (data are not shown), which might diminish the contribution of $\delta^{18}O$ of leaf water to $\Delta C^{18}O^{16}O$.

3.5.2 Validity of Keeling plots for use with $\delta^{18}O$ of ecosystem respiration

Our Keeling plot approach for use with $\delta^{18}O$ of ecosystem respiration over two years resulted in success during moist periods with no precipitation events. Apparently, assumptions behind the Keeling plot approach were violated for the rest of the measurements. For 2000, we observed an increase in the $\delta^{18}O$ of atmospheric CO_2 at night in connection with the increase in atmospheric CO_2 concentration. This suggested that soil respired CO_2 had equilibrated with water that was very enriched in ^{18}O. This might be explained by inactivity of plants due to severe water deficit and higher $\delta^{18}O$ of respired CO_2 equilibrated with soil water that was very enriched in $\delta^{18}O$. Weak relationships between $\delta^{18}O$ and the reciprocal of CO_2 have been reported (Flanagan et al. 1997; Sternberg et al. 1989), because there can be changes in $\delta^{18}O$ without corresponding change in CO_2 concentration, owing to isotopic equilibration between leaf and soil water, and in some cases moss water and dew (Bowling et al. 1999).

The $\delta^{18}O$ intercept for the dry season in 2000 was more negative than that of the wet season in 2001, indicating the low leaf respiration in dry periods would result in less input of CO_2 relatively enriched in ^{18}O from foliage respiration compared to the moist periods. However, the $\delta^{18}O$ intercept was very low during the nighttime measurements in May 2001 just after rainfall occurred. Relatively depleted precipitation primarily

controlled $\delta^{18}O_{SW}$. Very depleted leaf water was also modeled because the water had not yet gone through evaporative enrichment. The consequences of depleted $\delta^{18}O_{SR}$ and $\delta^{18}O_{LR}$ that were controlled by isotopic source water pools led to the lowest $\delta^{18}O_R$ in May 2001 (Fig.3.9 and 3.10). Lower $\delta^{18}O_R$ values of chamber respiration were also clearly shown (Fig.3.11).

The $\delta^{18}O$ of ecosystem respiration ($\delta^{18}O_R$) is expected to lie between that of leaf and soil respired CO_2. The $\delta^{18}O_R$ plotted beyond the theoretical bounds between leaf and soil respired CO_2 in 2000 (Table 3.4, Fig.3.9 and 3.10). In 2001, the $\delta^{18}O_R$ was more depleted than that expected from soil-respired CO_2 in equilibrium with soil water assuming precipitation water directly recharged to source water in May. Similar results were reported in Flanagan et al. (1994). Measured $\delta^{18}O_R$ was more negative than the predicted $\delta^{18}O_{SR}$ when samples were collected during intermittent mild rain events. Only when no rainfall events occurred and conditions were moist enough for plant activity were the values of $\delta^{18}O_R$ intermediate between $\delta^{18}O_{LR}$ and $\delta^{18}O_{SR}$; generally, $\delta^{18}O_R$ was more similar to $\delta^{18}O_{SR}$.

3.5.3 The role of plant functional group in respiratory $C^{18}O^{16}O$ fluxes

We observed significant linear relationships between $\delta^{18}O$ and $1/[CO_2]$ from the patch scale respiration chambers. Seasonal and diurnal variations of measured $\delta^{18}O$ of respiration from combined plant and soil chambers can be explained by environmental variables such as relative humidity, source water taken by plant roots, CO_2 production and $\delta^{18}O$ of water vapor to some degree.

In general, increases in averages of $\delta^{18}O$ of respired CO_2 from the chamber measurements ($\delta^{18}O_{CR}$) later in the growing season might be attributable to increases in the isotopic composition of leaf and soil water, which we expect to strongly control $\delta^{18}O$ of leaf respired and soil respired CO_2. The greater VPD experienced, the greater the enrichment of chloroplast $H_2{}^{18}O$ observed (Craig and Gordon, 1965; Flanagan, 1993). On the other hand, the higher VPD causes a decrease in stomatal conductance resulting in a decline in $C^{18}O^{16}O$ discrimination by plants (Farquhar et al. 1993). The dominant influence of evaporative enrichment of ^{18}O in source water appears to overshadow the stomatal response to VPD at our semi-arid grassland site.

$\delta^{18}O_{CR}$ of bare ground patches was lower relative to that of vegetated patches in June and July 2001 probably because it largely reflects CO_2 in equilibrium with depleted soil surface water with the exclusion of $\delta^{18}O_{LR}$.

In June 2001, $\delta^{18}O_{CR}$ of C_4 plots was considerably lower than C_3 plots. Relatively shallower roots were distributed in C_4 plants than C_3 plants suggesting different usage of source water by depth between the two species. However, the ^{18}O source soil water for both C_4 and C_3 plants are unlikely to be different in June 2001 (Fig.3.4). During this time period, modeled $\delta^{18}O_{LW}$ values for C_3 and C_4 grasses also displayed little differences (Fig.3.7). Additionally, the effect of CO_2 production on $\delta^{18}O_{SR}$ between the two plant communities might also be trivial as indicated by modeling results (Table 3.3). The sensitivity of model result between plant community treatments relied only upon CO_2 production with depth since different extent of isotopic equilibrium and different carbonic anhydrase (CA) hydration rates by C_3 versus C_4 plants was not accounted for in

the model, and identical $\delta^{18}O$ of source water and soil moisture were applied for each treatment as input variables. Therefore, $\delta^{18}O_{CR}$ from C_3 and C_4 plots might be sensitive to other factors such as Ci, Ca, Ccs, and $\theta_{eq.}$ In our study, less foliar retrodiffusional flux caused by low internal CO_2 concentrations and low CA activity appear to be more influential to $C^{18}O^{16}O$ fluxes in C_4 patches in relatively moist condition.

Interestingly, the explicit differences in $\delta^{18}O_R$ between C_3 and C_4 patches shown in June disappeared in July and September. We observed large $\delta^{18}O$ of soil water gradients between the upper-most soil depth (0-15cm) and the deep soil depth (50cm) in July and September 2001 (Fig.3.4) indicating increasing evaporative enrichment of surface soil water. This influenced $\delta^{18}O_{LW}$ variations of two species showing higher $\delta^{18}O_{LW}$ in C_4 grasses (Fig.3.7 b). The effect on $\delta^{18}O_{SR}$ between two plant communities might also be trivial (Table 3.3). For $\delta^{18}O$ of leaf respired CO_2 from C_4 plots, it is expected that there should be a compensation between enrichment of leaf water and incomplete isotopic equilibrium between CO_2 and H_2O with low CA activity in C_4 plants leading to more depleted values (Farquhar and Lloyd 1993; Gillon and Yakir 2000). There were also no apparent differences in the modeled $\delta^{18}O_{LR}$ values between C_3 and C_4 grasses (Fig.3.8). This supported the fact that relatively less foliar retrodiffusional flux and CA activity leading to low $\delta^{18}O_{LR}$ in C_4 plants might be compensated by use of more enriched soil surface water during dry seasons. Relatively high foliar retrodiffusional flux carrying enriched ^{18}O of leaf water in C_3 plants might be compensated by use of more depleted deep soil water. Three counteracting factors such as different root distribution and CA activity between two species, and a marked gradient in soil water

$\delta^{18}O$ profile probably resulted in no differences in $C^{18}O^{16}O$ fluxes between C_3 and C_4 patches.

3.5.4 Consideration of pulse precipitation events in $\delta^{18}O$ of soil water and soil respired CO_2

Ambient CO_2 diffuses into soil, exchanges oxygen atoms with soil water and diffuses back out (Tans 1998). This diffusion-equilibration-retrodiffusion process has been defined as "atmospheric invasion". Diffusing ambient CO_2 usually equilibrates with soil water to some degree determined by residence time in the soil (Miller et al. 1999). Considering that an invasion effect might have occurred during chamber measurements, there was a good correlation between modeled and measured $\delta^{18}O_{SR}$ from bare ground chamber during June and July (slope of 1.34 and R^2 of 0.85). However, modeled $\delta^{18}O_{SR}$ was overestimated during May 2001 compared to measured $\delta^{18}O$ from the respiration chamber.

On the first day of sampling in May, a very small precipitation event (0.3 mm) occurred. Since the size of water input was small, infiltration depth would also be small. Small rainfall events wet only the uppermost cm of the soil, where a large fraction of soil moisture could be lost via evaporation, due to high temperatures.

The response of soil moisture to precipitation events was dependent on the intensity of precipitation and history of water conditions. With large water inputs soil moisture increased drastically, however, little fluctuation was triggered by several small events (less than 7 mm) possibly because of strong evaporative forcing (Fig.3.2). Small intermittent rain events during dry weather conditions could lead to a drastic isotopic

influence on soil water isotopes and thus soil respired CO_2, if respiration is stimulated enough. Soil moisture inertia shown in the relation with small precipitation events might decrease the effective kinetic fractionation factor, which would result in overestimating $\delta^{18}O_{SR}$.

Pulse precipitation events can stimulate heterotrophic activity and lead to bursts of CO_2 production (Irvine and Law, 2002). The CO_2 production could occur near to the surface, which would also reduce the influence of fractionation during diffusion out of the soil and increase the $\delta^{18}O$ value of soil respiration (Hesterberg and Siegenthaler 1991). This may contribute a disproportionate amount of respired CO_2 equilibrated with surface water. The importance of CO_2 concentrations building up in the chamber headspace in calculating the $\delta^{18}O_{SR}$ from chamber data were indicated by Mortazavi et al. (2004) and highlight the influence of surface soil water on $\delta^{18}O_{SR}$. Therefore, the short-grass steppe which experiences pulsed rainfall events (Sala et al. 1992) may express soil respiration pulses which carry ^{18}O signature of the recent rainfall. Modeling such effects is difficult without an explicit soil hydrology model.

Additionally, other factors such as soil respiration distribution and advective transport within the soil might explain the discrepancy between the estimates of $\delta^{18}O_{SR}$ from the model and from respiration chamber (Stern et al. 1999).

3.5.5 Contributions of leaf and soil respiratory $C^{18}O^{16}O$ fluxes to total respiratory $C^{18}O^{16}O$ fluxes from fine to local scales

At the canopy scale, the values of $\delta^{18}O_R$ in June and July 2001 were more similar to $\delta^{18}O_{SR}$. The contribution of soil respiration to total respiratory $C^{18}O^{16}O$ flux

calculated from equation (4) was greater than 80% relative to leaf respired CO_2 for all measurements periods, and such contribution was more pronounced in July (Table 3.5). In an ecosystem where C_3 and C_4 plants coexist, $\delta^{18}O_{SR}$ might have a relatively large impact on the $\delta^{18}O_R$ because C_4 plants discriminate against $C^{18}O^{16}O$ less than C_3 plants (Riley et al. 2003). Interestingly, in respiration chamber measurements, the fractional contribution of soil respiration $C^{18}O^{16}O$ fluxes in C_4 plots was higher than in C_3 and mixed C_3 and C_4 plant plots during moist conditions indicating distinct influence of less foliar retrodiffusional flux due to low CA and low internal CO_2 concentrations in C_4 plants (Farquhar and Lloyd 1993; Gillon and Yakir 2000). The percentage of leaf participation in $C^{18}O^{16}O$ fluxes was approximately 35% in C_3 plots and 12% in C_4 plots during nocturnal moist conditions. On the contrary, the relative contributions of C_3 and C_4 plants to $C^{18}O^{16}O$ fluxes were indistinguishable under dry conditions. Both plant types showed disproportionately high contribution of $\delta^{18}O_{SR}$ to $\delta^{18}O_{CR}$ during dry conditions.

The fractional contribution of soil respiration $C^{18}O^{16}O$ fluxes at the canopy scale was close to that of soil respiration $C^{18}O^{16}O$ fluxes in mixed C_3 and C_4 patches indicating an importance of plant community dynamics in explaining the variability of $\delta^{18}O$ of ecosystem respiration.

3.6 Conclusion

Despite the importance of understanding $\delta^{18}O$ of ecosystem respiration dynamics in global scale models, few studies have been conducted in semi-arid ecosystems with brief periods of water availability (Sala et al. 1992) and of coexistence of C_3 and C_4 plant species. Keeling plot approach for use with respiratory $C^{18}O^{16}O$ fluxes was valid in

relatively moist conditions without pulse rainfall event in the ecosystem. Very low CO_2 production rates during dry periods caused decoupling between $\delta^{18}O$ of atmospheric CO_2 and inverse CO_2 concentrations.

In moist condition, $^{18}O_{CR}$ of C_4 plots was considerably lower than C_3 plots. The source soil water $\delta^{18}O$ signatures both C_4 and C_3 plants utilized were not significantly different, which reflected no apparent differences between separately modeled C_3 and C_4 $\delta^{18}O_{LW}$ values. On the other hand, consistently lower $\delta^{18}O_{LR}$ were modeled in C_4 grasses than C_3 grasses indicating less foliar retrodiffusional flux caused by low internal CO_2 appear to be more influential to $C^{18}O^{16}O$ fluxes in C_4 patches. There were no significant differences in $\delta^{18}O_R$ between C_3 and C_4 patches in dry condition. We observed large $\delta^{18}O$ of soil water gradients between the upper-most soil depth (0-15cm) and the deep soil depth (40-50cm) in dry season indicating increasing evaporative enrichment of surface soil water. This influenced $\delta^{18}O_{LW}$ and $\delta^{18}O_{LR}$ variations of two species showing higher $\delta^{18}O_{LW}$ in C_4 grasses and no significant difference in $\delta^{18}O_{LR}$ between the two. This supported the fact that relatively less foliar retrodiffusional flux leading to low $\delta^{18}O_{LR}$ in C_4 plants might be compensated by use of more enriched soil surface water during dry seasons. Three counteracting factors such as a) different root distribution, b) physiological traits in terms of internal CO_2 concentration and CA activity between two species, and c) a marked gradient in soil water $\delta^{18}O$ profile probably contributed to no differences in $C^{18}O^{16}O$ fluxes between C_3 and C_4 patches during these drier conditions.

$\delta^{18}O$ estimates of the contribution of soil respiration to total ecosystem respiration in shortgrass steppe averaged 89%. Fractional contribution of soil respiration to total

chamber respiration was greater in C_4 plots relative to C_3 plots indicating less foliar retrodiffusional flux caused by low CA and internal CO_2 concentrations might have dominant influence on $C^{18}O^{16}O$ fluxes during moist conditions.

3.7 References

Ball JT (1987) Calculations related to gas exchange In: E. Zeiger, GD Farquhar and IR Cowan (eds.), Stomatal function. Stanford University Press, Stanford, CA. pp. 446-476.

Bowling DR, Baldocchi DD, Monson RK (1999) Dynamics of isotopic exchange of carbon dioxide in a Tennessee deciduous forest. Global Biogeochemical Cycles 13:903-922.

Bowling DR, McDowell NG, Welker JM, Bond BJ, Law BE, Ehleringer JR (2003a) Oxygen isotope content of CO_2 in nocturnal ecosystem respiration: 1. Observations in forests along a precipitation transect in Oregon, USA. Global Biogeochemical Cycles 17, 1120, dio:10.1029/2003GB002081

Bowling DR, McDowell NG, Welker JM, Bond BJ, Law BE, Ehleringer JR (2003b) Oxygen isotope content of CO_2 in nocturnal ecosystem respiration: 2 Short-term dynamics of foliar and soil component fluxes in an old-growth ponderosa pine forest. Global Biogeochemical Cycles 17, 1124, dio:10.1029/2003GB002082.

Brenninkmeijer CAM, Kraft P, Mook WG (1983) Oxygen isotope fractionation between CO_2 and H_2O. Isotope Geosciences 1:181-190

Buchmann N, Ehleringer JR (1998) CO_2 concentration profiles, and carbon and oxygen isotopes in C_3 and C_4 crop canopies. Agricultural and Forest Meteorology 89:45-58.

Buchmann N, Guehl J-M, Barigah TS, Ehleringer JR (1997) Interseasonal comparison of CO_2 concentrations, isotopic composition, and carbon dynamics in an Amazonian rainforest (French Guiana). Oecologia 110:120-131.

Campbell GS, Norman JM (1989) Plant canopy structure. In: Plant Canopies: Their Growth, Form and Function. G Russell, B Marshall, PG Javis (eds.). Cambridge University Press, Cambridge, pp. 1-19.

Cappa CD, Hendricks MB, DePaulo DJ, Cohen RC (2003) Isotopic fractionation of water during evaporation. Journal of Geophysical Research 108, 4525, doi:10.1029/2003JD003597.

Cernusak LA, Farquhar GD, Wong SC, Stuart-Williams H (2004) Measurement and interpretation of the oxygen isotope composition of carbon dioxide respired by leaves in the dark. Plant Physiology 136:3350-3363.

Collatz GJ, Ball JT, Grivet C, Berry JA (1991) Physiological and environmental regulation of stomatal conductance, photosynthesis and transpiration: a model that includes a laminar boundary layer. Agricultural and forest meteorology 54:107-136

Conway TJ, Tans PP, Waterman LS, Thoning KW, Kitzis DR, Masarie KA, Zhang N (1994) Evidence of interannual variability of carbon cycle from the National Oceanic and Atmospheric Administration/Climate Monitoring and Diagnosis Laboratory Global Air Sampling Network. Journal of Geophysical Research 99:22831-22855.

Coplen TB (1996) New guidelines for reporting stable hydrogen, carbon, and oxygen isotope-ratio data. Geochemica et Cosmochimica Acta 60:3359-3360.

Craig H, Gordon LI (1965) Deuterium and oxygen 18 variations in the ocean and the marine atmosphere. Tongiorgi, E. Stable Isotopes in Oceanographic Studies and Paleotemperatures. Spoleto, Italy, Lab. Di Geol. Nucleare, Cons. Naz. Delle Ric.

Dawson TE, Ehleringer JR (1991) Streamside trees that do not use stream water. Nature 350:335-337.

Ehleringer JR, Bowling DR, Flanagan LB, Fessenden J, Helliker B, Martinelli LA, Ometto JP (2002) Stable isotopes and carbon cycle processes in forests and grasslands. Plant Biology 4:181-189.

Farquhar GD, Caemmerer Sv, Berry JA (1980) A biochemical model of photosynthetic CO_2 assimilation in leaves of C_3 species. Planta 149:78-90.

Farquhar GD, Hubick KT, Condon AG, Richards RA (1989) Carbon isotope discrimination and water use efficiency. In: Stable Isotopes in Ecological Research. PW Rundel, JR Ehleringer, KA Nagy (eds.) Springer-Verlag, New York, pp. 21-46.

Farquhar GD, Lloyd J (1993a) Carbon and oxygen isotope effects in the exchange of carbon dioxide between terrestrial plants and the atmosphere. In: Stable Isotope and Plant Carbon-Water Relations Academic, San Diego, California, pp 47-70.

Farquhar GD, Lloyd J, Taylor JA, Flanagan LB, Syvertsen JP, Ehleringer JR (1993b) Vegetation effects on the isotope composition of oxygen in atmospheric CO_2. Nature 363:493-443.

Ferretti DF, Pendall E, Morgan JA, Nelson JA, LeCain D, Mosier AR (2003) Partitioning evapotranspiration fluxes from a Colorado grassland using stable isotopes: Seasonal variations and ecosystem implications of elevated atmospheric CO_2. Plant and Soil 00:1-13.

Flanagan LW, Comstock JP, Ehleringer JR (1991) Comparison of modeled and observed environmental influences on the stable oxygen and hydrogen isotope composition of leaf water in Phaseolus vulgaris L. Plant Physiology 96:588-596.

Flanagan LB (1993) Environmental and biological influences on the stable oxygen and

hydrogen isotopic composition of leaf water. In: Stable Isotope and Plant Carbon-Water Relations Academic, San Diego, California, pp 71-90.

Flanagan LB, Phillips SL, Ehleringer JR, Lloyd J, Farquhar GD (1994) Effect of changes in leaf water oxygen isotopic composition on discrimination against $C^{18}O^{16}O$ during photosynthetic gas exchange. Australian Journal of Plant Physiology 21:221-234.

Flanagan LB, Varney GT (1995) Influence of vegetation and soil CO_2 exchange on the concentration and stable oxygen isotope ratio of atmospheric CO_2 within a Pinus resinosa canopy. Oecologia 101:37-44.

Flanagan LB, Brooks JR, Varney GT, Ehleringer JR (1997) Discrimination against $C^{18}O^{16}O$ during photosynthesis and the oxygen isotope ratio of respired CO_2 in boreal forest ecosystems. Global Biogeochemical Cycles 11:83-98.

Flanklin JF, Bledsoe CS, Callahan JT (1990) Contributions of the long-term ecological research program. BioScience 40:509-523.

Francey RJ, Tans PP (1987) Latitudinal variationin oxygen-18 of atmospheric CO_2. Nature 327:495-497.

Fung I, Field CB, Berry JA, Thompson MV, Randerson JT, Malmstrom CM, Vitousek PM, Collaz GJ, Sellers PJ, Randall DA, Denning AS, Badeck F, John J (1997) Carbon 13 exchanges between the atmosphere and biosphere. Global Biogeochemical Cycles 11:507-533.

Gillon JS, Yakir D (2000) Naturally low carbonic anhydrase activity in C_4 and C_3 plants limits discrimination against $C^{18}OO$ during photosynthesis. Plant, Cell and Environment 23:903-915.

Gillon JS, Yakir D (2001) Influence of carbonic anhydrase activity in terrestrial vegetation on the ^{18}O content of atmospheric CO_2. Science 291:2584-2587.

Helliker BR, Ehleringer JR (2000) Establishing a grassland signature in veins: ^{18}O in the leaf water of C_3 and C_4 grasses. Proceedings of the National Academy of Sciences 97:7894-7898.

Hesterberg R, Siegenthaler U (1991) Production and stable isotopic composition of CO_2 in a soil near Bern, Switzerland. Tellus Ser. B 43:197-205.

Irvine J, Law BE (2002) Contrasting soil respiration in young and old growth ponderosa pine forests. Global Change Biology 8:1183-1194.

Lauenroth WK, Milchunas DG (1991) Short-grass steppe. In: Ecosystems of the World 8A: Natural grasslands. RT Coupland (ed.), Elsevier, Amsterdam, pp. 183-226.

Majoube M (1971) Fractionnement en oxygene 18 et en deuterium entre L'eau et sa vapeur. Journal of Chemical Physics 58:1423-1436.

Merlivat L (1978) Molecular diffusivities of $H_2{}^{16}O$, $HD^{16}O$, and $H_2{}^{18}O$ in gases. Journal of Chemical Physics 69:2864-2871.

Milchunas DG, Lauenroth WK (2001) Belowground primary production by carbon isotope decay and long-term root biomass dynamics. Ecosystems 4:139-150.

Miller JB, Yakir D, White JWC, Tans PP (1999) Measurement of $^{18}O/^{16}O$ in the soil-atmosphere CO_2 flux. Global Biogeochemical Cycles 13:761-774.

Mortazavi B, Prater JL, Chanton JP (2004) A field based method for simultaneous measurements of the $\delta^{18}O$ and $\delta^{13}C$ of soil CO_2 efflux. Biogeosciences 1:1-9.

Nelson JA, Morgan JA, LeCain DR, Mosier AR, Milchunas DG, Parton BA (2003) Elevated CO_2 increases soil moisture and enhances plant water relations in a long-term field study in semi-arid shortgrass steppe of Colorado. Plant and Soil 259:169-179.

Parton WJ, Logan JA (1981) A model for diurnal variation in soil and air temperature. Agricultural Meteorology 23:205-216.

Pendall E, Del Grosso S, King JY, LeCain DR, Milchunas DG, Morgan JA, Mosier AR, Ojima DS, Parton WA, Tans PP, White JWC (2003) Elevated atmospheric CO_2 effects and soil water feedbacks on soil respiration components in a Colorado grassland. Global Biogeochemical Cycles 17, doi:10.1029/2001GB001821.

Riley WJ, Still CJ, Helliker BR, Ribas-Carbos M, Berry JA (2003) ^{18}O composition of CO_2 and H_2O ecosystem pools and fluxes in a tallgrass prairie: Simulations and comparisons to measurements. Global Change Biology 9:1567-1581.

Roden JS, Ehleringer JR (1999) Observations of hydrogen and oxygen isotopes in leaf water confirm the Craig-Gordon model under wide-ranging environmental conditions. Plant Physiology 120:1165-1173.

Rozanski KC, Sonntag C, Munnich KO (1982) Factors controlling stable isotope composition of European precipitation. Tellus 34:142-150.

Sala OE, Lauenroth WK, Parton WJ (1992) Long-term soil water dynamics in the shortgrass steppe. Ecology 73:1175-1181

Stern L, Baisden WT, Amundson R (1999) Processes controlling the oxygen isotope ratio of soil CO_2: Analytic and numerical modeling. Geochemica et Cosmochimica Acta 63:799-814.

Sternberg L da SL, Martinelli LA, Victoria RL, Barbosa EM, Bonates LCM (1998) The relationship between $^{18}O/^{16}O$ and $^{13}C/^{12}C$ ratios of ambient CO_2 in two Amazonian tropical forests. Tellus 50B:366-376.

Tans PP (1998) Oxygen isotopic equilibrium between carbon dioxide and water in

soils. Tellus Ser. B. 50:163-178.

Tans PP, White JWC (1998) In balance, with a little help from the plants. Science 281:183-184.

Trolier M, White JWC, Tans PP, Masarie KA, Germery PA (1996) Monitoring the isotopic composition of atmospheric CO_2:measurements from the NOAA global air sampling network. Journal of Geophysical Research 101:25897-25916.

Wang XF, Yakir D (1995) Temporal and spatial variations in the oxygen-18 content of leaf water in different plant species. Plant, Cell and Environment 18:1377-1385.

Wang XF, Yakir D, Avishai M (1998) Non-climatic variations in the oxygen isotopic composition of plants. Global Change Biology 4:835-849.

Williams TG, Flanagan LB, Coleman JR (1996) Photosynthetic gas exchange and discrimination against $^{13}CO_2$ and $C^{18}O^{16}O$ in tobacco plants modified by an antisense construct to have low chloroplastic carbonic anhydrase. Plant Physiology 112:319-326.

Yakir D, Wang X-F (1996) Fluxes of CO_2 and water between terrestrial vegetation and the atmosphere estimated from isotope measurements. Nature 380:515-517.

Table 3.1 Seasonal variations of precipitation, volumetric soil water content, ^{18}O of precipitation and vapor pressure deficit (VPD) over 2000 and 2001.

	Cumulative precipitation two weeks prior to sampling dates (mm)	Soil water content (%)	$\delta^{18}O$ of precipitation (‰)	VPD (kPa)
22-May, 2000	35.2	7.3	-8.67	1.69
6-June, 2000	3.7	3.3	-9.99	2.26
24-July, 2000	2.5	2.5	-5.14	2.99
4-September, 2000	3.3	3.4	-2.64	1.68
17-May, 2001	21.2	10.3	-12.36	0.32
21-June, 2001	20.5	14.1	-9.25	0.81
27-July, 2001	13.9	3.1	-5.12	1.71
7-September, 2001	14.9	3.1		1.00

Table 3.2 Leaf water potential (MPa)of two grass species (*Bouteloua gracilis and Pascopyrum smithii*) over two growing seasons of 2000 and 2001.

	Species	
	Bouteloua gracilis	*Pascopyrum smithii*
23-May, 2000	-1.3	-2.3
6-June, 2000	-2.1	-2.8
25-July, 2000	-3.0	-3.9
12-September, 2000	-2.4	-2.7
15-May, 2001	-1.8	-2.5
19-June, 2001	-1.7	-2
27-July, 2001	-1.8	-2.8

Table 3.3. Modeled $\delta^{18}O$ of soil respired CO_2 (‰, VSMOW) during growing season of 2001. D, N and E represent daytime, nighttime and dawn periods, respectively.

	May			June			July			September
	D	N	E	D	N	E	D	N	E	D
C_3	18.26	19.92	18.75	14.12	17.05	17.43	22.51	23.04	23.1	23.91
C_4	18.92	20.67	20.08	14.06	16.7	17.79	21.96	23.03	22.95	23.46
M	20.09	20.4	19.71	14.51	16.69	17.63	21.95	22.71	24.04	23.55
B	21.2	21.88	20.72	16.97	18.06	19	24.91	24.04	23.77	24.51

Table 3.4. Variation of vertical CO_2 concentrations, $\delta^{18}O$ values of air and $\delta^{18}O$ of ecosystem respiration from two selected heights each day of monthly air sampling over two years (2000 and 2001). Tropospheric $\delta^{13}C$ values were measured via aircraft at Carr close to study site. (Provided by P. Lang, NOAA CMDL)

	May-00			Jun-00			Jul-00			Sep-00			May-01			June-01			July-01		
	1m	2m	Δ	1m	2m	Δ	1m	2m	Δ	1m	2m	Δ	1m	2m	Δ	1m	2m	Δ	1m	2m	Δ
$[CO_2]$ (μmol mol^{-1})																					
CBL	372.02			369.52			368.67			367.54			374.25			373.67			370.17		
0-4	380.1	379.7	0.41	390.3	389.3	1.01	381.4	380.8	0.63	389.13	388.2	0.93	381.50	381.08	0.42	411.9	400.8	11.1	392.98	392.07	0.91
4-8	383	382	1.05	385.1	384.3	0.83	369.1	369.6	-0.56	386.03	384.1	1.94	384.24	384.12	0.12	427.8	428.3	-0.57	376.89	376.75	0.14
8-12	370.5	370.8	-0.31	370.3	370.8	-0.51	370.1	370.2	-0.12	378.58	379	-0.46	379.17	379.96	-0.79	361.6	361.8	-0.25	368.27	368.19	0.08
12-16	369.7	369.4	0.32	371.6	371.6	-0.01	370	369.9	0.09	368.15	368.5	-0.35	372.63	373.59	-0.96	365.6	366.8	-1.22	377.33	377.41	-0.08
16-20	369	368.9	0.1	371.1	371.3	-0.22	372	371.7	0.28	365.87	366.4	-0.49	373.63	373.34	0.29	364.6	365	-0.43	370.13	369.57	0.56
20-24	402.9	397.5	5.43	391.7	388.9	2.79	379.4	379.3	0.15	378.86	375.5	3.34	386.01	387.05	-1.04	407.2	395.4	11.81	382.84	381.46	1.38
$CO_{2\,D}$-$CO_{2\,N}$	-33.19	-28.08		-20.09	-17.29		-9.39	-9.33		-10.71	-7.02		-13.38	-13.46		-41.64	-28.61		-5.51	-4.05	
$\delta^{13}C$																					
CBL	-8.154									-7.809			-8.137			-8.095			-7.927		
0-4	-8.422	-8.408	-0.01	-8.671	-8.638	-0.03	-8.499	-8.517	0.02	-8.47	-8.434	-0.04	-8.372	-8.369	0.00	-8.981	-8.743	-0.24	-8.758	-8.753	0.00
4-8	-8.488	-8.464	-0.02	-8.598	-8.562	-0.04	-8.105	-8.13	0.03	-8.46	-8.42	-0.04	-8.521	-8.565	0.04	-9.554	-9.603	0.05	-8.265	-8.26	-0.01
8-12	-8.153	-8.28	0.13	-8.169	-8.203	0.03	-8.116	-8.13	0.01	-8.348	-8.366	0.02	-8.412	-8.403	-0.01	-7.629	-7.632	0.00	-7.95	-7.937	-0.01
12-16	-8.156	-8.096	-0.06	-8.18	-8.184	0.00	-8.098	-8.077	-0.02	-7.985	-8	0.01	-8.142	-8.199	0.06	-7.887	-7.883	0.00	-8.255	-8.269	0.01
16-20	-8.085	-8.061	-0.02	-8.147	-8.182	0.04	-8.153	-8.14	-0.01	-7.921	-7.912	-0.01	-8.107	-8.107	0.00	-7.849	-7.864	0.01	-8.007	-7.987	-0.02
20-24	-8.77	-8.668	-0.10	-8.571	-8.522	-0.05	-8.477		------	-8.182	-8.106	-0.08	-8.465	-8.473	0.01	-8.756	-8.518	-0.24	-8.435	-8.389	-0.05
$\delta^{13}C_{\,tros}$-$\delta^{13}C_{\,canopy}$	-0.069	-0.093	0.02							7.921	7.912		8.107	8.107		7.849	7.864		-0.13	-0.15	
$\delta^{13}C_{\,D}$ - $\delta^{13}C_{\,N}$	0.614	0.572		0.391	0.338		0.379			0.197	0.106		0.323	0.274		0.869	0.635		0.18	0.12	
$\delta^{18}O$																					
CBL	-0.341									0.152			-0.103			-0.016			0.082		
0-4	31.01	30.95	0.06	31.39	31.38	0.014	30.61	30.65	-0.04	31.357	31.15	0.21	28.9854	29.239	-0.25	29.29	29.89	-0.60	30.5304	30.563	-0.03
4-8	30.96	31.04	-0.08	31.11	31.12	-0.008	30.71	30.58	0.13	30.842	30.84	0.00	28.732	28.422	0.31	28.7	28.75	-0.05	30.6695	30.673	0.00
8-12	31.05	30.73	0.32	30.92	30.88	0.041	30.55	30.58	-0.03	30.952	30.88	0.07	28.9607	28.942	0.02	30.4	30.41	-0.01	30.5994	30.622	-0.02
12-16	30.83	30.84	-0.01	30.83	30.85	-0.023	30.65	30.65	0.00	30.895	30.88	0.02	29.8537	29.845	0.01	30.63	30.64	-0.02	30.9517	30.831	0.12
16-20	31	31	0.00	30.72	30.74	-0.024	30.83	30.79	0.04	31.052	30.98	0.07	29.7785	29.808	-0.03	30.69	30.66	0.03	30.9455	30.968	-0.02
20-24	31.74	31.5	0.24	31.31	31.28	0.028	30.45	30.86	-0.41	31.057	30.97	0.09	28.7537	28.622	0.13	29.91	29.9	0.01	30.7622	30.706	0.06
$\delta^{18}O_{\,D}$ - $\delta^{18}O_{\,N}$	-0.903	-0.657		-0.478	-0.427		0.20	-0.211		-0.1617	-0.089		1.10004	1.2236		0.718	0.747		0.18952	0.1257	
$\delta^{18}O$ of ecosystem respiration																					
D	---------			8.76 (4.26)**<8-12>			---------			8.24 (3.39)**<12-16>			x			x			x		
N	---------			---------			---------			---------			-5.18 (8.1)*<21-2>			x			23.49 (1.55)**<21-0>		
E	---------			---------			---------			---------			x			19.59 (0.2)**<4.2-6.8>			27.93 (0.45)**<5.8-8.8>		

D, N, E represent daytime, nighttime and dawn periods, respectively.

Δ : 1m - 2m

--------; No positive relations were formed between ^{18}O and inverse $[CO_2]$

Parentheses represent standard error of intercept for Keeling plot

<> represents duration of collection of fasks

x represents positive relations between $\delta^{18}O$ of CO_2 and inverse $[CO_2]$ were shown, but no significant relations were formed.

Geometric mean regressions were performed to calculate intercepts (*; p<0.1, **; p<0.05)

Table 3.5. Soil respired fraction calculated from total ecosystem respiration ($\delta^{18}O_R$) and chamber respiration ($\delta^{18}O_{CR}$) for year 2001. Modeled $\delta^{18}O$ of leaf respired and soil respired CO_2 were used for the calculation of a fraction of soil respiration from total ecosystem and chamber respirations (Eq. 3.6 and 3.7). Scale dependent invasion effects were considered in modeling of soil respired CO_2. C_3, C_4 and M represent C_3, C_4 and mixed C_3 and C_4 plots, respectively. D, N and E indicate daytime, nighttime and dawn periods, respectively.

		Ecosystem	C_3	C_4	M
June, 2001	D	------	0.59	0.77	0.57
	N	------	0.58	0.87	0.74
	E	0.88	0.53	0.95	0.85
July, 2001	D	------	------	------	0.69
	N	0.94	0.76	0.82	0.83
	E	0.84	0.9	0.87	0.89

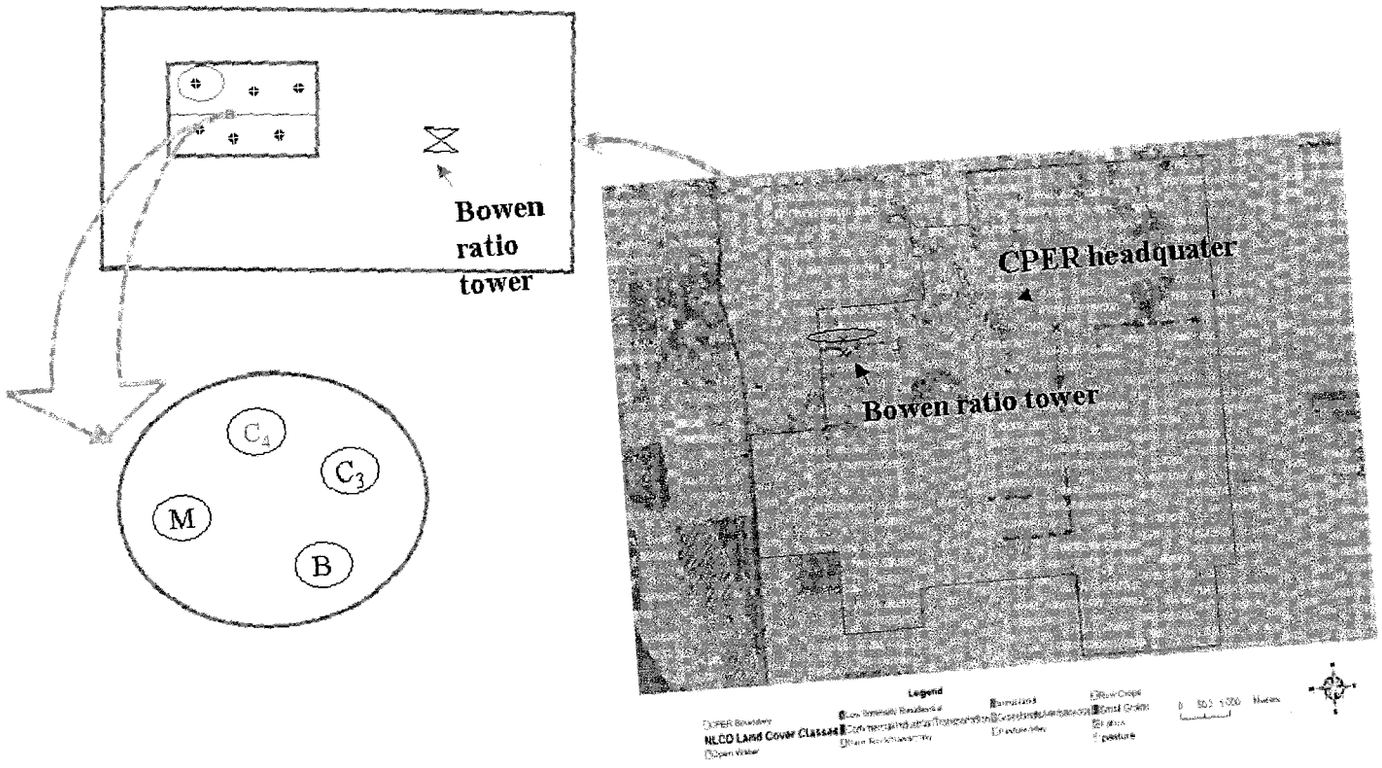

Fig.3.1 Location of Bowen ration towers, chambers and CPER headquarter

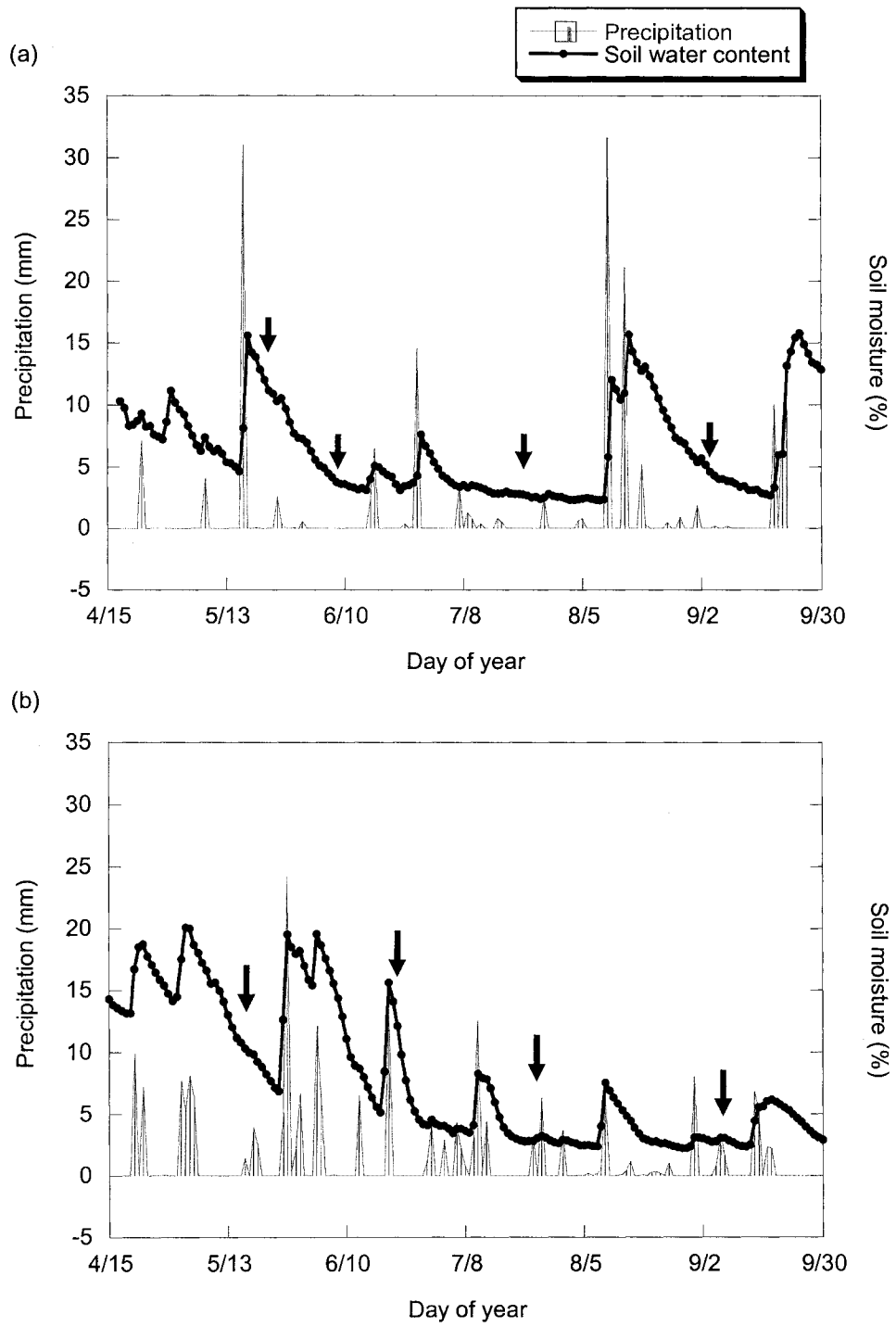

Fig.3.2 Seasonal variations in precipitation and soil moisture on (a) 2000 and (b) 2001. Volumetric soil water was measured with soil moisture probe connected with BREB data logger (Campbell Scientific, CS615) and averaged 0-15 cm corrected to specific soil type (Morgan J.A, unpublished data). Arrows represent sampling periods over growing seasons of 2000 and 2001.

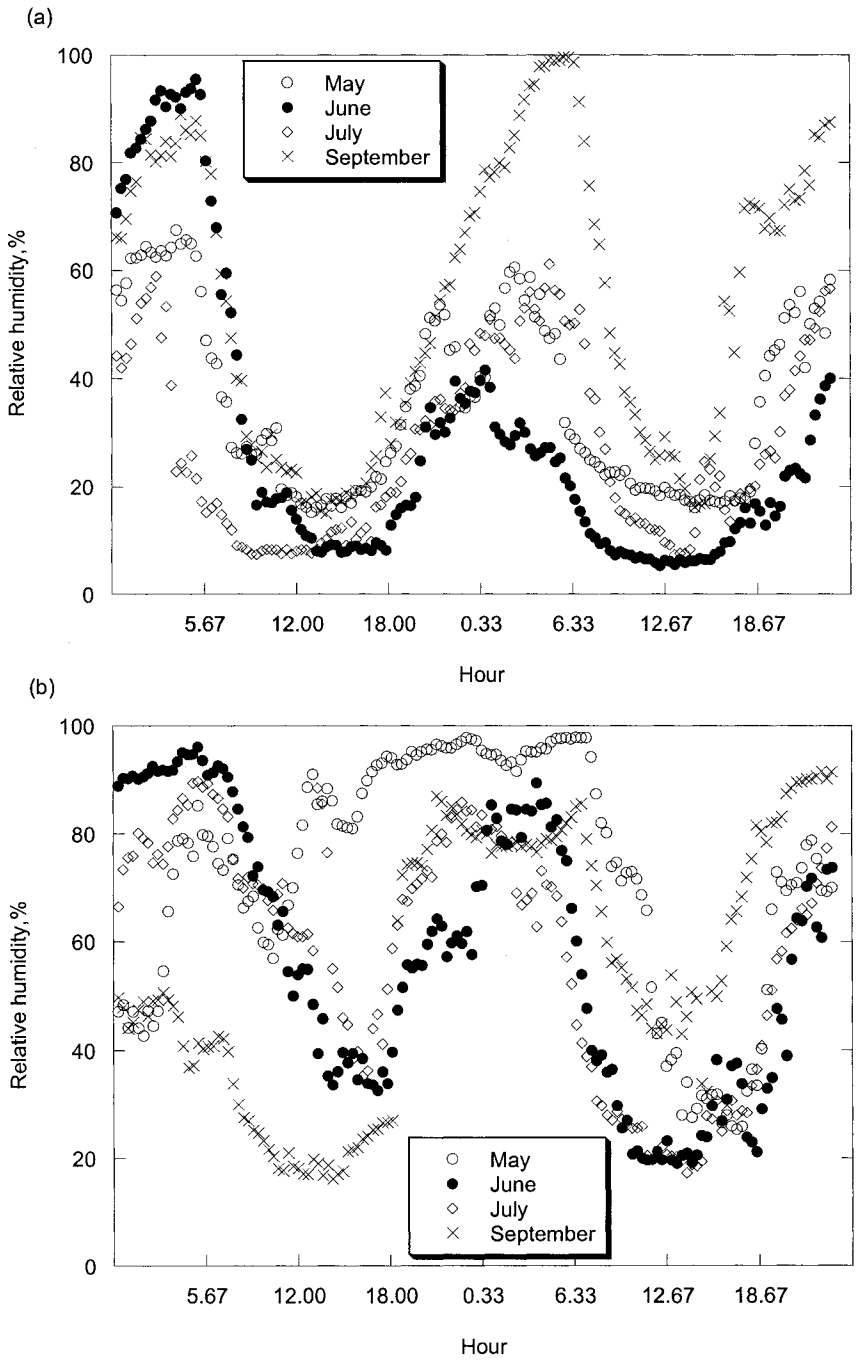

Fig. 3.3 Diurnal variations in relative humidity for sampling periods of (a) 2000 and (b) 2001

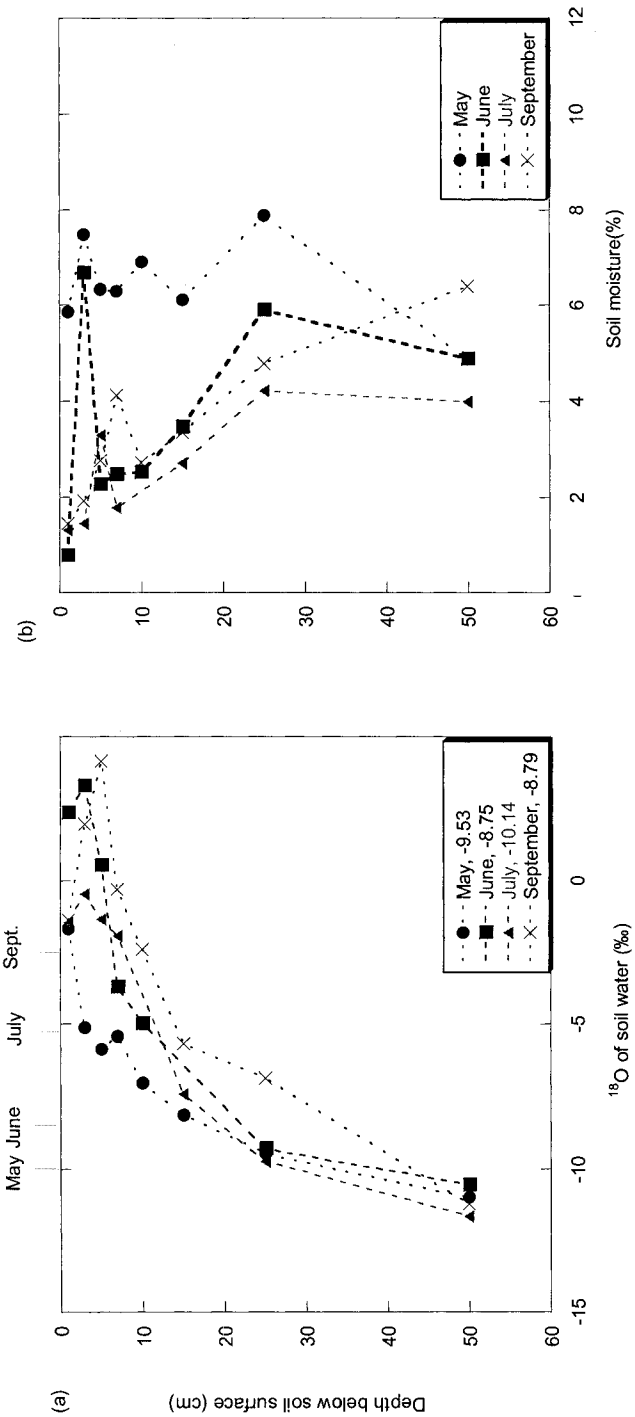

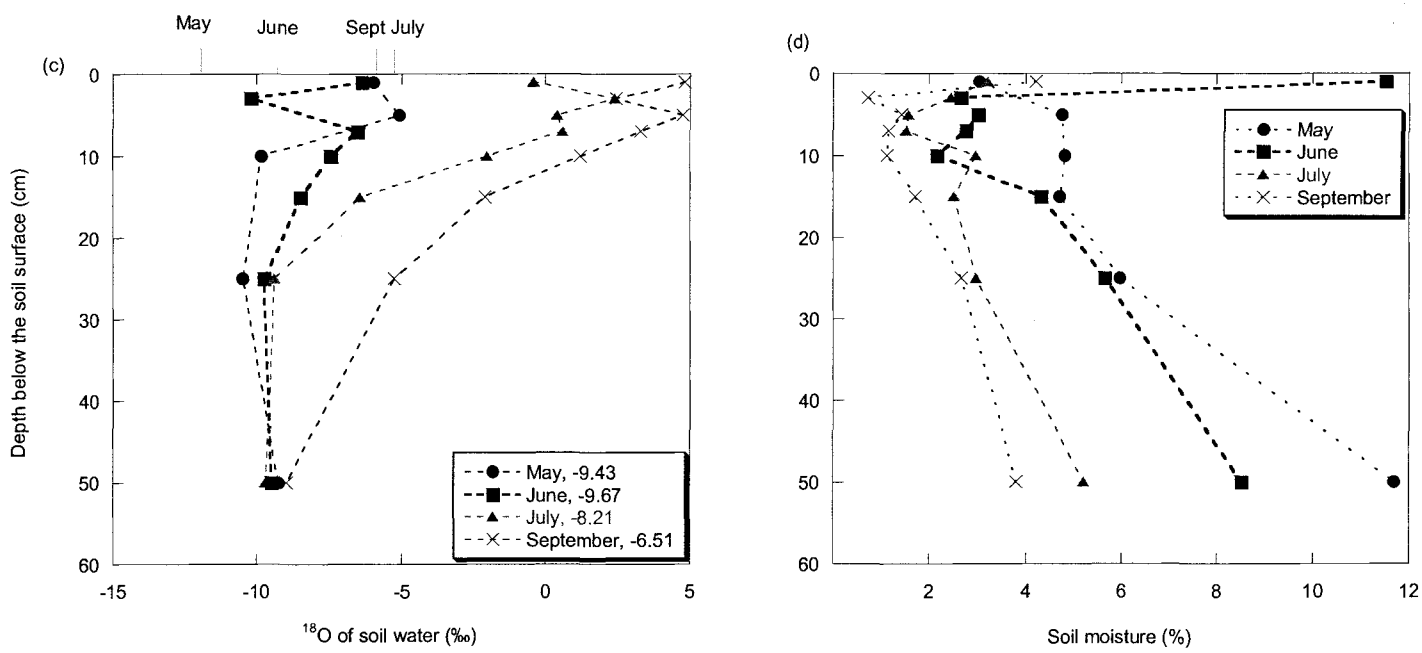

Fig.3.4 Soil water ^{18}O values and soil water content over 2000 and 2001. (a) and (c) show $\delta^{18}O$ of soil water for 2000 and 2001;(b) and (d) show soil water content for 2000 and 2001, respectively. The precipitation ^{18}O values each month for two years were written on the top of left graphs. The depth weighted $\delta^{18}O$ values of soil water were expressed in the legend boxes.

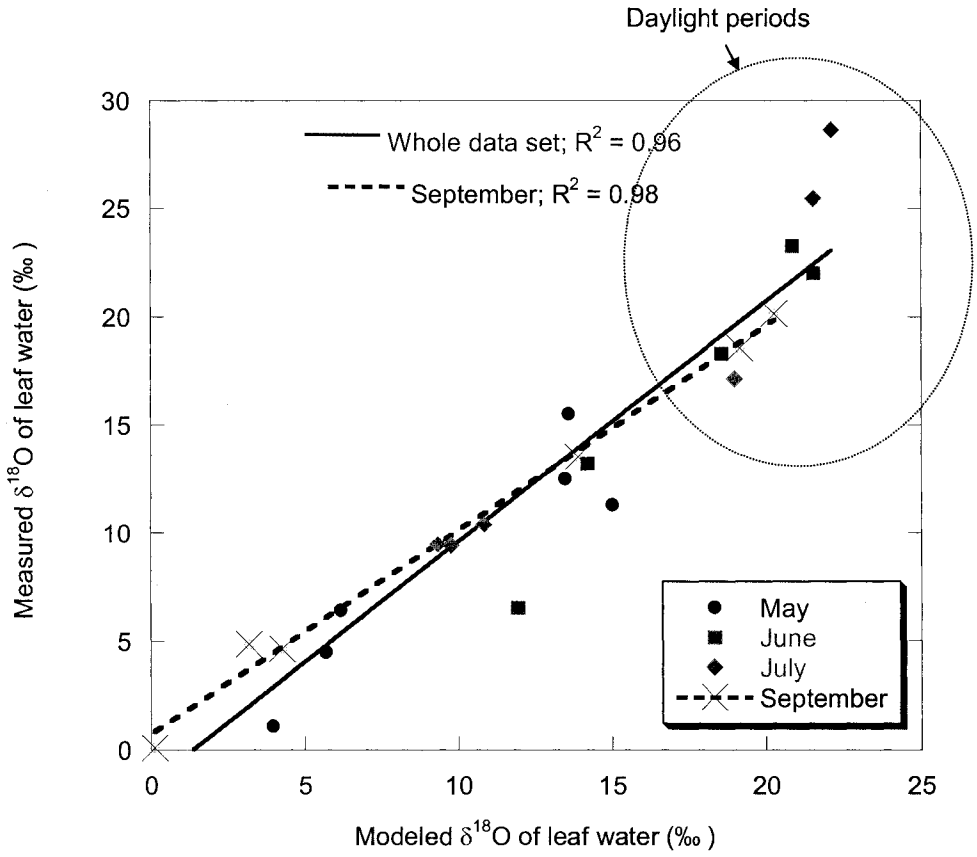

Fig.3.5 Comparisons between observed and modeled leaf water oxygen isotope ratio. Observed values are the average of two leaf collections in 2000. Leaf collections were conducted approximately 5-6 times a day each month. The ^{18}O values are expressed relative to SMOW. the source water for plant use (δ_{sw}) is average of top 25 cm of soil water for both C_3 and C_4 plants The ellipse refers to daylight periods.

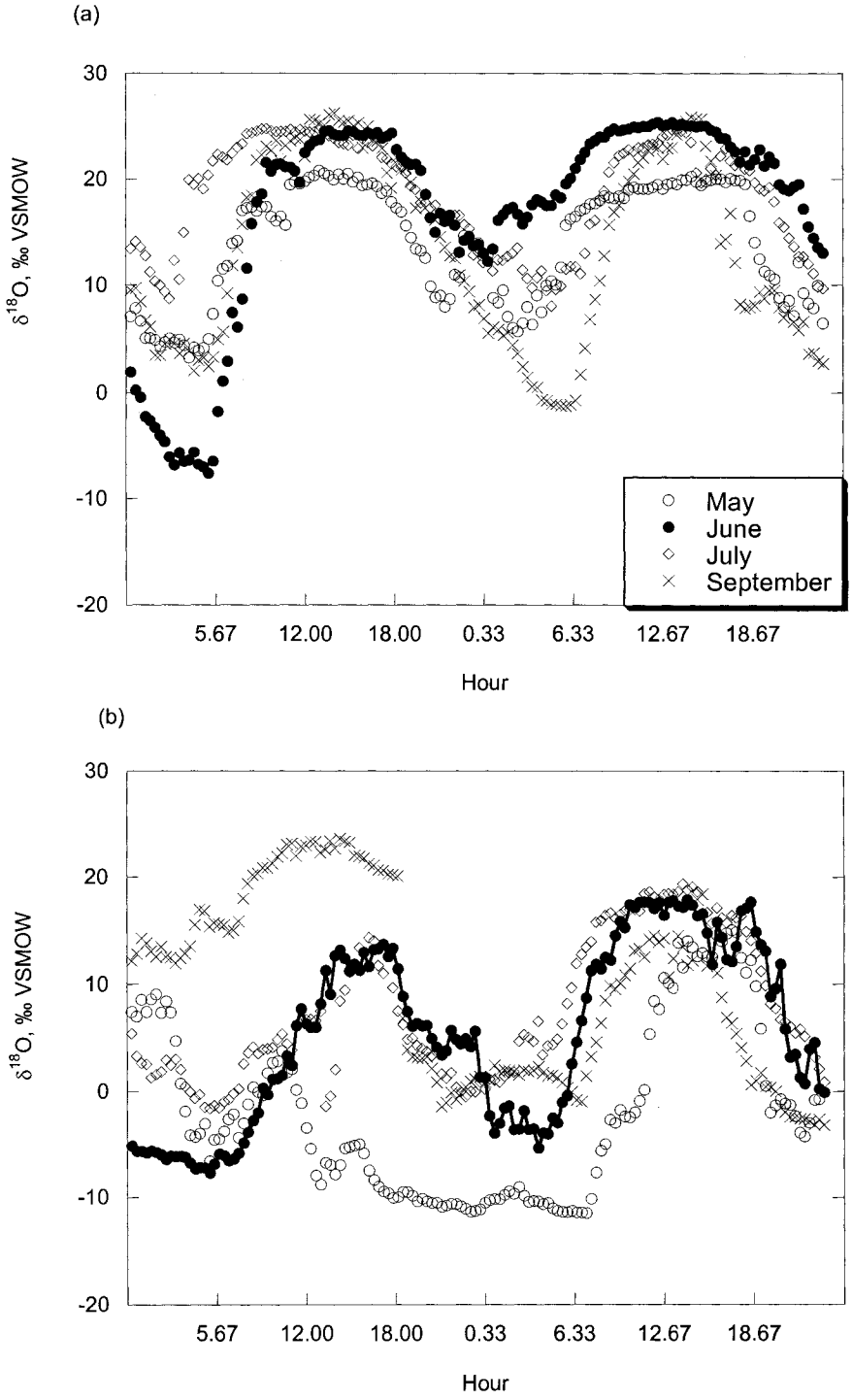

Fig.3.6 Modeled diurnal $\delta^{18}O$ of leaf water patterns for (a) 2000 and (b) 2001. We assumed that the source water for plant use (δ_{sw}) is average of top 25 cm of soil water for both C_3 and C_4 plants

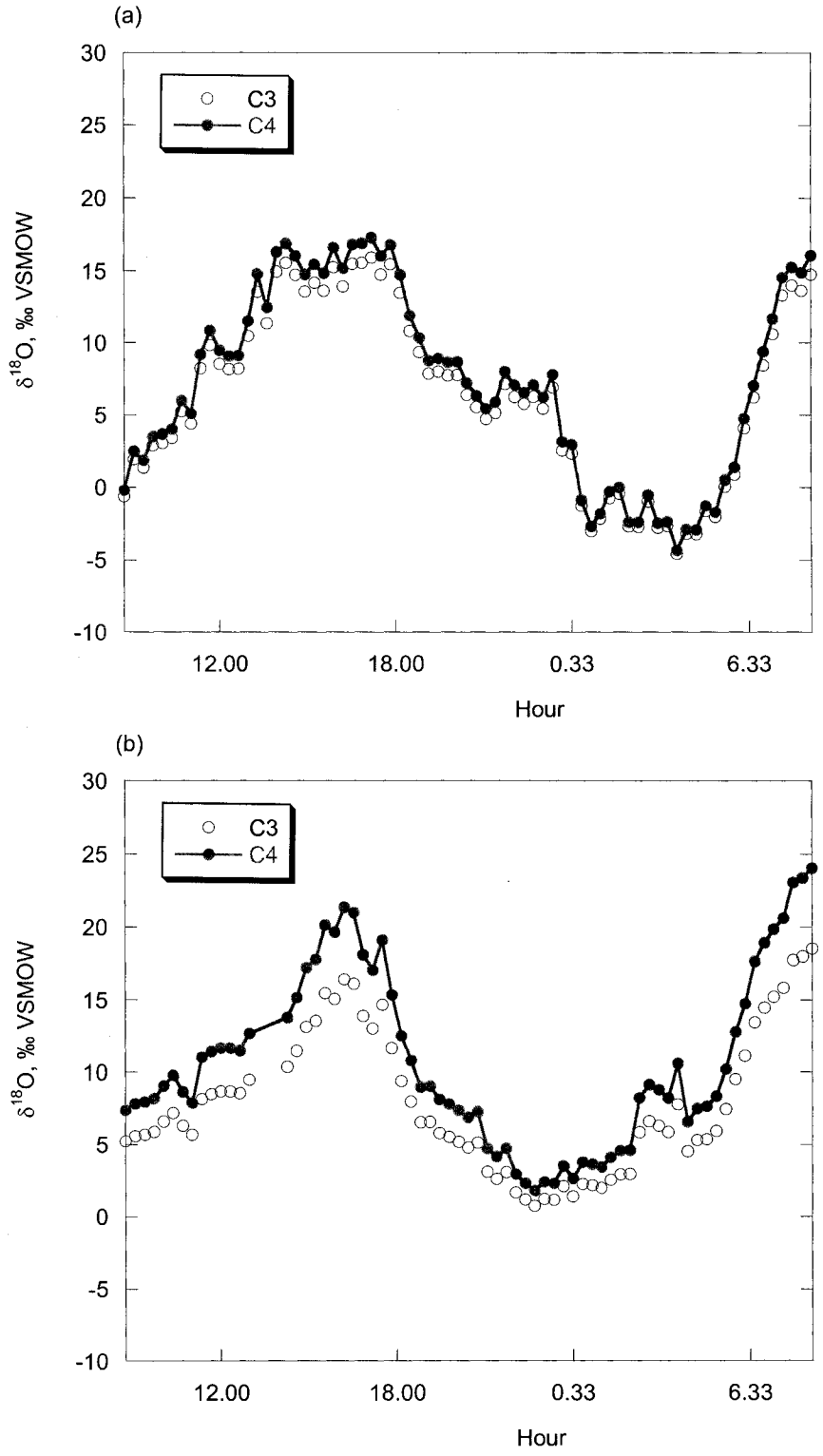

Fig. 3.7 Modeled $\delta^{18}O$ of leaf water patterns of C_3 and C_4 grasses for (a) June 2001 and (b) July 2001. We used $\delta^{18}O$ of soil water at 50 cm for the representative source water for C_3 plants and at 10 cm for C_4 plants.

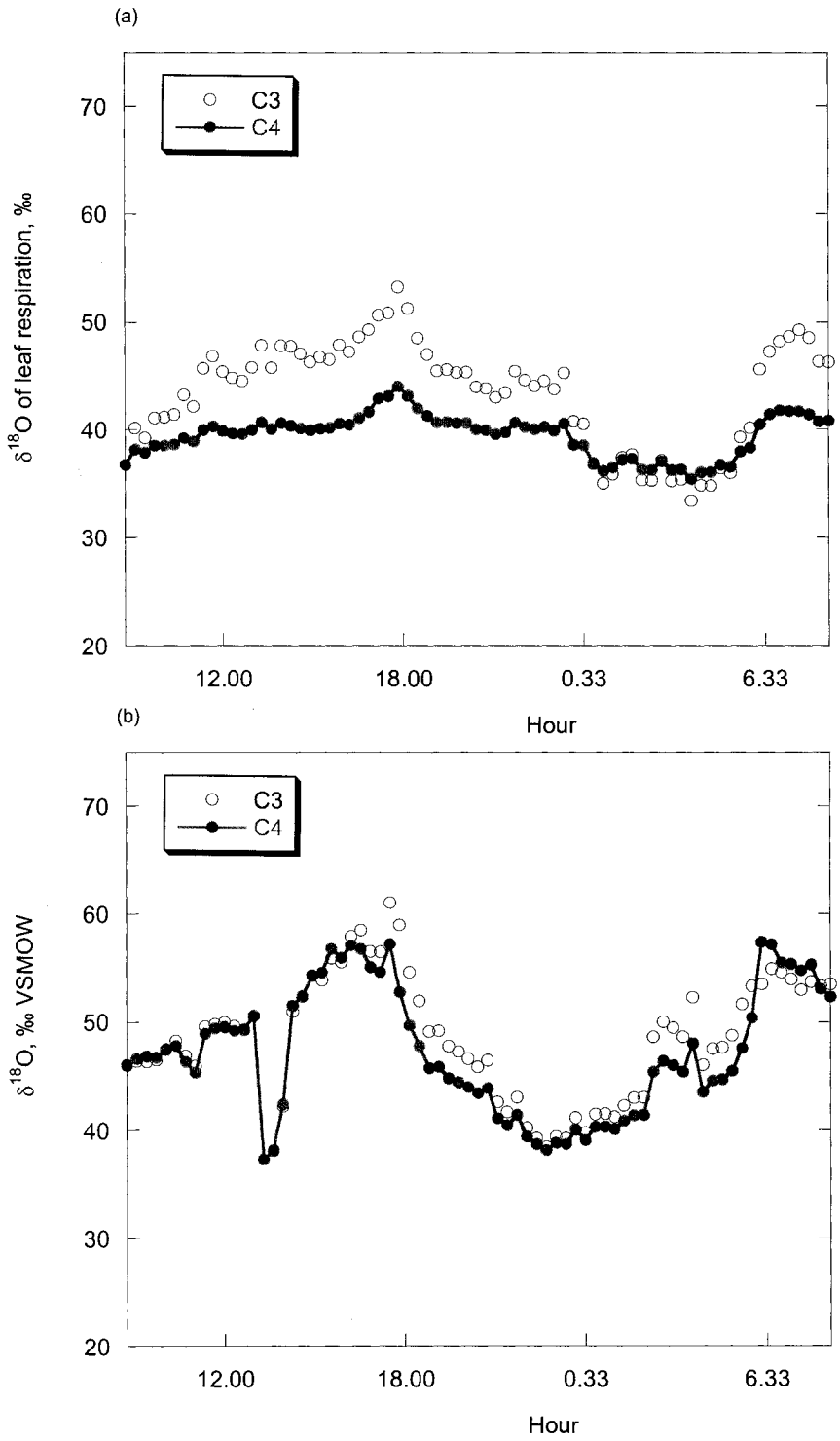

Fig. 3.8 Modeled values for $\delta^{18}O$ of leaf respired CO_2 separated by C_3 and C_4 grasses for (a) June 2001 and (b) July 2001. The isotopic signature of leaf respiration was calculated based on source water, leaf temperature, relative humidity, and Craig-Gordon model of evaporative enrichment. Different CA activity, internal CO_2 concentrations and source water between C_3 and C_4 plants were taken account.

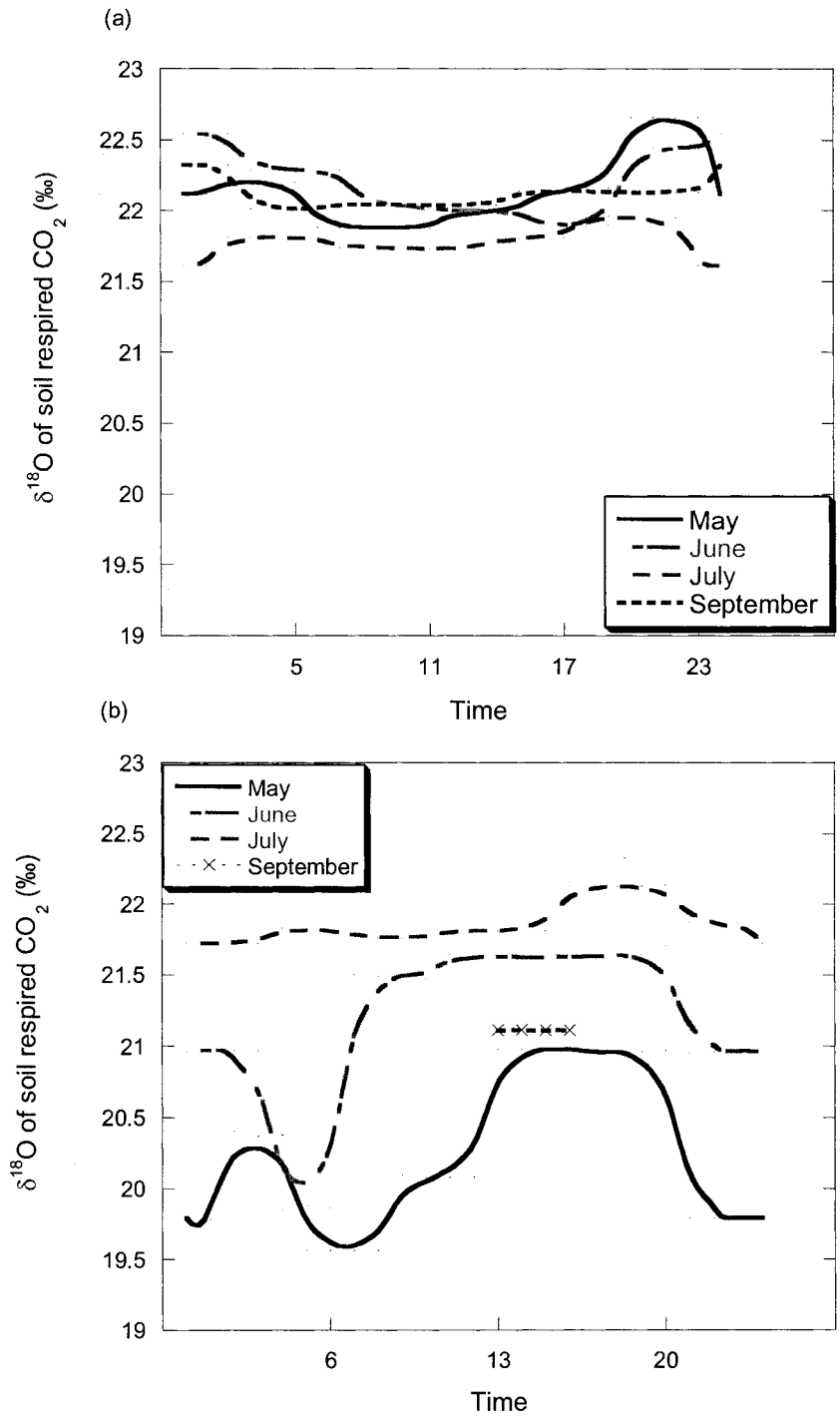

Fig.3.9 Modeled diurnal variations in $\delta^{18}O$ of soil respired CO_2 on (a) 2000 and (b) 2001. The $\delta^{18}O_{SR}$ was calculated based on measured source water, temperature dependent equilibrium and kinetic fractionation with some modification to take account of inherent soil properties and diffusional variations (Tans, 1998).

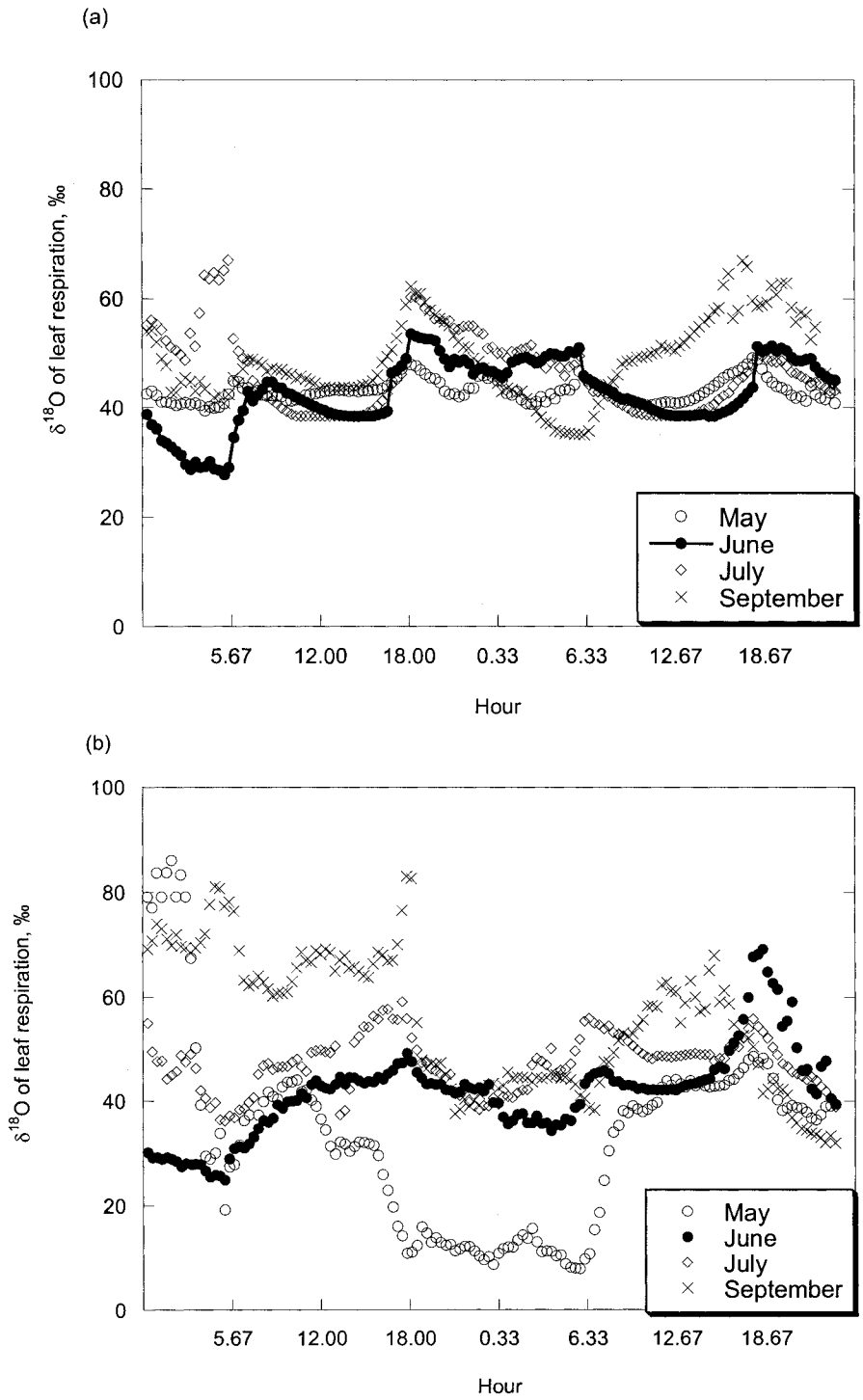

Fig.3.10 Modeled values for $\delta^{18}O$ of leaf respired CO_2 for (a) 2000 and (b) 2001. The isotopic signature of leaf respiration was calculated based on source water, leaf temperature, relative humidity, and Craig-Gordon model of evaporative enrichment. Different CA activity, internal CO_2 concentrations between C_3 and C_4 plants and monthly productivity were taken account.

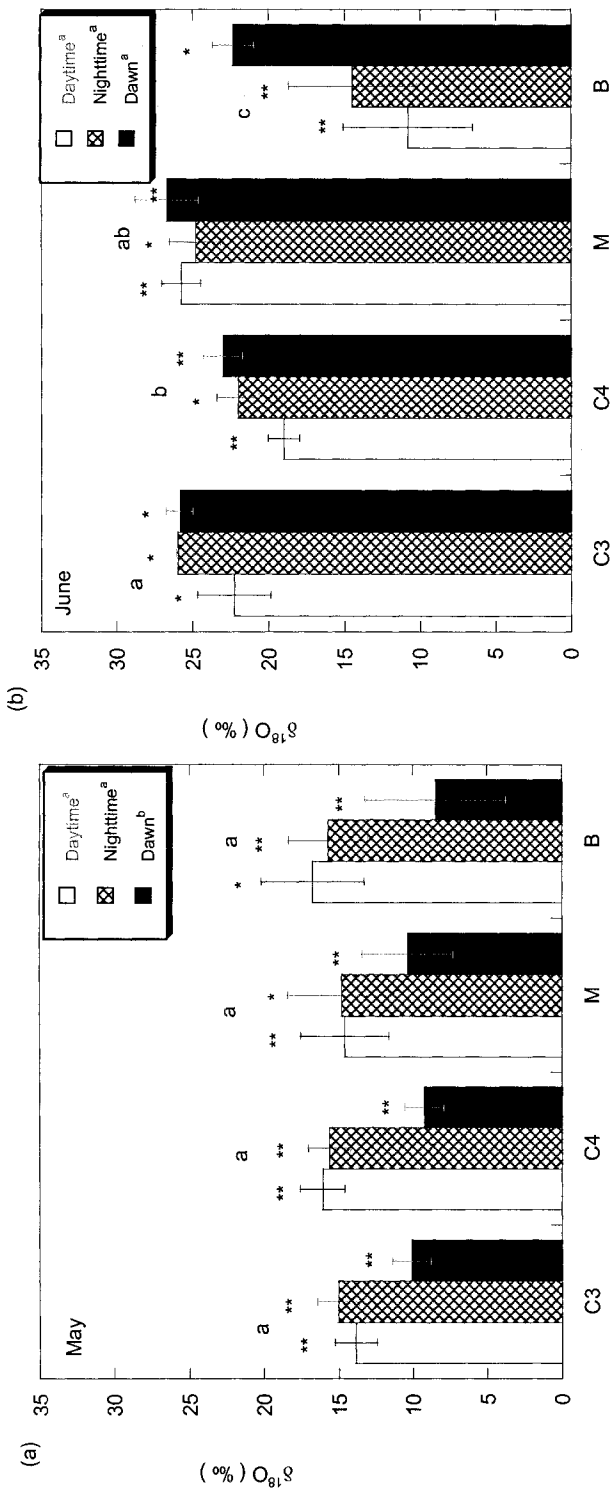

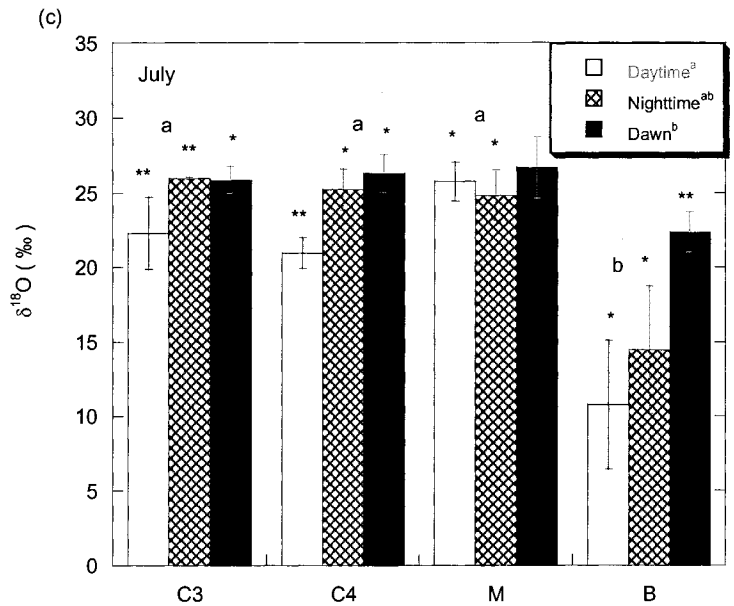

Fig.3.11 $\delta^{18}O$ of CO_2 respired from four different cover types (C_3, C_4, mixed C_3 and C_4 and bareground patches) in 2001. Different letters represent significant difference among chambers (LSMEANS, $p<0.05$). Different letters in the legend box represent significant difference among times of day. Error bars represent standard error for intercept. Geometric mean regressions were performed to calculate intercepts (*; $p<0.1$; **;$p<0.05$).

4. Partitioning gross photosynthesis and respiration in the Colorado shortgrass steppe ecosystem: Relation to climatic and plant community dynamics

4.1 Abstract

Partitioning net ecosystem exchange (NEE) into gross photosynthesis and respiration is a critical issue for ecology because environmental perturbations may influence these fluxes differentially. This study evaluated whether or not isotopic fluxes of $^{13}CO_2$ and $C^{18}O^{16}O$ could be used for partitioning NEE into gross photosynthesis and respiration of the shortgrass steppe over two consecutive growing seasons. Day and night time Keeling plot approaches for ^{13}C discrimination for net ecosystem exchange ($\delta^{13}C_B$) and for ecosystem respiration ($\delta^{13}C_R$) were applied. Carbon assimilation and stomatal conductance were modeled from the leaf to canopy scale to estimate ^{13}C photosynthetic discrimination ($\delta^{13}C_P$). For partitioning with oxygen isotopes, daytime Keeling plot intercepts were used for combined photosynthetic and respired $C^{18}O^{16}O$ signal ($\delta^{18}O_R$). A set of techniques was used to compute canopy scale of ^{18}O photosynthetic discrimination ($\delta^{18}O_P$) including photosynthesis model, measured and modeled values for $\delta^{18}O$ of leaf water, and analysis of carbonic anhydrase (CA) hydration rates specific to plant functional type (C_3 versus C_4). A numerical model was applied to estimate $\delta^{18}O$ of soil respired CO_2 ($\delta^{18}O_R$). In order to partition NEE into photosynthesis and respiration,

considerable differences between $\delta^{13}C_B$ (or $\delta^{18}O_B$) and $\delta^{13}C_R$ (or $\delta^{18}O_R$) are required. Photosynthesis did not contribute a $C^{18}O^{16}O$ signal during prolonged dry conditions, and water vapor and carbon were weakly coupled during rainy sampling periods. Restricted application of carbon isotopes for partitioning was also revealed in dry condition on July 2001. Despite the limitations, photosynthetic CO_2 fluxes partitioned by both stable isotopes agreed well, and the relationship was stronger where isotopic disequilibrium between $\delta^{13}C_p$ and $\delta^{13}C_R$ were strong.

4.2 Introduction

Net ecosystem exchange (NEE) plays a significant role in the balance of the global carbon cycle and in rate of the atmospheric increase in CO_2. Our current understanding of what controls NEE in most ecosystems is limited. Changes in the environment have differential effects on the carbon assimilation rates, respiration and decomposition rates, and on the net storage of carbon in plant and soil components of the ecosystem. Researchers have recently been utilizing direct observations of NEE using eddy correlation technique in the worldwide FLUXNET network (Baldocchi et al. 2001). Detecting the magnitude of changes in NEE is not enough to fully understand the process governing NEE nor to predict ecosystem functioning accurately. Increasing net ecosystem uptake results from increases in gross photosynthesis and/or decreases in respiratory activity. Because environmental perturbations may influence gross photosynthesis and respiration differentially, a need exists to independently evaluate these fluxes.

Numerous modeling approaches have been developed to partition NEE into

photosynthesis and respiration such as estimating total ecosystem respiration based on regressions of nocturnal NEE versus soil or air temperature (Goulding et al. 1996; Valentini et al. 1995), estimating the respiration term relative to a light-response curve model (Gilmanov et al. 2003), and a process oriented approach from leaf level fraction model (Farquhar et al. 1989) to global scale models (Lloyd et al. 1996).

Each partitioning method has advantages and disadvantages. For example, the regression model between soil temperature and night time NEE is not labor intensive and it is possible to achieve continuous data sets if several assumptions are valid; light induced inhibition to photosynthesis must be trivial (Brooks and Farquhar 1985) and consistent relations between soil temperature and night time NEE are maintained. This approach may perform poorly in hot and dry conditions because the accuracy of respiratory flux tends to drop (Goulding et al. 1996; Suyker and Verma. 2001).

A partitioning approach applying isotopic mass balance is of particular interest. ^{13}C or ^{18}O of air reflect eco-physiological signals transferred from plants and soils, which may contain enough information to partition net ecosystem exchanges into gross fluxes. Photosynthesis discriminates against the heavier ^{13}C isotope via diffusion (+4.4 ‰) and enzymatic fractionation (about 27 ‰ for C_3 plants and very low for C_4 plants), consequently enriching ^{13}C of CO_2 in the atmosphere. By contrast, respiration dilutes ^{13}C of CO_2 in the atmosphere because the source of respiratory CO_2 is organic metabolites and ^{13}C depleted plant (foliage, stem and roots) and soil organic materials. The difference in carbon isotope ratio ($^{13}C/^{12}C$) between C_3 and C_4 plants provides a way to evaluate their relative contributions to CO_2 fluxes by imprinting an isotopic signal to the atmosphere. The ^{18}O of CO_2 is also enriched when photosynthetic activity occurs

(Flanagan et al. 1991), and expresses similar behavior as ^{13}C of CO_2. A large proportion of CO_2 that enters stomata is not fixed by photosynthesis and diffuses back out with enriched ^{18}O signal in the process of dissolution with leaf water via the chloroplastic enzyme carbonic anhydrase (CA) (Williams et al. 1996). Leaf water is inherently enriched in ^{18}O relative to source water because transpiration is an evaporative and fractionating process (Flanagan et al. 1991; Wang and Yakir 1995). Therefore, ^{18}O of CO_2 diffusing out of leaves (retrodiffusing) contains the $\delta^{18}O$ signal of enriched leaf water.

Isotopic mass balance approach for partitioning was first applied in concert with meteorological measurements by Yakir and Wang (1996) in wheat, cotton and corn fields, followed by Bowling et al. (1999, 2003) in forests and Lai et al. (2003) in the tallgrass prairie. However, an isotopic partitioning approach has never been applied to the short grass steppe. Further, few studies regarding the use of stable isotopes to study ecosystem CO_2 exchange have been reported in semi-arid systems while many studies have been conducted in forests (Bowling et al. 1999; Buchmann et al. 1997 a b; Lloyd et al. 1996; Ekblad and Högberg 2001).

Yakir and Wang (1996) stated accurate estimations of end members is critical for the applicability of isotopic partitioning to more heterogeneous ecosystems. Bowling et al. (1999 and 2001) developed field techniques to estimate net ecosystem exchange of $^{13}CO_2$, allowing for partitioning NEE into photosynthesis and respiration with ^{13}C measurements in forests. For mixed C_3 and C_4 ecosystems, Lai et al. (2003) employed a direct modeling approach using two photosynthetic pathway models to estimate canopy conductance. They partitioned NEE into photosynthesis and respiration only for wet periods due to

insufficient isotopic labeling of end members to discern them during drought. If sufficient difference in $\delta^{18}O$ between photosynthetic and respiratory end members is imposed by large ^{18}O enrichment in leaf water, using $\delta^{18}O$ isotopic partitioning should have a major advantage over using only $\delta^{13}C$ isotopic partitioning methods, even in dry conditions.

Our objective is to determine whether or not isotopic fluxes of $^{13}CO_2$ and $C^{18}O^{16}O$ could be used for partitioning NEE into gross photosynthesis and respiration on shortgrass steppe over the growing season for two consecutive years.

4.3 Methods

4.3.1 Site description

This study was conducted during growing seasons of 2000 and 2001 at the USDA-ARS Central Plains Experimental Range (CPER), in the shortgrass steppe region of north-eastern Colorado, 56 km north-east of Fort Collins, CO (lat. 40 40 N, long. 104 45 W). Vegetation of this region is dominated by warm-season, C_4 grasses (*Bouteloua gracilis* and *Buchloe dactyloides),* but contains an abundance of cool-season, C_3 grasses (e.g. *Pascopyrum smithii* and *Stipa comata*), as well as a variety of C_3 forbs and woody vegetation. C_4 forbs and woody vegetation occur primarily in landscape positions with very deep sandy soils. Root biomass is responsible for ~70% of net primary production in the shortgrass steppe (Milchunas and Lauenroth, 2001). Long term (55 year) mean annual precipitation averaged 320mm, with the majority occurring during May, June and July. Mean air temperatures are 15.6 ^{0}C in summer and 0.6 ^{0}C in winter with maximum July temperatures averaging 30.6 ^{0}C (Lauenroth and Milchunas, 1991). The pasture

around Bowen ratio tower had historically been moderately grazed, although cattle were removed from the pasture in late spring of 2000 due to severe drought. Cattle were returned to the pasture in the Spring of 2001 and moderate grazing resumed.

4.3.2 Midday leaf water potential

Leaf water potential was measured over two growing seasons of 2000 and 2001 on 1-2 leaves *P. smithii* with a Scholander-type pressure chamber (PMS instrument Company, Corvallis, OR, USA). Measurements were taken mid-morning (1000-1145 hrs MST) when plants were typically active and sampled leaves were processed immediately after being cut.

4.3.3 Meteorological Parameters and Bowen Ratio technique

Relevant meteorological parameters were measured above the canopy every 20 min from a Bowen ratio energy balance technique (BREB). Measurements included air temperature, relative humidity and soil temperature. Temperature gradients were obtained at 1 and 2 m heights from fine wire chromel-constantan thermocouples. Soil temperatures were measured at 2cm and 6cm depths and were averaged over 4 sensors. Volumetric soil water was measured with soil moisture probe connected with BREB data logger (Campbell Scientific, CS615) and averaged 0-15 cm corrected to specific soil type.

Fluxes of CO_2 (net ecosystem exchange, NEE) and relevant meteorological parameters were measured from a Bowen ratio tower. CO_2 fluxes were measured above the canopy every 20 min via Bowen ratio energy balance technique using an infra-red gas analyzer (Model LI-6262, LiCor, Inc., Lincoln, NE, USA). Ancillary measurements

of net radiation and soil heat flux were used to calculate fluxes of CO_2 every 20 minutes with the data logger that collected the micrometeorological data (21X data logger, Campbell Scientific, Inc., Logan, UT, USA). Turbulent transfer coefficients were assumed to be same for heat, water vapor and CO_2 and calculated using the 20 minute average sensible heat flux and temperature gradients. Fluxes were calculated using methods described by Dugas (1993) and Dugas et al. (1999). They were adjusted for the variation in air density resulting from the transfer of water vapor (Webb et al. 1980) and calculated as a product of turbulent diffusivity and the 20 minute average CO_2 gradient that was measured along with the humidity. We represent fluxes towards the land surface as negative values, and fluxes into the atmosphere as positive values.

4.3.4 Flask measurements

We observed diurnal and seasonal changes of CO_2, and associated isotopic signatures of ^{13}C and ^{18}O from air flasks above canopy at 1 and 2m heights. The heights were selected based on the fact that the flux-profile relationships are valid above the roughness sub layer at vertical distances 2-3 times canopy height (Kaimal and Finnigan, 1994).

Atmospheric samples were pumped through a large glass flask (2.5L) with two stopcocks. Flask samples from the two heights were collected simultaneously. All flask samples were dried using $Mg(ClO_4)_2$ trap prior to collection to avoid contamination of the $\delta^{18}O$ values. These flasks representing 20-30 minute time averages were obtained approximately every 4 hours. Flasks were analyzed for CO_2 using the high-precision non-dispersive infrared gas analysis system used for the NOAA global flasks (Conway et

al. 1994) and analyzed for ^{13}C and ^{18}O using a continuous-flow mass spectrometer at the stable isotope laboratory with precision of ± 0.03 ‰ for $\delta^{13}C$ and ± 0.05 ‰ for $\delta^{18}O$ (Trolier et al. 1996) at University of Colorado at Boulder. The measurement precision for CO_2 concentration is 0.1 ppm.

4.3.5 ^{18}O of leaf water and soil water

Leaf samples were collected for analysis of $\delta^{18}O$ of water during collection of air samples from flasks over the growing season in 2000. Samples were stored in glass vials wrapped with wax film, and kept frozen until analysis. Leaf water was extracted by cryogenic vacuum distillation. Extracts were equilibrated with CO_2 and analyzed for $\delta^{18}O$ by dual-inlet mass spectrometry.

Soil samples were collected from 8 depths (1, 3, 5, 7, 10, 15, 25 and 50cm) once each diurnal set over the 2000 and 2001 growing seasons to conduct analysis of changes in soil water content and isotopic composition of soil water. In 2001, samples were collected from two separate soil pits located within two blocks to examine variability in the depth profile of $\delta^{18}O$ of soil water. Collected soil samples were sealed and stored frozen in glass vials until analysis for gravimetric soil water content and soil water $\delta^{18}O$. $\delta^{18}O$ of the water was analyzed by direct equilibration (12 hrs) with CO_2 using dual-inlet isotope ratio mass spectrometry. Leaf and soil water isotopic composition is reported with respect to the Vienna Standard Mean Ocean Water (V-SMOW) (Coplen 1996). The data were used for modeling leaf water, leaf and soil respired CO_2.

4.3.6. Partitioning approach

Tower samples allow detection of diurnal, seasonal and interannual differences in gross fluxes of photosynthesis (F_P) and respiration (F_R). We partitioned gross fluxes using the ^{13}C and ^{18}O isotopic mass balance method that is similar to the Yakir and Wang (1996) approach in principle, however, slightly different estimations of ^{13}C discrimination for net ecosystem exchanges ($\delta^{13}C_B$ or $\delta^{18}O_B$) during daytime periods, photosynthetic assimilation ($\delta^{13}C_P$ or $\delta^{18}O_P$), and combined ecosystem respiration ($\delta^{13}C_R$ or $\delta^{18}O_R$) were applied to our study.

$$F_B (=NEE) = F_P + F_R \tag{4.1}$$

$$\delta^{13}C_{B*} F_B (=\delta^{13}C_B NEE) = \delta^{13}C_R * F_R + \delta^{13}C_P * F_P \tag{4.2}$$

$$\delta^{13}C_B = f_P * \delta^{13}Cp + (1\text{-}fp) * \delta^{13}C_R \tag{4.3}$$

$$fp = \frac{\delta^{13}C_B - \delta^{13}C_R}{\delta^{13}C_p - \delta^{13}C_R}, \quad f_R = \frac{\delta^{13}C_B - \delta^{13}C_p}{\delta^{13}C_R - \delta^{13}C_p} \tag{4.4}$$

$$Fp = F_B * fp \ (= NEE*fp) \tag{4.5}$$

$$F_R = F_B * f_R (= NEE*f_R) \tag{4.6}$$

Where F_B (=NEE): net CO_2 exchanges derived from Bowen ratio energy balance (BREB); F_P: canopy photosynthetic flux density ($\mu mol\ m^{-2}\ s^{-1}$);F_R: ecosystem

respiratory flux density (μmol m^{-2} s^{-1}); fp: fraction from photosynthesis; f_R: fraction from respiration. Isotopic terms are defined below.

4.3.6.1 Estimate of $\delta^{13}C_B$

We estimated $\delta^{13}C_B$ (= 2m' $\overline{C}$ + b') by collecting air samples during the day. The terms m' and b' can be obtained by following equation

$$\delta^{13}C_a = m'C_a + b' \quad (4.7)$$

Where m' and b' are coefficients of linear regression for C versus $\delta^{13}C_a$. The C_a is CO_2 concentration and overbar indicates time averaging over daylight measurements from flask samplings.

4.3.6.2 Estimate of $\delta^{13}Cp$ by modeling canopy assimilation and conductance from leaf to canopy scale

Independent modeling of canopy assimilation and conductance by plant functional group (C_3 versus C_4) was performed to estimate canopy scale of discrimination against ^{13}C (Δ_E) through C_i/C_a. The mixed C_3 and C_4 ecosystem was simulated by running photosynthesis subroutines cycle twice, once for each physiological type, and separate photosynthetic assimilation rate and overall surface conductance from the two components were calculated. The parameterizations of photosynthesis and stomatal and canopy conductance are based on equations in Farquhar et al. (1980), Collatz et al. (1991)

and Ball et al. (1987). Parameters used for the photosynthesis model are listed in Table 4.2. An appendix to this article provides definition of terms and equations used in the photosynthesis model. The photosynthetic model is combined with the Ball (1987) semi-empirical model for leaf stomatal conductance.

$$g_s = \frac{m_s \cdot A_n \cdot h}{Cs} + b_s \tag{4.8}$$

where g_s= leaf stomatal conductance (mol m^{-2} s^{-1}). The m_s and b_s are stomatal slope and intercept factors. A_n is net assimilation. h is the relative humidity. The Cs is the CO_2 concentration at the leaf surface.

Cs is calculated as

$$Cs = C_a - \frac{1.4 \times A_n}{g_b} \tag{4.9}$$

where C_a is ambient CO_2 concentration and g_b is the leaf boundary layer conductance (mol m^{-2} s^{-1}).

The bulk canopy conductance and intercellular CO_2 concentration should be flux-weighted, based on relative contributions of C_3 and C_4 species.

The bulk canopy boundary layer resistance (under neutral conditions) is given by

$$r_B = 1/g_b = \frac{C_l}{u^{1/2}} \tag{4.10}$$

where C_l = bulk canopy boundary layer resistance coefficient (m s^{-1})$^{-1/2}$; u = wind

speed (m s^{-1})

A modification to the soil water stress function suggested by Colello et al. (1998) was adopted.

$$V_m = f_w(\theta)V_{c\max} \tag{4.11}$$

$$f_w = \frac{\theta - \theta_w}{\theta_i - \theta_w} \tag{4.12}$$

where θi is surface soil moisture at the onset of water stress. We set this value as 0.14. θw is surface soil moisture at wilting point (=0.03). The V_m is Rubisco capacity, μmol m^{-2} s^{-1}. V_{max} is maximum Rubisco capacity per unit leaf area (μmol m^{-2} s^{-1})

To integrate these equations over the canopy scale, we used scaling factor (Π) addressed by Sellers et al. (1996).

$$A = A_{no}\Pi \tag{4.13}$$

$$\Pi \approx FPAR / \bar{k} \tag{4.14}$$

$$FPAR \approx \lambda\nu(1 - e^{-kLAI/\lambda}) \tag{4.15}$$

where A is canopy photosynthesis, FPAR is the fraction of incident radiation absorbed by the green canopy. The A_{no} is the net photosynthesis for the leaves at the top of the canopy, λ is the clumping factor, ν is canopy greenness, L_T is the leaf area index. $\bar{k}$ is the mean canopy extinction coefficient , weighted by daily mean radiation. The diurnal Sun Zenith angle was calculated according to the formulation by Campbell and Norman (1989).

Bulk intercellular CO_2 concentration (Ci) can be calculated by

$$C_i = C_a - \frac{1.6A}{G_c} \tag{4.16}$$

where Gc is bulk canopy conductance (mol m^{-2} s^{-1}) and A is the canopy photosynthesis.

The next step is to calculate Δ to estimate $\delta^{13}Cp$. Discrimination against ^{13}C during photosynthesis can be calculated by (Farquhar et al. 1989)

$$\Delta = a + (b-a) \times \frac{C_i}{C_a} \tag{4.17}$$

where a is diffusion fractionation (4.4 ‰), b is enzymatic fractionation (27.5 and 0.6 for C_3 and C_4 plants, respectively).

Canopy scale discrimination Δ_E can be estimated by weighted leaf area index (LAI) of C_3 and C_4 plants.

$$\Delta_E = \frac{\sum_{i=3,4} LAI\Delta_i}{LAI} \tag{4.18}$$

where i = 3 represents C_3 species and i = 4 represents C_4 species.

Finally, $\delta^{13}Cp$ can be calculated by (Bowling et al. 2001)

$$\delta^{13}C_p = \delta_{a\_CO_2} - \Delta_E \tag{4.19}$$

4.3.6.3 Estimate $\delta^{13}C_R$

$\delta^{13}C_R$ values obtained from the intercept of a geometric mean regression between the measured isotopic composition vs. $1/[CO_2]$ from night-time flasks. Sources of $\delta^{13}C$ values of respired CO_2 include both plant and soil organic carbon respiration.

4.3.6.4 Estimate $\delta^{18}O_B$

$\delta^{18}O_B$ values were obtained from a similar equation used for the estimation of $\delta^{13}C_B$. Daytime air samples were used for the calculation.

$$\delta^{18}O_B = 2m' \bar{C} + b' \quad (4.20)$$

where m and b can be obtained by following equation.

$$\delta^{18}O_a = m'C_a + b' \quad (4.21)$$

Where m' and b' are coefficients of linear regression for C versus $\delta^{18}O_a$. C_a is CO_2 concentration and overbar indicates time averaging over daylight measurements of flask sampling to obtain m and b.

4.3.6.5 Estimate $\delta^{18}O_p$

Due to different extent of isotopic equilibrium and different carbonic anhydrase (CA) hydration rates by C_3 versus C_4 plants, the following equations were applied (Gillon and Yakir 2000) and then productivity weighted $\delta^{18}Op$ scaled to the canopy. Measured and modeled values for $\delta^{18}O$ of leaf water ($\delta^{18}O_{LW}$) were used to compute $\delta^{18}O_P$.

$$\delta^{18}O_p = -\varepsilon_k' - c_\varepsilon[\theta_{eq}(\delta_e - \delta^{18}O_a) - (1-\theta_{eq})\varepsilon_k'/(c_\varepsilon + 1)] \quad (4.22)$$

where ε_k' is the weighted mean of discrimination during the diffusion from ambient air to the sites of carboxylation within the chloroplast including smaller fractionations in the laminar boundary layer and during diffusion through solution (7.4‰; Farquhar et al. 1993); δ_e refers to the $\delta^{18}O$ of CO_2 in equilibrium with chloroplast water. The $\delta^{18}O_a$ is the oxygen isotope ratio of CO_2 in the atmosphere; $C\varepsilon = c_{cs}/(c_a - c_{cs})$; c_{cs} and c_a are CO_2 concentrations at the site of CO_2-H_2O exchange in leaves and in ambient air, respectively. The c_{cs} was estimated from $(c_i - c_{cs})/c_a = 0.1$ (Wang et al. 1998). The c_i is CO_2 concentration in the stomatal cavity, estimated from the photosynthesis model addressed above. The definition of c_{cs} is necessary because CO_2 mixing ratios between at the site of Rubisco (c_c) and the chloroplast can be significantly different due to large internal resistances (Gillon and Yakir, 2000)

The θ_{eq} is isotopic equilibrium addressed by Gillon and Yakir (2000). We assumed θ_{eq} is constant and used mean estimates of isotopic equilibrium values (0.7 and 0.52 for C_3 and C_4 plants, respectively) derived from Gillon and Yakir (2000).

Relative contribution of plant functional types was taken account in scaling leaf to canopy level.

$$\Delta^{18}O_{canopy} = \sum_{i=3,4} P_i \Delta^{18}O_i \quad (4.23)$$

P represents % weighted aboveground plant biomass. i represents plant functional types.

Since no $\delta^{18}O$ signatures for leaf water were measured during 2001, evaporative enrichment of leaf water was modeled using the Craig-Gordon model (Craig and Gordon 1965) as described by Flanagan et al. (1991, 1997).

$$\delta^{18}O_{LW} = \delta_{sw} + \varepsilon_{eq} + \varepsilon_{\kappa} + h\,(\delta_{\alpha} - \varepsilon_{\kappa} - \delta_{sw}) \qquad (4.24)$$

Where δ_{sw} is $\delta^{18}O$ of source water that plants use. We assumed C_3 and C_4 plants should have different δ_{sw} because of their different root distribution patterns. We used $\delta^{18}O$ of soil water at 25 cm for the representative source water for C_3 plants and at 10 cm for C_4 plants. ^{18}O of soil water weighted by volumetric water content corresponding to each depth was used for δ_{sw}. h is relative humidity at the leaf surface temperature. We calculated leaf temperature by the energy budget of the leaf (Campbell and Norman 1989). Assuming the boundary layer of grass is rather smooth, the leaf temperature was higher by 1-2 $^{\circ}C$ than air temperature during daytime. ε_{κ} is the kinetic fractionation factor. ε_{κ} can be calculated as (Farquhar et al. 1989)

$$\varepsilon_{\kappa} = \frac{32r_s + 21r_b}{r_s + r_b} \qquad (4.25)$$

where r_s and r_b are the stomatal and boundary layer resistances to water vapor diffusion (m^2 s mol^{-1}), and 32 and 21 are fractionation factors (‰). These fractionation values have been revised based on recent experiments showing $^{16}O/^{18}O$=1.032 (Cappa et al. 2003) rather than 1.028 (Merlivat 1978).

The $\delta^{18}O$ of atmospheric water vapor (δ_a) was estimated by assuming air moisture is near equilibrium with the local precipitation at air temperature during sampling time. The equations of Majoube (1971) were used to calculate the temperature dependent fractionation factor for water liquid-vapor equilibrium.

4.3.6.6 Modeled soil temperature and moisture profiles

For data entry of soil temperature depth profile in Pieter Tans' model (1998) described as below, we used a model developed by Parton and Logan (1981) for estimating diurnal variations in soil temperature by depth ranging from 0-50 cm given the maximum and minimum soil temperature. A truncated sine wave was used to predict variation of daytime temperature and an exponential function to predict nighttime temperatures (Parton and Logan, 1981).

We estimated diurnal variations in the soil moisture profile by depth, using automatic 20 minute –volumetric soil moisture measurements averaged 0-15cm and soil moisture profile from 0 to 50 cm around 3-5 cm interval measured on each sampling period. Polynomial equations (provided by KaleidaGraph software) were derived to predict diurnal variations in soil moisture profile. Soil moisture gradients by depth were corrected based on measured soil moisture profile from 0 to 50 cm depth around 3-5 cm interval on each sampling date. Polynomial equation depicting diurnal pattern of soil moisture was applied to each soil layer. When little diurnal variations in surface soil moisture were observed, we assumed measured soil moisture profile by depth was constant throughout a day.

4.3.6.7. Estimate of $\delta^{18}O_R$

We used Tans' model to estimate $\delta^{18}O$ of soil respired CO_2 (Tans 1998; Miller et al. 1999). This model calculates $\delta^{18}O$ of root and soil respiration as a function of soil water, temperature-dependent equilibrium (ε_{eq}) and kinetic fractionation (Tans 1998; Miller et al. 1999). The model also incorporates the influence of abiotic or invasion fluxes and develops analytical solutions for the $\delta^{18}O$ value of soil gas CO_2 and surface CO_2 fluxes for a range of environmental conditions. The real boundary conditions of atmospheric ^{13}C and ^{18}O signatures from flasks, estimated soil moisture and temperature profile by each layer on hourly basis and CO_2 production from chamber measurements were used to run the model. We assumed the residence time of air was not greater than tens of seconds and contributions of invasion to δ_a would be small.

The $\delta^{18}O$ values of soil water measured one per each diurnal were used to produce a continuous time series by assuming that the measured value was representative of a period 12 hours before and after the measurement. Effective kinetic fractionation related to volumetric soil water content was subtracted from the isotopic value of the CO_2 equilibrated with surface soil water.

4.4 Integration of NEE and gross photosynthetic fluxes, and linear regression analyses

We integrated NEE derived from BREB and gross photosynthetic fluxes estimated from isotopic partitioning approach using KaleidaGraph (version 3.5). Linear regression analyses were conducted to test if any environmental variables were coupled with integrated gross photosynthetic fluxes. The variables expected to influence gross photosynthesis included vapor pressure deficit (VPD), soil water content and midday

leaf water potential.

4.4 Results

4.4.1 Local weather and meteorology

Mean annual precipitation was similar between 2000 and 2001 (311mm and 348mm, respectively), but the structure of the seasonal precipitation regime was different between the two years. More frequent precipitation events including small (<10mm) and moderate size events (10mm to 25mm) occurred in 2001 than in 2000 while a large precipitation event (>25mm) occurred in August 2000 (Fig.4.1). Monthly mean precipitation was greater in growing season of 2001 than in 2000 with maximum of 73.8 mm in May, 2001 (Table4.1). Daily mean air and soil temperatures during sampling periods in 2000 were relatively higher than during those days in 2001. In general, 2000 had higher VPD values and lower June-July soil moisture levels than were observed in 2001. In addition, the 2000 season had the lower soil moisture from June to July.

4.4.2 Midday leaf water potential

Average leaf water potential for *P. smithii* (C_3) was lower in 2000 than in 2001 (Table 4.1). The lowest leaf water potential was recorded in July, 2000 indicating severe water stress on the plants.

4.4.3 Daytime and seasonal patterns of net CO_2 exchange (NEE) and integrated values of day/night time NEE

For the days that we measured, the CO_2 uptake was lower in 2000 than in 2001 except for July 2001 (Fig.4.2). Diurnal cycles of net CO_2 exchange in relatively moist conditions were different from drought periods. During the dry season of 2000, a gradual increase in CO_2 uptake occurred in the early morning, then decreased or stopped toward noon, suggesting canopy scale-stomatal closure. The CO_2 uptake was resumed about 1 to 2 hours after mid-day and reached maximum rates around 1400 to 1500 STD in drought periods. During another dry period in July 2001, the CO_2 uptake gradually declined from early morning to completely cease shortly after midday and then the system became a CO_2 source. By contrast, during moist periods of 2001, maximum CO_2 uptake occurred around 10 a.m. and persisted for 2-3 hours. Photosynthesis gradually decreased toward late afternoon. These differences in daytime pattern of CO_2 uptake during dry versus wet periods were comparable to northern temperate grassland (Flanagan et al. 2002) and tall grass prairie (Suyker and Verma, 2001; Lai et al. 2003).

Integrated values of day and night time NEE indicate seasonal differences in net fluxes (Table 4.3). Despite similar net CO_2 exchange between DOY 143 and 207, a greater daytime integrated CO_2 uptake was estimated on DOY 143. In 2000, the daytime CO_2 uptake was lowest in July with concurrent high air and soil temperature, high vapor pressure deficit, and low soil moisture (Table 4.1). There was a brief relief of moisture stress following precipitation in late August (Fig.4.1), so uptake increased in September. In 2001, rates of daytime CO_2 uptake were highest in May and June under conditions of low air/soil temperatures and vapor pressure deficit, high soil moisture and cumulative monthly precipitation (Table 4.3). The daytime integrated CO_2 uptake was lowest on DOY 208 when soil moisture had declined to 3.1 %.

4.4.4 Partitioning net ecosystem exchange into gross photosynthesis and respiration using ^{13}C and ^{18}O signatures

4.4.4.1 Variations of end members for $\delta^{13}C$ partitioning

We estimated three end members for $\delta^{13}C$ partitioning; ^{13}C discrimination of net ecosystem exchange ($\delta^{13}C_B$), photosynthetic assimilation ($\delta^{13}C_p$), and ecosystem respiration ($\delta^{13}C_R$). There were significant intra-annual and inter-annual differences in $\delta^{13}C_R$ (Table 4.4). The $\delta^{13}C_R$ values varied by as much as 5 ‰ and 7 ‰ over both growing seasons. The $\delta^{13}C_R$ ranged from –14 ‰ (May 2000) to –22 ‰ (June 2001).

The net ecosystem exchange $\delta^{13}C$ values ($\delta^{13}C_B$) during daytime were always more depleted than the $\delta^{13}C_R$ values. In July 2001, the estimate of mean $\delta^{13}C_B$ was very similar to the mean value of $\delta^{13}C_R$ eliminating the potential that ^{13}C of CO_2 can be used to partition NEE into gross photosynthesis and respiration for that date.

Variations in $\delta^{13}C_p$ are dependent on C_i/C_a in association with Δ_E. The modeled values of C_i/C_a were relatively consistent during nighttime (data are not shown) then gradually decreased as air temperature and VPD increased indicating gradual closure of stomata (data are not shown). Severe dry conditions during June and July of 2000 caused almost complete stomatal closure for 1000-1200 LST. Moist conditions followed by precipitation events in the first sampling dates in May and July 2001 and second dates in September 2000 (Fig.4.1) provided conditions to maintain stomata open during the morning hours. In May and July of 2001, the magnitude of decreasing C_i/C_a became

greater toward afternoon as relative humidity decreased.

Modeled estimates of canopy discrimination of C_4 plants (Δ_{C4}) inversely followed the pattern of modeled C_i/C_a since enzymatic fractionation against ^{13}C is smaller than diffusion fractionation resulting in a negative relationship between Δ_{C4} and C_i/C_a (Fig.4.4). However, the pattern of Δ_{C3} showed a positive relationship to C_i/C_a due to greater enzymatic fractionation of RUBISCO in C_3 plants at higher C_i/C_a.

The modeled canopy scale ^{13}C discrimination (Δ_E) varied on diel time scales suggesting a controlling relationship to environmental variables such as vapor pressure deficit (Fig.4.5). Generally, minimum Δ_E and more positive $\delta^{13}Cp$ ($\delta_a - \Delta_E$) occurred when VPD was highest. Seasonal variations in Δ_E were sensitive to changes in relative productivity of C_3 and C_4 plant species in pattern and magnitude of bulk canopy discrimination against ^{13}C. Greater relative productivity of C_3 plants in 2001 likely dominated patterns of canopy scale ^{13}C discrimination. Lower canopy ^{13}C discrimination was observed in 2000 than in 2001 due to a lower C_3/C_4 LAI in 2000 than in 2001.

An important pre-requisite for partitioning is distinctive end members to distinguish both photosynthetic and respiratory fluxes. Isotopic equilibrium prevailed during daylight periods on May 2000, so partitioning was not attempted. Equilibrium occurred around noon in June 2000 (Fig.4.6a) and $\delta^{13}C_p$ values were even lower than $\delta^{13}C_R$ before noon, which restricted application of equations to partitioning. Isotopic equilibrium between $\delta^{13}C_p$ and $\delta^{13}C_R$ never occurred in September 2000 and other months of 2001.

4.4.4.2 Variations of end members for $\delta^{18}O$ partitioning

For $\delta^{18}O_B$, there were no positive relations between $\delta^{18}O$ and inverse $[CO_2]$ in May and July, 2000 during daytime measurements (Table 4.4). We observed an increase in the $\delta^{18}O$ value of atmospheric CO_2 at night in connection with the increase in CO_2 concentration during those periods of flask measurements. Positive relations were shown in 2001; however, no significant relations were formed during daytime measurements. Discernable end members of photosynthesis and respiration in June and September 2000 enabled partitioning NEE into gross photosynthesis and respiration.

Modeled variations in the other two end members are displayed in Fig.4.6b. The $\delta^{18}Op$ values were generally higher than $\delta^{18}O_R$ but there were exceptional periods such as late afternoon in June and early morning in September. Isotopic equilibrium between the two occurred around 0820 (local time) in both months and around 1620 in September.

4.4.4.3 ^{13}C partitioning approach

Partitioning approach with isotopes requires explicit differences among end members. Failure of this requirement makes the partitioning approach with carbon isotopes unavailable in May 2000 and July 2001. For the dates we used, modeled gross photosynthesis was generally lower in 2000 than in 2001 (Fig.4.7). Gross photosynthetic CO_2 fluxes were greatest for two consecutive days in June 2001 (Fig.4.7) compared to May 2001 even though greatest integrated CO_2 uptake were observed for the second day of May (Table 4.3).

There was a significant relationship between integrated photosynthetic CO_2 fluxes derived from ^{13}C labeled partitioning approach and integrated CO_2 uptake calculated from Bowen Ratio technique ($R^2 = 0.69$). Integrated daily estimates of gross

photosynthesis from isotopic partitioning method were generally higher than those of CO_2 uptake by Bowen Ratio technique (Fig.4.8).

4.4.4.4. Comparison of partitioning approach between $\delta^{13}C$ and $\delta^{18}O$ signatures

Due to restricted usage of ^{18}O signatures for partitioning as addressed before, only two months can be used for comparison of partitioning derived from both ^{13}C and ^{18}O. Partitioning using ^{13}C signatures was tightly associated with same method using ^{18}O signatures in June 2000 (R^2=0.81) while they had less strong linear relations in September 2000 (R^2=0.48) (Fig.4.9). Photosynthetic CO_2 fluxes partitioned with oxygen isotope were overestimated relative to those with carbon isotopes in most time periods in September. We excluded conditions when isotopic equilibrium among end members prevailed and when stomatal conductance limited influence of photosynthetic activity on $\delta^{13}Cp$ or $\delta^{18}Op$. We applied partitioning approach with carbon isotopes on appropriate time periods when signals from both end members were big enough to separate NEE, which resulted in good regression coefficients between the two methods.

4.4.4.5 Linear regression model of integrated gross photosynthetic fluxes with environmental variables

Soil moisture and leaf water potential were good indicators of variations in integrated gross photosynthesis (R^2 = 0.71, R^2 = 0.45, respectively, $p < 0.05$) (Fig.4.10). VPD was negatively related to variations in integrated gross photosynthesis (R^2=0.4, $p < 0.05$). Gross respiration had no significant relations with environmental variables.

4.5 Discussion

In order to partition NEE into photosynthesis and respiration successfully, considerable differences among end members should be required (Yakir and Wang 1996; Bowling et al. 2003; Lai et al. 2003). If isotopic measurements fail to provide information for labeling associated bi-directional fluxes, partitioning will not work appropriately. The difference between $\delta^{13}C_B$ and $\delta^{13}C_R$ was too small to use those signatures for partitioning in July 2000 and 2001. Similar results were reported in tall grass prairie under drought periods (Lai et al. 2003). No significant differences between two end members in dry conditions in 2001 constrained the application of using ^{13}C labeled partitioning.

In dry time periods, isotopic mass balance approach using ^{18}O signatures can be used as an alternative to ^{13}C partitioning due to the large ^{18}O enrichment in leaf water (Yakir and Sternberg 2000). However, in our study, obtaining significant linear relations between $\delta^{18}O$ and inverse $[CO_2]$ during daytime measurements was limited in many cases such as dry spring, severe water stress conditions and intermittent rain events. The dry spring conditions in 2000 reduced early onset of growth of cool season grasses (C_3 grasses) and led to no apparent signal of photosynthetic activity on $\delta^{18}O$ of atmospheric CO_2 in the early growing season. In severe water stress periods as in July 2000, no enriched ^{18}O signal associated with photosynthetic activity was observed during daytime. This is most likely associated with stomatal closure and a general lack of exchange between atmospheric CO_2 and leaf water. Variations in ^{18}O of CO_2 without explicit photosynthetic resulted in poor regression coefficients for Keeling plots during prolonged dry conditions in 2000 (Table 4.4). In addition to lack of photosynthetic $C^{18}O^{16}O$ signal during prolonged dry conditions, less coupling between water vapor and carbon

occurred in rainy sampling periods as in May and July 2001, possibly due to condensation.

Time-dependent isotopic disequilibrium between $\delta^{13}Cp$ (or $\delta^{18}Op$) and $\delta^{13}C_R$ (or $\delta^{18}O_R$) is the next criteria for partitioning. Variations in $\delta^{13}C_p$ (or $\delta^{18}Op$) are dynamic on diel time scales in response to environmental variables, possibly through diel changes in stomatal conductance. The $\delta^{13}C_R$ is relatively conservative and varied with longer term of environmental variables such as relative humidity (Ekblad and Hogberg 2001) and vapor pressure deficit (Bowling et al. 2001). The effects were observed over days to weeks due to different turn over rates of respired carbon residues that contribute to signal of $\delta^{13}C_R$. Under prolonged dry conditions, transfer of newly fixed photosynthate to $\delta^{13}C_R$ took longer than 2 weeks; this lag reflects a shift of respiration from labile to recalcitrant carbon pools in the soil (Schonwitz et al. 1986). Isotopic equilibrium ($\delta^{13}C_R = \delta^{13}Cp$) would be a function of the interplay between recalcitrant and labile pools of carbon and the aboveground photosynthetic mixture in mixed C_3 and C_4 ecosystems. Sensitivities of seasonal variations in photosynthetic mixture coupled to precipitation regimes such as timing, frequency and amount of precipitation affected $\delta^{13}C_R$ (See chapter 2), which consequently determined the timing of isotopic equilibrium. In this study, isotopic equilibrium occurred around noon and $\delta^{13}Cp$ was even more depleted than $\delta^{13}C_R$ before noon in June. The severe dry conditions resulted in almost complete stomatal closure for 1000-1200 LST and enriched $\delta^{13}C_R$ reflected the lack of new C inputs from the C_3 community during dry spring in 2000. The $\delta^{18}Op$ was in equilibrium with $\delta^{18}O_R$ in the early mornings in both months. Transition periods have no clear distinction between end

members and consequently, reduced correlations between carbon and oxygen labeled partitioning approaches. Under conditions of isotopic disequilibrium among end members, significant relations between ^{13}C and ^{18}O partitioning for gross photosynthesis can be observed in June and September 2000.

The photosynthetic fluxes separated by ^{13}C labeled partitioning approach for growing seasons of two years had good correlations with integrated CO_2 uptake calculated from Bowen ratio data. However, nearly all gross photosynthesis partitioned by ^{13}C signals were higher than estimates based on integrated values of CO_2 uptake from Bowen Ratio technique. There is a possibility that CO_2 uptake from BREB may be underestimated. We obtained integrated CO_2 uptake values from the subtraction of integrated night time NEE from integrated values of net CO_2 exchange (calculated from Bowen ratio data) because both CO_2 uptake and loss contributed to net CO_2 exchange. An assumption behind the calculation is that nighttime respiration should approximate daytime respiration. However, daytime total ecosystem respiration is likely to differ from nighttime respiration. Increasing leaf temperature caused by restricted transpiration following increased sensible heat transfer could promote respiration over assimilation (Baldocchi 1997). This increase in daytime respiration would result in an increase in daytime CO_2 uptake.

Soil moisture and leaf water potential were good indicators of variations in integrated gross photosynthesis ($R^2 = 0.72$) (Fig.4.10). In this semi-arid grassland ecosystem, water availability is the most important limiting factor of primary production (Sala et al. 1988; Lauenroth and Sala 1992). The greatest net CO_2 uptake was observed in the middle of the rainy season, at peak leaf area index in a semiarid grassland and

shrubland (Emmerich 2003) indicating the importance of plant physiological responses to water in influencing ecosystem- scale CO_2 uptake. Significant relationships between gross photosynthetic fluxes and VPD suggested that stomatal conductance tightly regulated by relative humidity in leaf level also controlled gross photosynthetic fluxes at ecosystem level to some degree.

4.6 Conclusions

Partitioning approach with carbon isotope had more applicability compared to that with oxygen isotopes in shortgrass steppe. Lack of photosynthetic $C^{18}O^{16}O$ signal during prolonged dry conditions and less coupling between water vapor and carbon in rainy sampling periods constrained the separation of NEE into gross photosynthesis and respiration. However, restricted usage of partitioning with carbon isotope was also revealed in dry condition in July 2001.

Despite the limitations, photosynthetic CO_2 fluxes partitioned by both stable isotopes agreed well, and the relationship was stronger when isotopic disequilibrium between $\delta^{13}C_p$ and $\delta^{13}C_R$ was strong.

Notation

A_{no} net photosynthesis for the leaves at the top of the canopy, μmol m^{-2} s^{-1}

A_n net photosynthetic rate, μmol m^{-2} s^{-1}

a diffusion fractionation, ‰

a' leaf absorption to photosynthetically active radiation

$\bar{a}$ mean diffusional fractionation of CO_2 from air to leaf, ‰

b enzymatic fractionation, ‰

b_s stomatal intercept factor

C_a ambient CO_2 concentration, μmol mol^{-1}

Ci bulk canopy intercellular CO_2 concentration, μmol mol^{-1}

Cl bulk canopy boundary layer resistance coefficient, $(m\ s^{-1})^{-1/2}$

Cs CO_2 concentration at the leaf surface, μmol mol^{-1}

c_{cs} CO_2 concentrations at the site of CO_2-H_2O exchange in leaves, μmol mol^{-1}

F_p canopy photosynthetic flux density, μmol m^{-2} s^{-1}

F_R ecosystem respiratory flux density, μmol m^{-2} s^{-1}

F_B net CO_2 exchanges derived from Bowen ratio energy balance (BREB), μmol m^{-2} s^{-1}

FPAR fraction of incident radiation absorbed by the green canopy

Gc bulk canopy conductance, mol m^{-2} s^{-1}

g_b leaf boundary layer conductance, mol m^{-2} s^{-1}

g_s leaf stomatal conductance, mol m^{-2} s^{-1}

h relative humidity, %

J_C Rubisco-limited rate of assimilation, μmol m^{-2} s^{-1}

J_E light limited rate of assimilation , μmol m^{-2} s^{-1}

J_S Carbon compound export limitation, μmol m^{-2} s^{-1}

Kc Michaelis constant for CO_2

Ko Michaelis constant for oxygen inhibition

$\bar{k}$ mean canopy extinction coefficient weighted by daily mean radiation

LAI leaf area index for C_3 or C_4, $m^2 m^{-2}$

NEE net ecosystem exchange for CO_2 fluxes, μmol m^{-2} s^{-1}

r_B bulk canopy boundary layer resistance, m^2 s mol^{-1}

rb leaf boundary layer resistance, m^2 s mol^{-1}

rs stomatal resistance, m^2 s mol^{-1}

u wind speed, m s^{-1}

α intrinsic quantum efficiency for CO_2 uptake, mol mol^{-1}

m_s stomatal slope factor

Q_p PAR photon flux density incident on the leaf, μmol m^{-2} s^{-1}

R_d leaf respiration rate, μmol m^{-2} s^{-1}

T_l leaf temperature (° C)

τ a ratio of kinetic parameters indicating the partitioning of RuBP to the carboxylase or oxygenase reactions of Rubisco

Vm Rubisco capacity, μmol m^{-2} s^{-1}

V_{max} maximum Rubisco capacity per unit leaf area (μmol m^{-2} s^{-1})

ν canopy greenness

λ clumping factor

Π scaling factor

$\delta^{13}C_B$ carbon isotopic composition of CO_2 associated with net ecosystem exchange, ‰

$\delta^{13}C_R$ $\delta^{13}C$ of ecosystem respiration, ‰

$\delta^{13}C_P$ carbon isotopic composition of the CO_2 assimilated via photosynthesis, ‰

$\delta^{18}O_B$ oxygen isotope composition of CO_2 associated with net ecosystem exchange,

‰

$\delta^{18}O_R$ $\delta^{18}O$ of ecosystem respiration, ‰

$\delta^{18}O_P$ oxygen isotope composition of CO_2 assimilated via photosynthesis, ‰

$\delta^{13}C_a$ $\delta^{13}C$ of canopy air, ‰

$\delta^{18}O_a$ $\delta^{18}O$ of canopy air, ‰

$\delta^{18}O_{LW}$ $\delta^{18}O$ of leaf water, ‰

$\delta_{a\_CO_2}$ $\delta^{13}C$ of background CO_2, ‰

δ_e $\delta^{18}O$ of CO_2 in equilibrium with chloroplast water, ‰

δ_{sw} Oxygen isotopic composition of source water, ‰

δ_a $\delta^{18}O$ of atmospheric water vapor, ‰

Δ discrimination against ^{13}C during photosynthesis, ‰

Δ_E canopy-scale carbon discrimination, ‰

$\Delta^{18}O_{canopy}$ canopy-scale oxygen discrimination, ‰

ε_{eq} temperature-dependent equilibrium factor, ‰

ε_κ kinetic fractionation factor, ‰

θ surface soil moisture, $m^3\ m^{-3}$

θi surface soil moisture at the onset of water stress, $m^3\ m^{-3}$

θw surface soil moisture at willing point, $m^3\ m^{-3}$

θ_{eq} isotopic equilibrium associated with CA activity

4.7 References

Baldocchi DD (1997) Measuring and modeling carbon dioxide and water vapor exchange over a temperate broad-leaved forest during the 1995 summer drought. Plant, Cell and Environment 20:1108-1122.

Baldocchi D, Falge E, Wilson K (2001) A spectral analysis of biosphere-atmosphere trace gas flux densities and meteorological variables across hour to multi-year time scales. Agricultural and Forest Meteorology 107:1-27.

Ball JT (1987) Calculations related to gas exchange In: E. Zeiger, GD Farquhar and IR Cowan (eds.), Stomatal function. Stanford University Press, Stanford, CA. pp. 446-476.

Bowling DR, McDowell NG, Bond B.J., Law BE, Ehleringer JR (2002) ^{13}C content of ecosystem respiration is linked to precipitation and vapor pressure deficit. Oecologia 131:113-124.

Bowling DR, Pataki DE, Ehleringer JR (2003) Critical evaluation of micrometeorological methods for measuring ecosystem-atmosphere isotopic exchange of CO_2. Agricultural and Forest Meteorology 116: 159-179.

Bowling DR, Baldocchi DD, Monson RK (1999) Dynamics of isotopic exchange of carbon dioxide in a Tennessee deciduous forest. Global Biogeochemical Cycles 13:903-922.

Bowling DR, Tans PP, Monson RK (2001) Partitioning net ecosystem carbon exchange with isotopic fluxes of CO_2. Global Change Biology 7:127-145.

Brenninkmeijer CAM, Kraft P, Mook WG (1983) Oxygen isotope fractionation between CO_2 and H_2O. Isotope Geoscience 1:181-190.

Brooks A, Farquhar GD (1985) Effect of temperature on the CO_2-O_2 specificity of ribulose-1, 5- biphosphate carboxylase/oxygenase and the rate of respiration in the light: estimates from gas exchange measurements on spinach. Planta 165:397–406.

Buchmann N, Guehl J-M, Barigah TS, Ehleringer JR (1997a) Interseasonal comparison of CO_2 concentrations, isotopic composition, and carbon dynamics in an Amazonian rainforest (French Guiana). Oecologia 110:120-131.

Buchmann N, Kao W-Y, Ehleringer J (1997b) Influence of stand structure on carbon-13 of vegetation, soils, and canopy air within deciduous and evergreen forests in Utah, United States. Oecologia 110:109-119.

Campbell GS, Norman JM (1989) Plant canopy structure. In: Plant canopies: their growth, form and function. G Russell, B Marshall, PG Javis (eds.), Cambridge University Press, Cambridge, pp. 1-19.

Campbell GS, Norman JM (1998) An introduction to Environmental Biophysics. Springer-Verlag, New York, 240 pages.

Cappa CD, Hendricks MB, DePaulo DJ, Cohen RC (2003) Isotopic fractionation of water during evaporation. Journal of Geophysical Research 108:4525, doi:10.1029/2003JD003597.

Ciais P, Tans PP, Trolier M, White JWC, Francey RJ (1995) A large Northern Hemisphere terrestrial CO_2 sink indicated by the $^{13}C/^{12}C$ ratio of atmospheric CO_2. Science 269:1089-1102.

Colello GD, Grivet C, Sellers PJ, Berry JA (1998) Modeling of energy, water, and CO_2 flux in a temperate grassland ecosystem with SiB2: May-October 1987. Journal of the Atmospheric Sciences 55:1141-1169.

Collatz GJ, Ball JT, Grivet C, Berry JA (1991) Physiological and environmental regulation of stomatal conductance, photosynthesis and transpiration: a model that includes a laminar boundary layer. Agricultural and Forest Meteorology 54:107-136.

Conway TJ, Tans PP, Waterman LS, Thoning KW, Kitzis DR, Masarie KA, Zhang N (1994) Evidence of interannual variability of carbon cycle from the National Oceanic and Atmospheric Administration/Climate Monitoring and Diagnosis Laboratory Global Air Sampling Network. Journal of Geophysical Research 99:22831-22855.

Coplen TB (1996) New guidelines for reporting stable hydrogen, carbon, and oxygen isotope-ratio data. Geochemica et Cosmochimica Acta 60:3359-3360.

Craig H, Gordon LI (1965) Deuterium and oxygen 18 variations in the ocean and the marine atmosphere. In: Stable Isotopes in Oceanographic Studies and Paleotemperatures, E. Tongiorgi (ed.), Spoleto, Italy, Lab. Di Geol. Nucleare, Cons. Naz. Delle Ric.

Dugas WA (1993) Micrometeorological and chamber measurements of CO_2 flux from bare soil. Agricultural and Forest Meteorology 67:115-128.

Dugas WA, Heuer ML, Mayeux HS (1999) Carbon dioxide fluxes over bermudagass, native prairie, and sorghum. Agricultural and Forest Meteorology 93:121-139.

Emmerich WE (2003) Carbon dioxide fluxes in a semiarid environment with high carbonate soils. Agricultural and Forest Meteorology 116:91-102.

Ekbland A, Högberg P (2001) Natural abundance of ^{13}C in CO_2 respired from forest soils reveals speed of link between tree photosynthesis and root respiration. Oecologia 127:305-308.

Farquhar GD, Caemmerer Sv, Berry JA (1980) A biochemical model of photosynthetic CO_2 assimilation in leaves of C_3 species. Planta 149:78-90.

Farquhar GD, Ehleringer JR, Hubick KT (1989) Carbon isotope discrimination and photosynthesis. Annual Review of Plant Physiology and Plant Molecular Biology 40: 503-537.

Farquhar GD, Lloyd J, Taylor JA, Flanagan LB, Syvertsen JP, Ehleringer JR (1993) Vegetation effects on the isotope composition of oxygen in atmospheric CO_2. Nature 363:493-443.

Ferretti DF, Pendall E, Morgan JA, Nelson JA, LeCain D, Mosier AR (2003) Partitioning evapotranspiration fluxes from a Colorado grassland using stable isotopes: Seasonal variations and ecosystem implications of elevated atmospheric CO_2. Plant and Soil 00:1-13.

Flanagan LW, Comstock JP, Ehleringer JR (1991) Comparison of modeled and observed environmental influences on the stable oxygen and hydrogen isotope composition of leaf water in Phaseolus vulgaris L. Plant Physiology 96:588-596.

Flanagan LB, Brooks JR, Varney GT, Ehleringer JR (1997) Discrimination against $C^{18}O^{16}O$ during photosynthesis and the oxygen isotope ratio of respired CO_2 in boreal forest ecosystems. Global Biogeochemical Cycles 11:83-98.

Flanagan LB, Wever LA, Carlson PJ (2002) Seasonal and interannual variation in carbon dioxide exchange and carbon balance in a northern temperate grassland. Global Change Biology 8:599-615.

Gillon JS, Yakir D (2000) Naturally low carbonic anhydrase activity in C_4 and C_3 plants limits discrimination against $C^{18}OO$ during photosynthesis. Plant, Cell and Environment 23:903-915.

Gilmanov TG, Verma SB, Sims PL, Meyers TP, Bradford JA, Burba GG, Suyker AE (2003) Gross primary production and light response parameters of four Southern Plains ecosystems estimated using long-term CO_2-flux tower measurements. Global Biogeochemical Cycles 17, 1071, doi:10.1029/2002 GB002023, 40-1-40-16.

Goulden ML, Munger JW, Fan S-M, Daube B, Wofsy SC (1996) Measurements of carbon sequestration by long-term eddy covariance: methods and a critical evaluation of accuracy. Global Change Biology 2: 169-182.

Kaimal JC, Finnigan JJ (1994) Atmospheric Boundary Layer Flows, Their Structure and Measurement. New York, Oxford Univ. Press, 289 pages.

Lai C-T, Schauer AJ, Owensby C, Ham JM, Ehleringer JR (2003) Isotopic air sampling in a tallgrass prairie to partition net ecosystem CO_2 exchange. Journal of Geophysical Research 08, 4566, doi:10.1029/2002JD003369.

Lauenroth WK, Milchunas DG (1991) Short-grass steppe. In: Ecosystems of the World 8A: Natural Grasslands. RT Coupland (ed.), Elsevier, Amsterdam, pp 183-226.

LeCain DR, Morgan JA, Mosier AR, Nelson JA (2003) Soil and plant water relations determine photosynthetic responses of C_3 and C_4 grasses in a semi-arid ecosystem under elevated CO_2. Annals of Botany 92:41-52.

Lloyd J, Kruijt B, Hollinger DY, Grace J, Francey RJ, Wong S-C, Kelliher FM, Miranda AC, Farquhar GD, Gash JHC, Vygodskaya NN, Wright IR, Miranda HS, Schulze E-D (1996) Vegetation effects on the isotopic composition of atmospheric CO_2 at local and regional scales: Theoretical aspects and comparison between a rain forest in Amazonia and a boreal forest in Siberia. Australian Journal of Plant Physiology 23:371-399.

Merlivat L (1978) Molecular diffusivities of $H_2{}^{16}O$, $HD^{16}O$, and $H_2{}^{18}O$ in gases. Journal of Chemical Physiology 69:2864-2871.

Milchunas DG, Lauenroth WK (2001) Belowground primary production by carbon isotope decay and long-term root biomass dynamics. Ecosystems 4:139-150.

Miller JB, Yakir D, White JWC, Tans PP (1999) Measurement of $^{18}O/^{16}O$ in the soil-atmosphere CO_2 flux. Global Biogeochemical Cycles 13:761-774.

Parton WJ, Logan JA (1981) A model for diurnal variation in soil and air temperature. Agricultural Meteorology 23:205-216.

Sala OE, Lauenroth WK, Parton WJ (1992) Long-term soil water dynamics in the shortgrass steppe. Ecology 73:1175-1181.

Sellers PJ, Randall DA, Collatz GJ, Berry JA, Field CB, Dazich DA, Zhang C, Collelo GD, Bounoua L (1996) A revised land surface parameterization (SiB2) for atmospheric GCMs. Part I: Model formulation. Journal of Climate 9:676-705.

Schonwits R, Stichler W, Ziegler H (1986) $\delta^{13}C$ values of CO_2 from soil respiration on sites with crops of C_3 and C_4 type of photosynthesis. Oecologia 69:305-308.

Suyker AE, Verma SB (2001) Year-round observations of the net ecosystem exchange of carbon dioxide in a native tallgrass prairie. Global Change Biology 7:279-289.

Tans PP (1998) Oxygen isotopic equilibrium between carbon dioxide and water in soils. Tellus Ser. B. 50:163-178.

Trolier M, White JWC, Tans PP, Masarie KA, Germery PA (1996) Monitoring the isotopic composition of atmospheric CO_2:measurements from the NOAA global air

sampling network. Journal of Geophysical Research 101:25897-25916.

Valentini R, Gamon JA, Field CB (1995) Ecosystem gas exchange in a California grassland: seasonal patterns and implications for scaling. Ecology 76:1940-1952.

Wang XF, Yakir D (1995) Temporal and spatial variations in the oxygen-18 content of leaf water in different plant species. Plant, Cell and Environment 18:1377-1385.

Wang XF, Yakir D, Avishai M (1998) Non-climatic variations in the oxygen isotopic compositions of plants. Global Change Biology 4:835-849.

Webb EK, Pearman GI, Leuning R (1980) Correction of flux measurements for density effects due to heat and water vapor transfer. Quarterly Journal of the Royal Meteorological Society 106:85-100.

Williams TG, Flanagan LB, Coleman JR (1996) Photosynthetic gas exchange and discrimination against $^{13}CO_2$ and $C^{18}O^{16}O$ in tobacco plants modified by an antisense construct to have low chloroplastic carbonic anhydrase. Plant Physiology 112:319-326.

Yakir D, Wang X-F (1996) Fluxes of CO_2 and water between terrestrial vegetation and the atmosphere estimated from isotope measurements. Nature 380:515-517.

Table 4.1 Meteorological conditions on sampling dates over 2000 and 2001. Daily averaged values of air temperature (Tair), soil temperature (Tsoil), vapor pressure deficit (VPD) and volumetric soil water content (%) for sampling periods were listed. Cumulative monthly precipitation values were listed. Leaf water potential (MPa) was measured over two growing seasons of 2000 and 2001 on 1-2 leaves of *P. smithii*.

	Tair (^{0}C)	T soil (^{0}C)	VPD (kPa)	Soil moisture (%)	Precipitation (mm)	Leaf water potential (Mpa)
May-00	20.15	19.01	1.69	12.06	38.86	-2.3
Jun-00	21.95	26.24	2.26	4.5	23.9	-2.8
Jul-00	26.2	28.18	2.99	2.54	6.45	-3.9
Sep-00	20.84	23.79	1.68	4.64	33.2	-2.7
May-01	15.15	14.04	0.32	10.81	73.8	-2.5
June-01	16.62	21.51	0.81	15.64	44.6	-2
July-01	22.28	25.86	1.71	3.08	43.8	-2.8

Table 4.2 Physiological parameters used in the C_3 and C_4 photosynthesis models. The parameterizations of photosynthesis and stomatal and canopy conductance are based on equations in Farquhar et al. (1980) (C_3 photosynthesis), Collatz et al. (1991) (C_4 photosynthesis) and Ball et al. (1987).

	C_3	C_4	Unit	References
Maximum Rubisco capacity, Vcmax at 25°C	63.3	30	μmol m^{-2} s^{-1}	LeCain et al.(2003)
Quantum yield, α	0.066	0.047	mol mol^{-1}	LeCain et al.(2003)
Leaf absorpticity, a	0.8	0.8		Cambell and Norman (1998)
Stomatal slope factor, m_s	9	4		Sellers et al. (1996)
Stomatal intercept factor, b_s	0.01	0.04		Sellers et al. (1996)
Leaf clumping factor, λ	0.95	0.95		Sellers et al. (1996)
co limitation factor,θ	0.95	0.83		Cambell and Norman (1998)
co limitation factor, β	0.98	0.93		Cambell and Norman (1998)
Temperature coefficients of				
Kc	0.074			Cambell and Norman (1998)
Ko	0.018			Cambell and Norman (1998)
τ	-0.056			Cambell and Norman (1998)

Table 4.3 Integrated NEE partitioned into daytime (uptake) and nighttime (respiration) for two growing seasons of 2000 and 2001. Fluxes were calculated as a product of turbulent diffusivity and the 20 min average CO_2 gradient that was measured along with the humidity from a Bowen ratio tower. Integrated CO_2 uptake values were obtained from the subtraction of integrated night time NEE from integrated values of net CO_2 exchange (calculated from Bowen ratio data). Net carbon exchange is also listed.

	Intergrated NEE (g C m-2)		
	Uptake	Respiration	Net
May, 2000			
DOY 143	-5.1	1.62	-3.48
DOY 144	-5.47	0.61	-4.86
June, 2000			
DOY 158	---------	---------	---------
DOY 169	-7.8	1.19	-6.61
July, 2000			
DOY 206	-4.14	0.17	-3.97
DOY 207	-3.73	0.22	-3.51
September, 2000			
DOY 248	-7.5	1.15	-6.35
DOY 249	-6.46	2.3	-4.16
May, 2001			
DOY 137	-7.87	4.07	-3.8
DOY 138	-18.39	6.15	-12.24
June, 2001			
DOY 172	-12.84	2.9	-9.94
DOY 173	-13.84	4.91	-8.93
July, 2001			
DOY 207	-3.19	2.05	-1.14
DOY 208	-1.57	1.52	-0.05

Table 4.4 Isotopic end members used in the isotopic g approach for partitioning gross photosynthesis and respiration.

	$\delta^{13}C$		$\delta^{18}O$	
	$\delta^{13}C_B$	$\delta^{13}C_R$	$\delta^{18}O_B$	$\delta^{18}O_R$
May-00	-15.52	-14.35	------	15.93
Jun-00	-15.51	-14.74	9.61	13.08
Jul-00	-17.17	-15.91	-------	13.08
Sep-00	-20.97	-19.56	8.84	18.24
May-01	-22.59	-15.57	x	13.09
June-01	-28.51	-22.7	x	14.73
July-01	-21.51	-21.38	23.49	17.75

-------; No positive relations were formed between ^{18}O and inverse $[CO_2]$
'x' indicates positive relations between $\delta^{18}O$ of CO_2 and inverse $[CO_2]$ were shown, but no significant relations were formed
^{18}O values averaged time periods of associated flask measurements

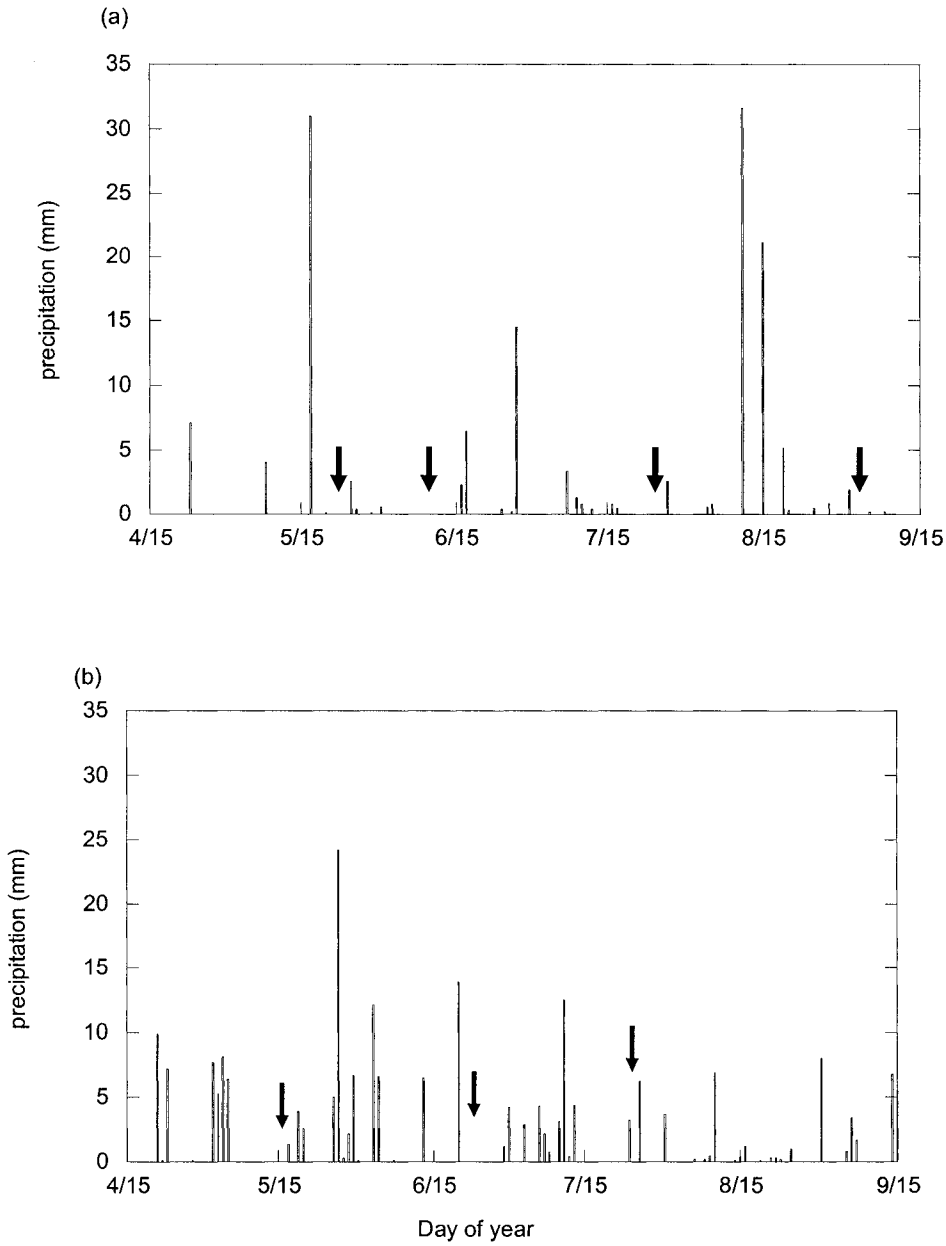

Fig.4.1 Variations of precipitation over two consecutive years beginning (a) April 2000 through (b) mid-September measured at the tower located the air sampling site (Morgan J.A, unpublished data). Arrows represent dates which field experiments were conducted.

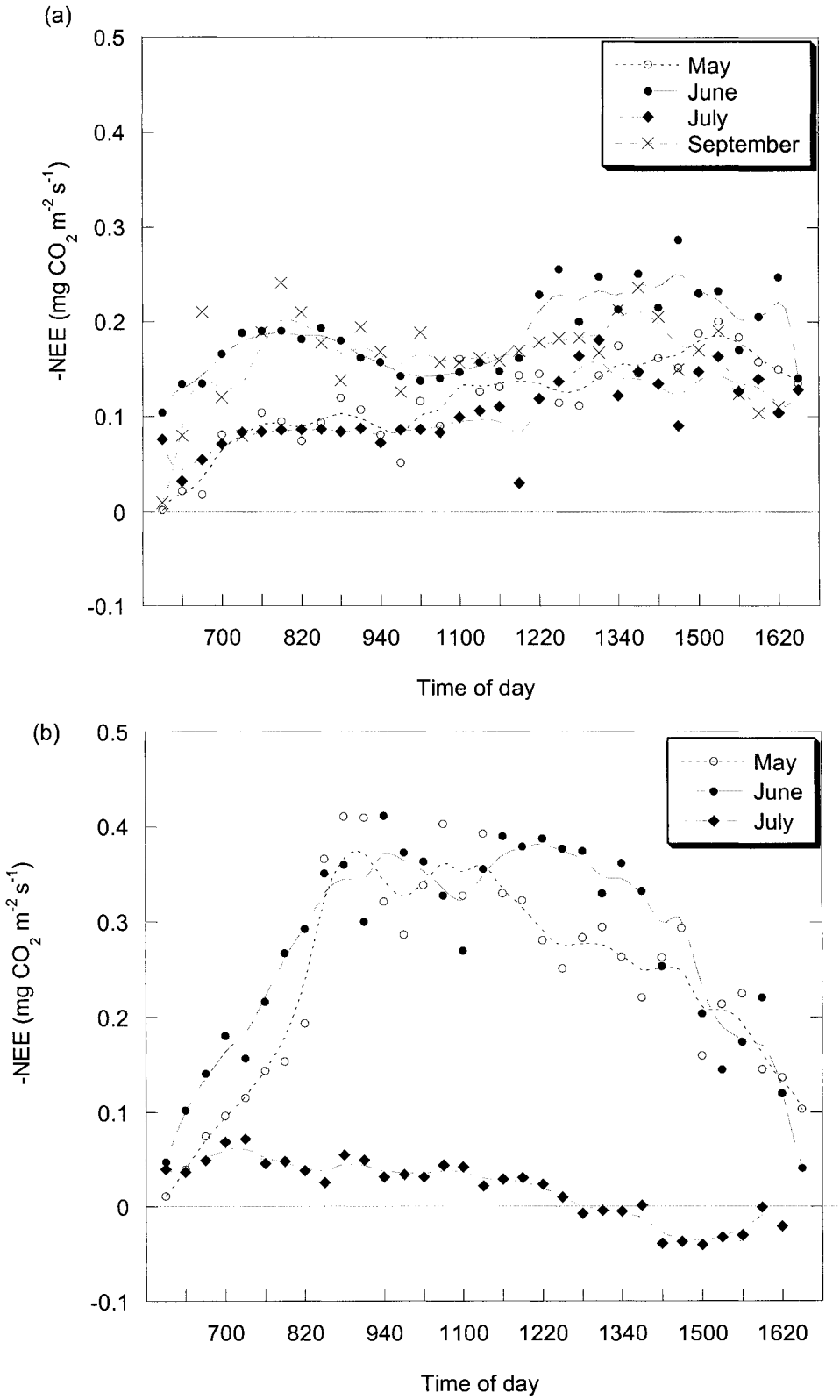

Fig.4.2 Daytime cycles of net CO_2 exchange rates in (a) 2000 and (b) 2001. Data points are 20 minute averages from Bowen Ratio tower (Morgan J.A, unpublished data). Note that the direction of CO_2 flux is upward during photosynthetic periods. Lines represent smoothed curves.

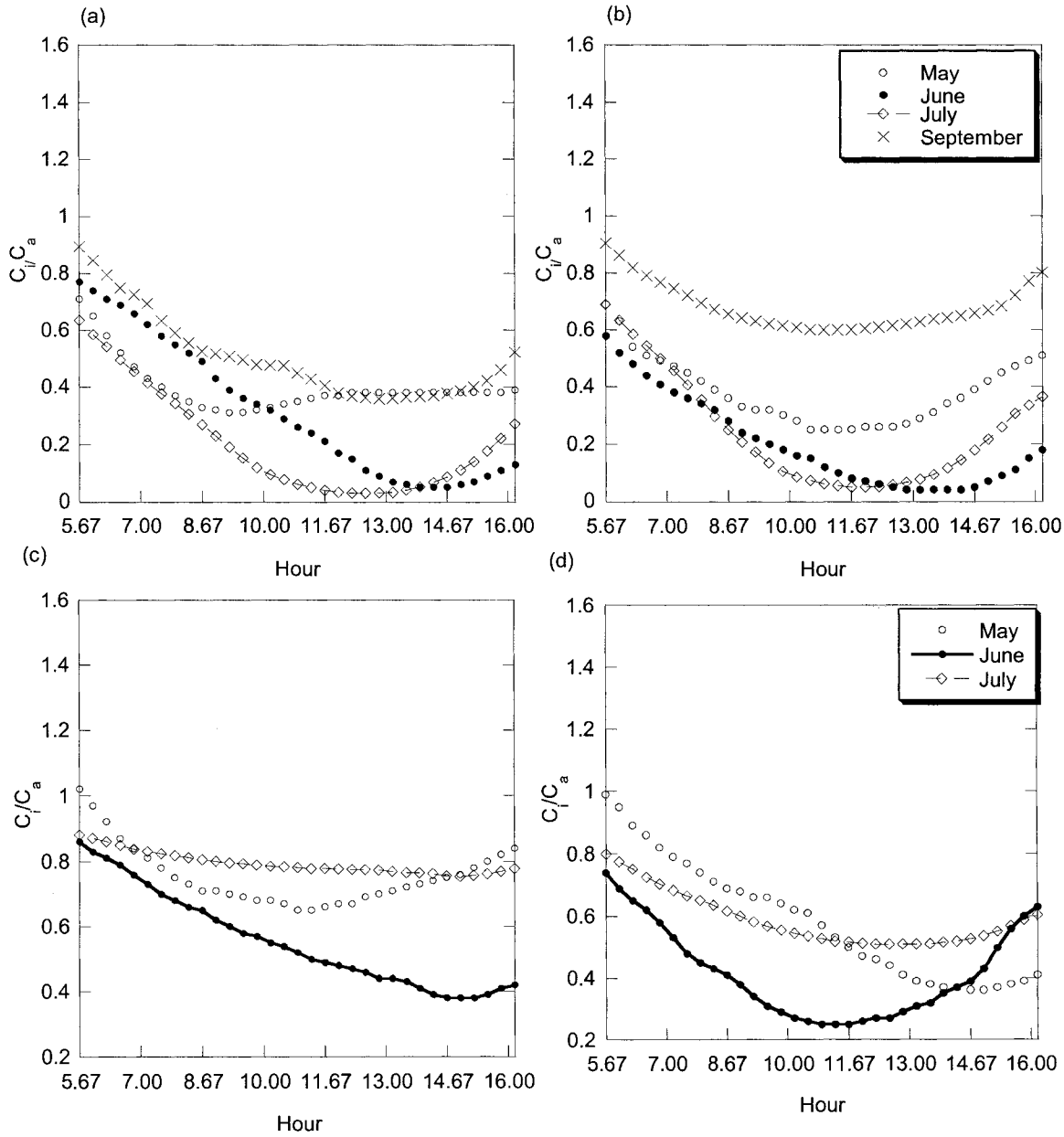

Fig.4.3 Modeled daytime ratios of intercellular (Ci) ambient (Ca) CO_2 concentrations for 2000 (a and b) and 2001 (c and d). Two consecutive days were displayed as 1st day on left side (a and c) and 2nd day (b and d) on right side.

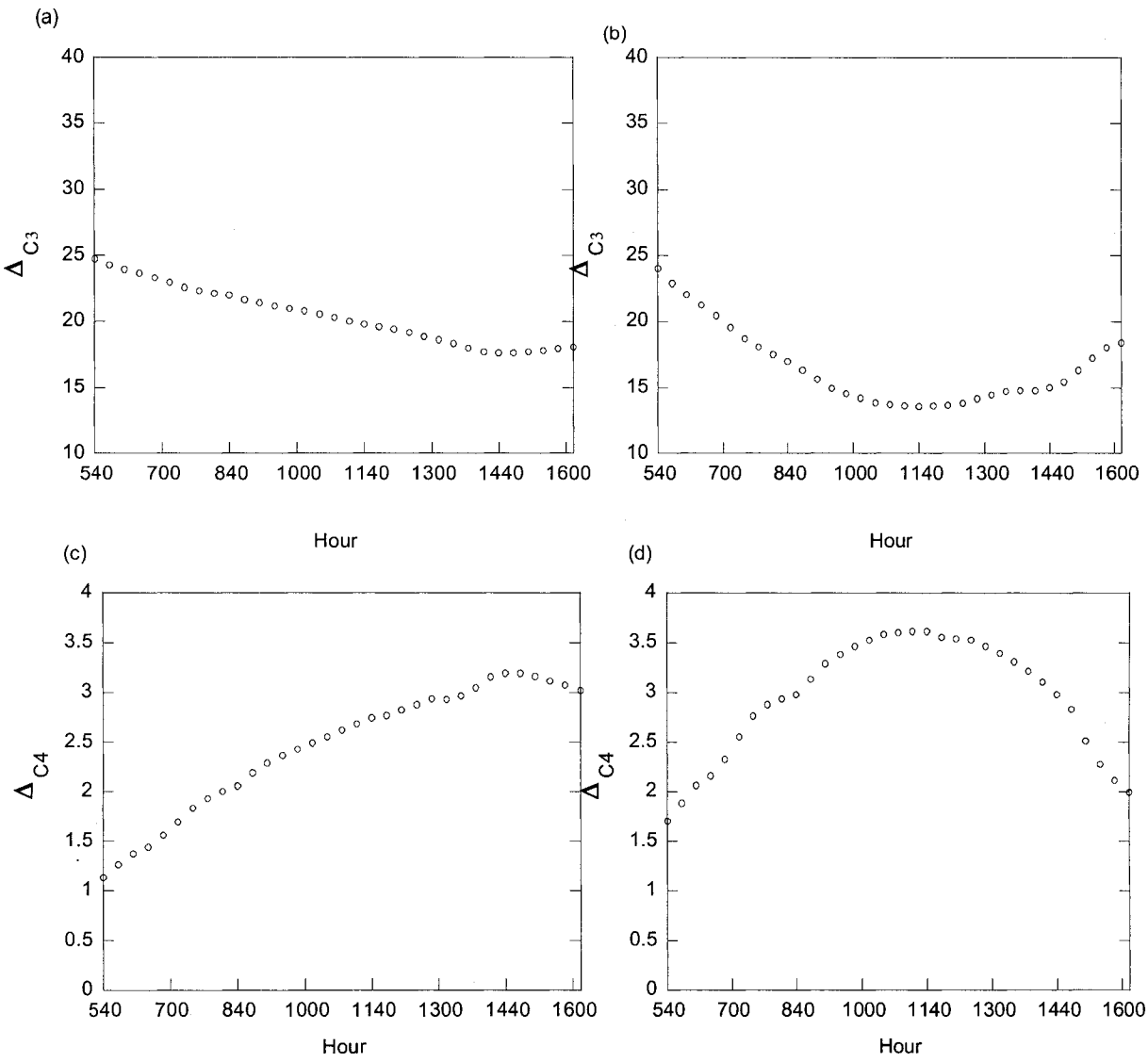

Fig.4.4 Modeled daytime canopy integrated photosynthetic discrimination against ^{13}C (Δ) separated by C_3 (a and b) plants and C_4 plants (c and d) in June, 2001. Two consecutive days were displayed as 1st day on left side (a and c) and 2nd day (b and d) on right side.

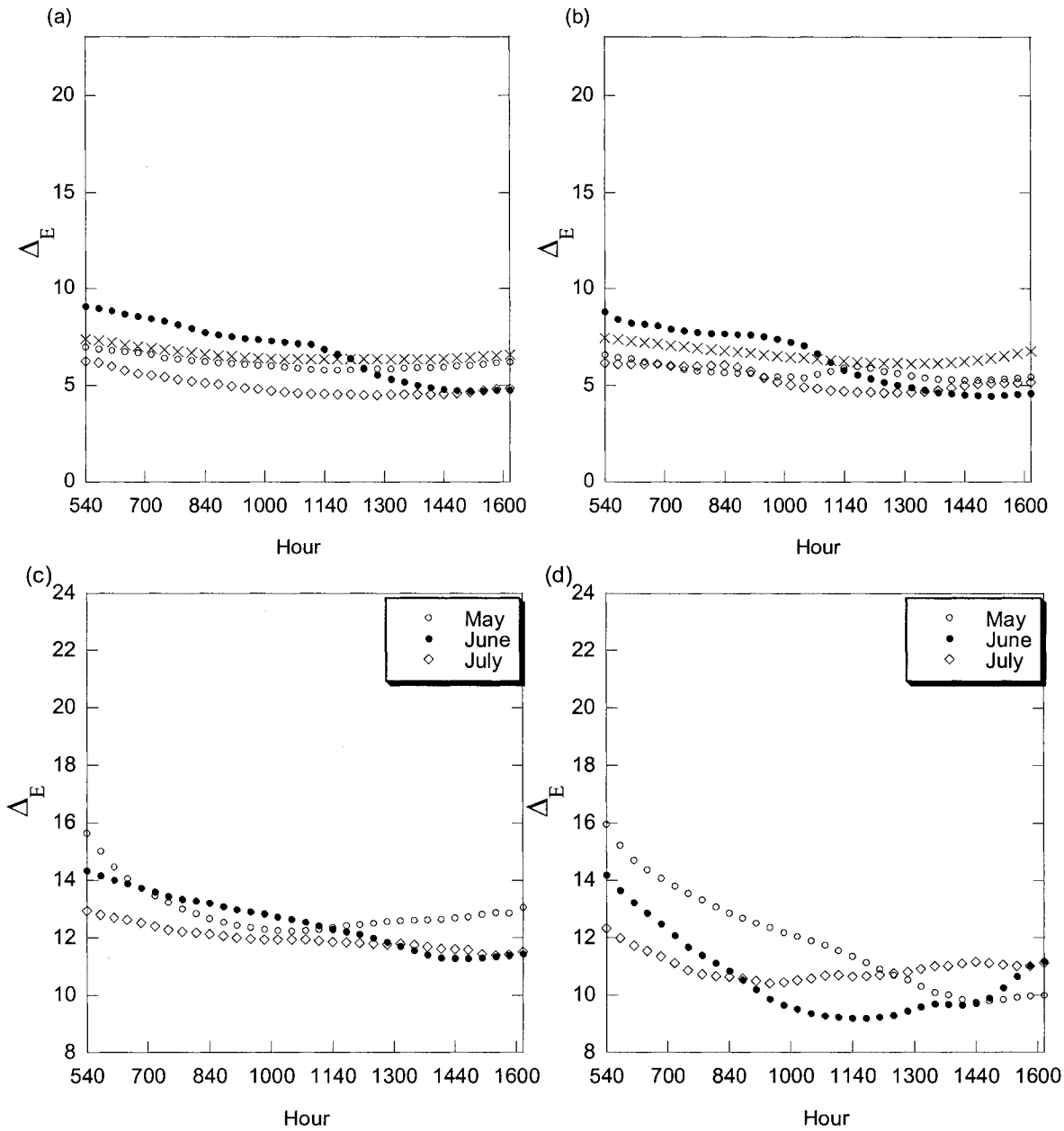

Fig.4.5 Modeled daytime bulk canopy discrimination against ^{13}C during photosynthesis (Δ_E) for 2000 (a and b) and 2001 (c and d). Two consecutive days were displayed as 1st day on left side (a and c) and 2nd day (b and d) on right side.

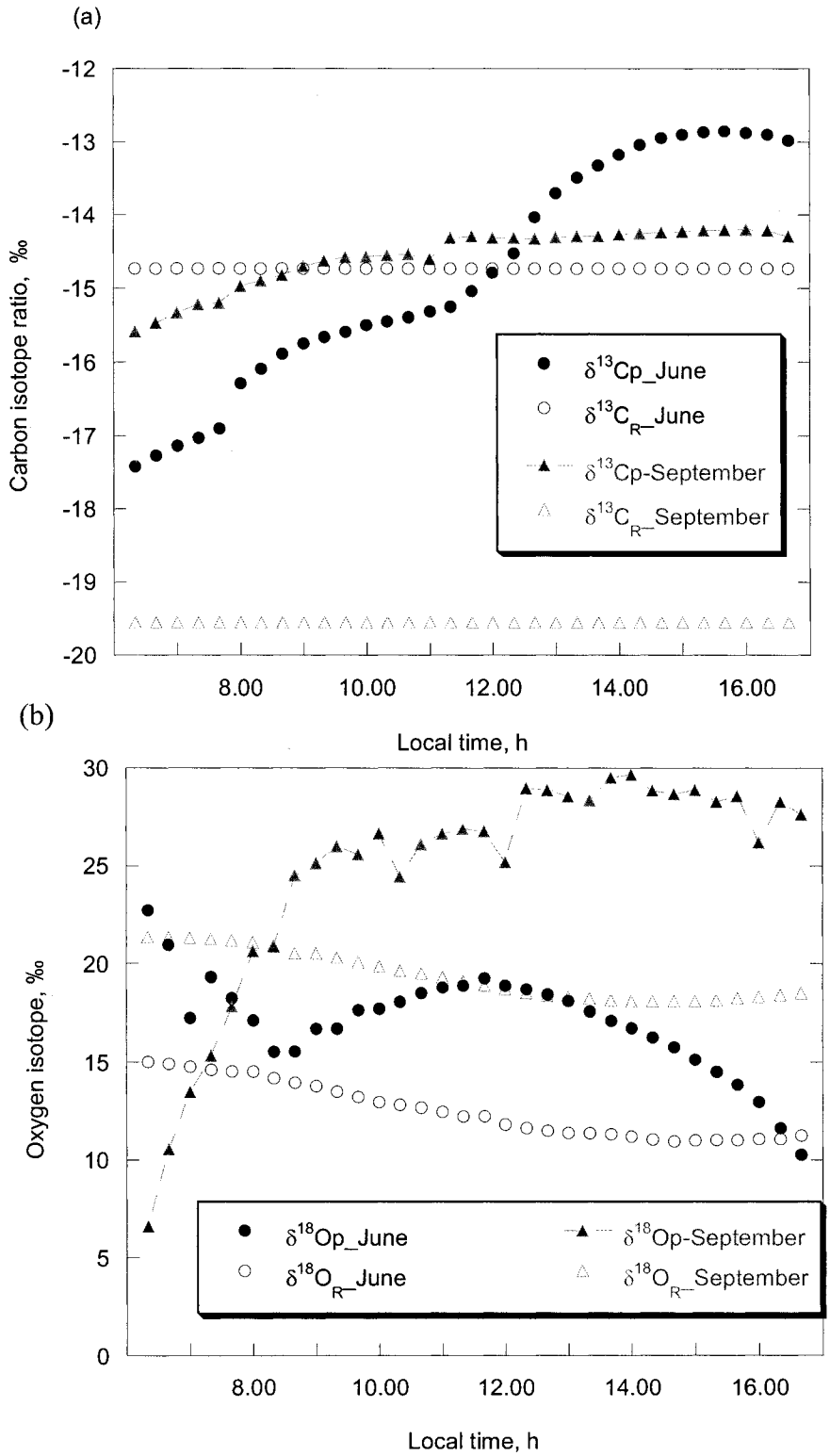

Fig.4.6 Model results of (a) carbon isotopic composition of the photosynthetic flux ($\delta^{13}C_p$), and of the respired flux ($\delta^{13}C_R$) for June and September 2000. (b) Oxygen isotopic composition of photosynthetic flux ($\delta^{18}Op$), and of the respired flux ($\delta^{18}O_R$) for June and September 2000.

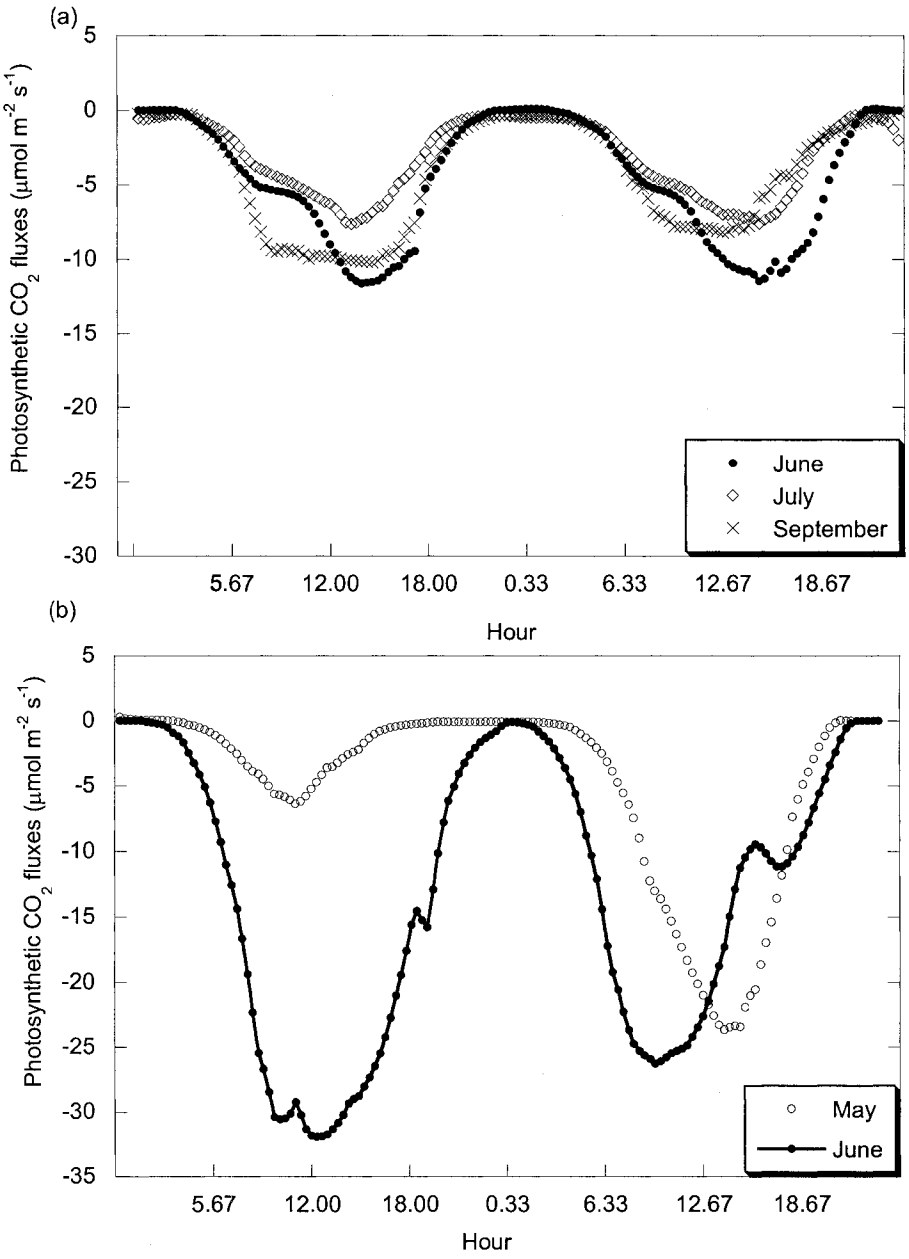

Fig.4.7 Two diurnal cycles of gross photosynthesis partitioned by $\delta^{13}C$ approach for (a) 2000 and (b) 2001.

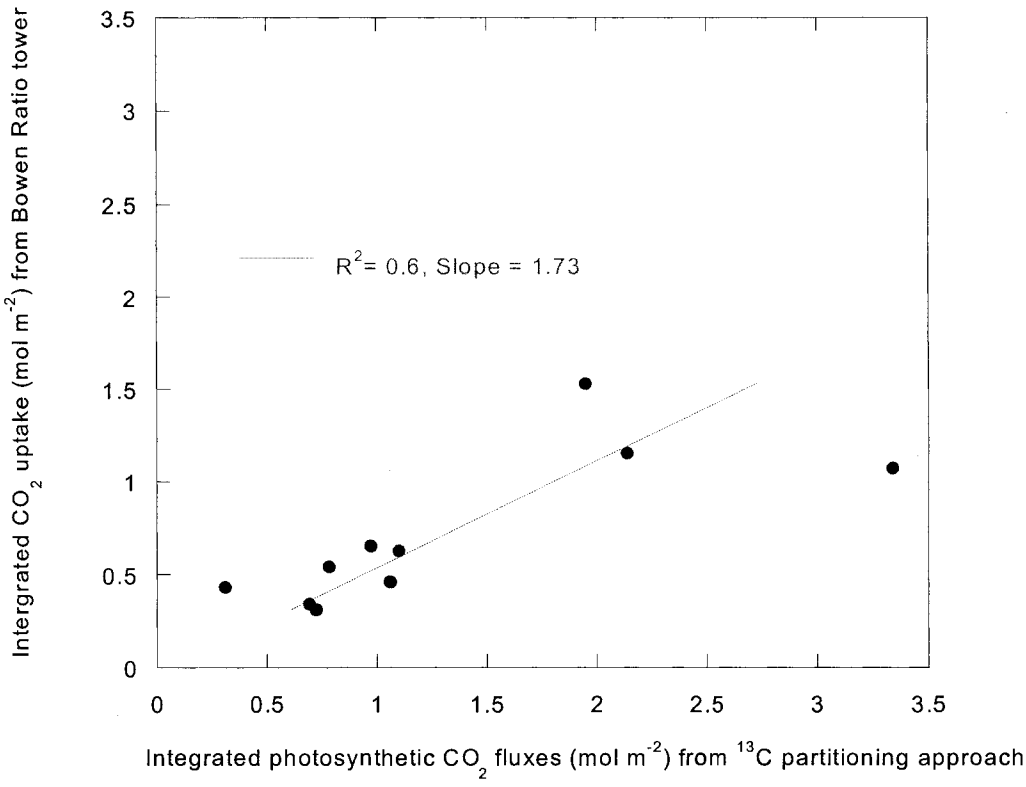

Fig.4.8 Comparison between daily integrated CO_2 uptake from Bowen Ratio tower and photosynthetic CO_2 fluxes calculated from $\delta^{13}C$ labeled partitioning approach for two consecutive years.

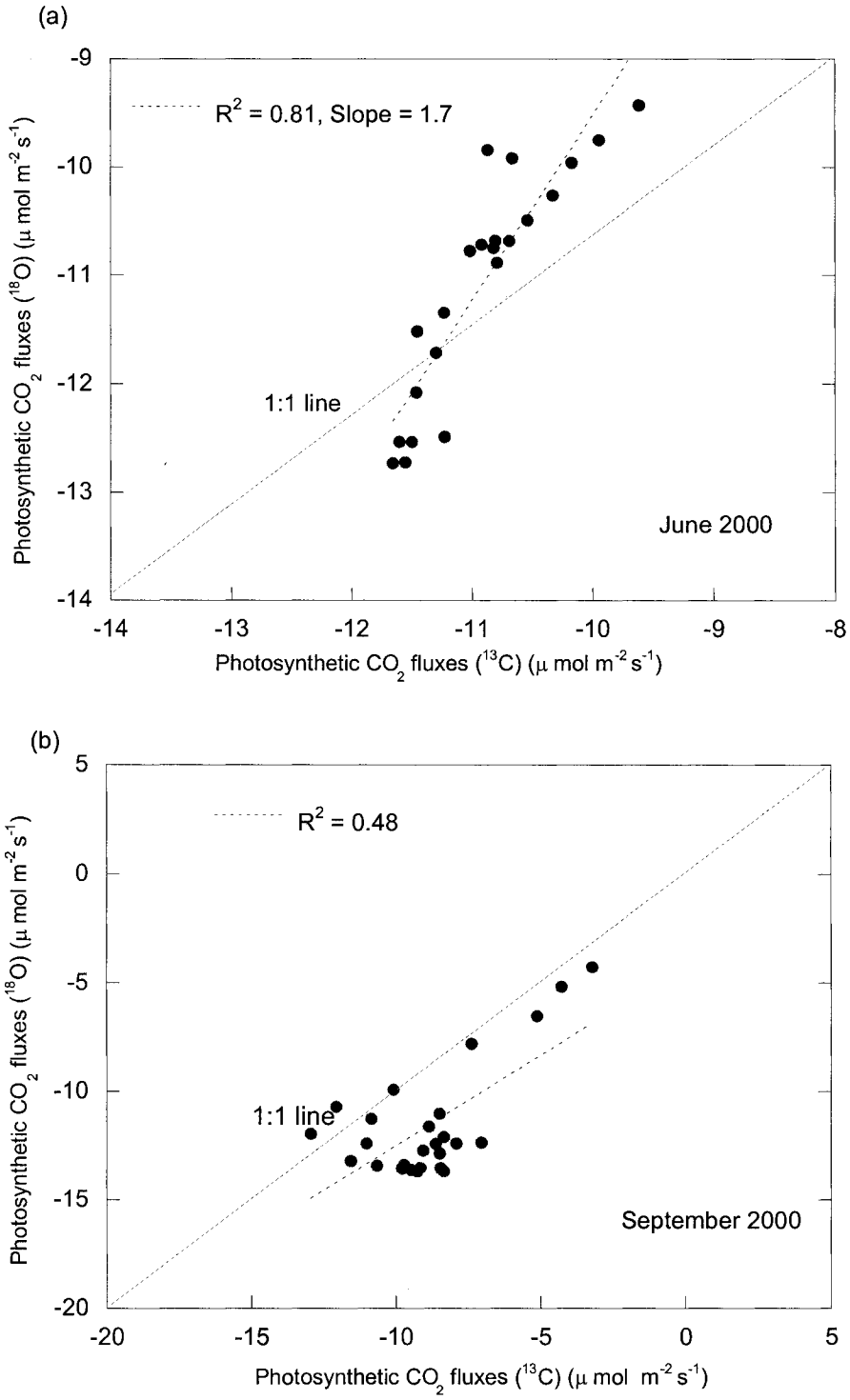

Fig.4.9 Comparison of gross photosynthesis between partitioned by $\delta^{13}C$ and $\delta^{18}O$ labeled approaches in (a) June and (b) September 2000. The data points are 20 minute averages. Situations where isotopic equilibrium between carbon/oxygen compositions of photosynthetic flux and of respiratory flux prevailed were excluded.

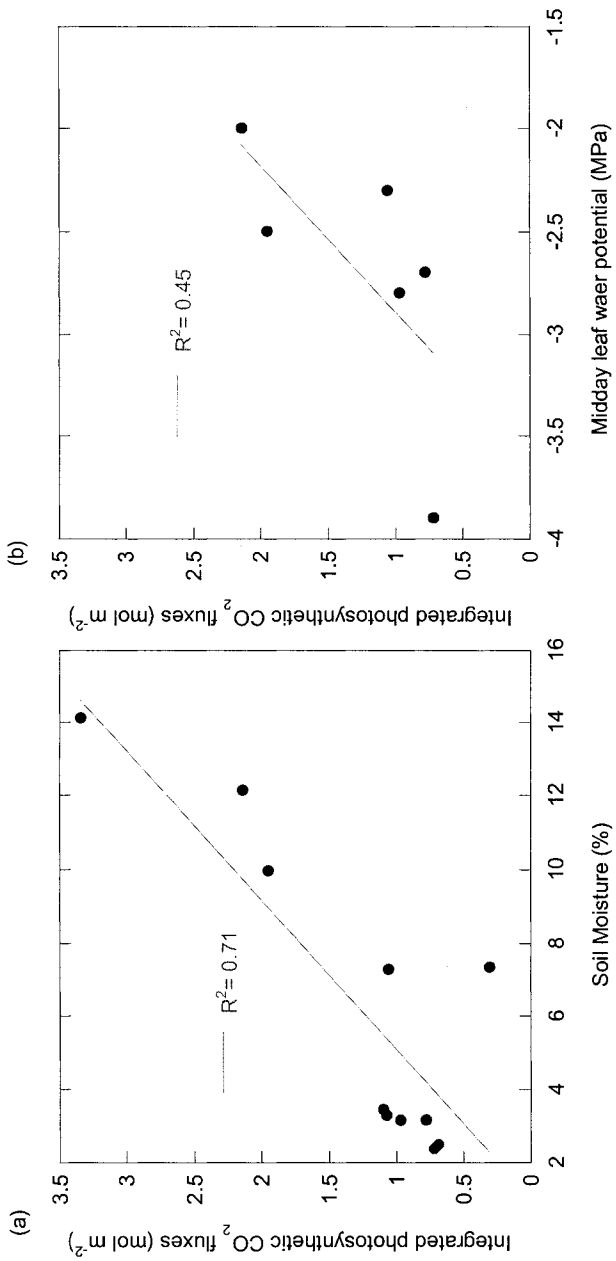

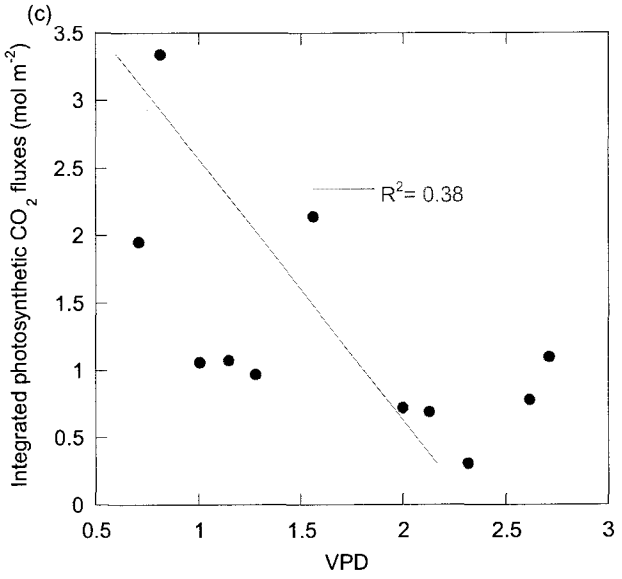

Fig.4.10 Relationship between integrated gross photosynthesis and (a) soil moisture, (b) (b) leaf water potential and (c) vapor pressure deficit (VPD) for two consecutive years.

APPENDIX

C_3 photosynthesis model

We used the C_3 photosynthesis model of Farquhar et al. (1980) coupled with a stomatal conductance model developed by Ball et al. (1987).

Net photosynthesis (A_n) is described as the minimum of three components

$$A_n = \min\begin{Bmatrix} J_E\ (Q_p, T_l) \\ J_C\ (V_m, T_l) \\ J_S \end{Bmatrix} - R_d\ (V_m, T_l) \tag{A1}$$

Where J_E = light limited rate of assimilation (μmol m^{-2} s^{-1}), J_C = Rubisco-limited rate of assimilation (μmol $m^{-2} \cdot s^{-1}$), J_S=Carbon compound export limitation (μmol m^{-2} s^{-1}), R_d=leaf respiration rate (μmol m^{-2} s^{-1}) , Vm = Rubisco capacity, μmol m^{-2} s^{-1}

$$J_E = \frac{a' \times \alpha \times Q_p \times (c_i - \Gamma)}{(c_i + 2\Gamma)} \tag{A2}$$

where a' is leaf absorption to photosynthetically active radiation, α is the intrinsic quantum efficiency for CO_2 uptake (mol mol^{-1}), Q_p is the PAR photon flux density incident on the leaf (μmol m^{-2} s^{-1}) and Γ is defined by the equation

$$\Gamma = \frac{[O_2]}{2\tau} \tag{A3}$$

where τ is a ratio of kinetic parameters indicating the partitioning of RuBP to the carboxylase or oxygenase reactions of Rubisco. $[O_2]$ is assumed constant (210000 μmol/mol). Ci is the intercellular CO_2 concentration

$$Jc = \frac{V_{\max}(c_i - \Gamma)}{(c_i + Kc(1 + [O_2]/Ko))} \tag{A4}$$

where V_{max} is the maximum Rubisco capacity per unit leaf area (μmol m^{-2} s^{-1}), Kc and Ko are the Michaelis constant for CO_2 and for oxygen inhibition, respectively.

$$Js = V_{\max} / 2 \tag{A5}$$

$$R_d = 0.015 \times V_{max} \tag{A6}$$

Five parameters need adjustment for temperature response of photosynthesis such as Kc, τ, Ko, V_m, and R_d. The first three temperature adjustments take the same form, respectively:

$$k = k_{25} \exp[q(T_l - 25)] \tag{A7}$$

where k represents the value of any of the parameters at leaf temperature T_l, k_{25} is the value of that parameter at 25°C, and q is the temperature coefficient for that parameter. The temperature response of V_m and R_d is:

$$V_m = \frac{V_{m,25} \exp[0.088(T_l - 25)]}{1 + \exp[0.29(T_l - 41)]} \tag{A8}$$

$$R_d = \frac{R_{d,25} \exp[(0.069 \times (T_l - 25)]}{1 + \exp[1.3(T_l - 55)]} \tag{A9}$$

C_4 photosynthesis model

$$J_E = a \times \alpha \times Q_p \tag{A10}$$

$$J_c = V_m \tag{A11}$$

$$J_s = 0.02 \times V_m \times c_i \tag{A12}$$

$$R_d = 0.025 \times V_m \tag{A13}$$

The temperature response of V_m and R_d is

$$V_m = \frac{V_{m,25} Q_{10}^{(\frac{T_l - 25}{10})}}{(1 + e^{0.3(13 - T_l)})(1 + e^{0.3(T_l - 36)})} \tag{A14}$$

where $Q_{10} = 39$ μmol m^{-2} s^{-1}

$$R_d = \frac{R_d Q_{10}^{\frac{T_l - 25}{10}}}{1 + e^{1.3(T_l - 55)}} \tag{A15}$$

where Q_{10} is 0.8 μmol m^{-2} s^{-1}

In order to avoid a sharp transition from one rate limiting process to another, empirical quadratic functions are used to generate a more gradual transition. The minimum of J_E and J_C is first computed from:

$$J_p = \frac{J_E + J_C - \sqrt{(J_E + J_C)^2 - 4\theta J_E J_C}}{2\theta} \quad \text{(A16)}$$

The second limitation is imposed by computing the minimum of Jp with Js:

$$A = \frac{Jp + Js - \sqrt{(Jp + Js)^2 - 4\beta JpJs}}{2\beta} \quad \text{(A17)}$$

Separate values for θ and β by C_3 and C_4 plants are listed in Table 4.2.